Spring 2015

Structural Requirements for Ribosome-Dependent GTPase Activity and Binding

Markus A. Carlson
Western Washington University, carlso55@students.wwu.edu

Structural Requirements for Ribosome-Dependent GTPase Activity and Binding

By

Markus A. Carlson

Accepted in Partial Completion

Of the Requirements for the Degree

Master of Science

Kathleen L. Kitto, Dean of the Graduate School

ADVISORY COMMITTEE

Chair, Dr. P. Clint Spiegel

Dr. Gerry Prody

Dr. Sergey Smirnov

MASTER'S THESIS

In presenting this thesis in partial fulfillment of the requirements for a master's degree at Western Washington University, I grant to Western Washington University the non-exclusive royalty-free rights to archive, reproduce, distribute, and display the thesis in any and all forms, including electronic format, via any digital library mechanisms maintained by WWU.

I represent and warrant this is my original work, and does not infringe or violate any rights of others. I warrant that I have obtained written permissions for the owner of any third party copyrighted material included in these files.

I acknowledge that I retain ownership rights to the copyright of this work, including but not limited to the right to use all or part of this work in future works, such as articles or books.

Library users are granted permission for individual, research and non-commercial reproduction of this work for educational purposes only. Any further digital posting of this document requires specific permission from the author.

Any copying or publication of this thesis for commercial purposes, or for financial gain, is not allowed without my written permission.

Markus Carlson

June 1st, 2015

Structural Requirements for Ribosome-Dependent GTPase Activity and Binding

A Thesis

Presented to

The Faculty of

Western Washington University

In Partial Fulfillment

Of the Requirements for the Degree

Master of Science

By

Markus A. Carlson

June 2015

Abstract

The two billion years of evolution since the divergence of prokaryotes and eukaryotes has left earth with very few molecules conserved across these two domains of life. One such molecule, the ribosome, is an enormous ribonucleoprotein responsible for translation, the process of converting the information contained within an organism's genetic code into functional proteins. Translation is facilitated by a number of other proteins, termed translation factors, required to catalyze the synthesis of these proteins. A large number of antibiotics prescribed today target either the ribosome or translation factors, and with increasing antibiotic resistance being found in infectious bacteria there is a greater need for understanding the ribosome and its associated molecules. While knowledge of the ribosome has increased considerably over the past two decades there are still many unknowns surrounding its transition states, how it interacts with translation factors, and even the role some of these translation factors play in the cell. A more thorough understanding of the interactions between ribosomes and translation factors will lead to the generation of more diverse and possibly more potent antibiotics for the treatment of bacterial infections.

The goals of this work were threefold. First, based on the work of previous Spiegel lab graduate student Justin Walter, we aimed to further characterize the role of the L12 ribosomal protein in activation of several translation factors that

utilize the hydrolysis of guanosine 5'-triphosphate (GTP), called GTPases, to exert their function. Walter had shown that removal of L12 led to decreased GTP hydrolysis by these proteins, but was unable to ensure L12 had been completely removed from the ribosomes. Here it is shown that when L12 is completely absent from functional prokaryotic ribosomes the GTPase activity of three translation factors, elongation factor G (EF-G), release factor 3 (RF3), and initiation factor 2 (IF2) all unequivocally cease, showing no activity beyond that of uncatalyzed GTP hydrolysis. A fourth translational GTPase, leader peptidase A (LepA), exhibited a different response, with activity dropping by effectively 50% upon the removal of L12. Reconstitution of these depleted ribosomes with externally purified L12 caused an unambiguous return to full activity for all investigated GTPases.

A second ambition of this work was to analyze the role of the L12 ribosomal protein in binding of translation factors. GTPase binding assays through ultracentrifugation demonstrated that absolute removal of L12 led to a nearly complete abrogation of binding between 70S ribosomes and EF-G, IF2, and RF3. LepA exhibited diminished binding in the presence of L12 deficient ribosomes, but maintained a level significantly above baseline. To further assess the effect of L12 depletion on binding, BioLayer Interferometry was utilized to quantitatively measure the binding affinity between EF-G and 70S or 70SΔL12. EF-G and 70S interactions fell within previously established K_D values, averaging ~160 nM. Preincubation of EF-G with 70SΔL12 maintained this affinity, suggesting that little

to no EF-G associates with depleted ribosomes, while preincubation of EF-G with intact 70S ribosomes caused a > 10,000 fold increase in the K_D, indicating EF-G has a strong association with 70S ribosomes when L12 is present.

The final objective herein was to determine the roles of domains 4 and 5 and subdomain G' of EF-G in the hydrolysis of GTP. EF-GΔ5 and EF-GΔ4,5 were previously produced in the Spiegel lab. Here it is shown that EF-GΔ4 and EF-GΔG' are both expressed in the soluble fraction of *E. coli* cells and are readily isolated. The GTPase activity of each mutant relative to full length EF-G was calculated. EF-GΔ4 and EF-GΔ4,5 exhibited an activity of roughly 65% of wild type EF-G, suggesting the loss of the 4 domain confers the same disadvantage as the loss of the 4 and 5 domains. Meanwhile, EF-GΔ5 maintained 85% activity, showing the loss of the 5 domain is less detrimental to GTPase activity than either the Δ4 or Δ4,5 mutants. EF-GΔG' confers a loss of around 90% activity compared to EF-G, suggestive of a crucial role of this domain in EF-G activity or binding, despite being absent in other homologous translational GTPases.

Acknowledgements

Many thanks are extended to Dr. P. Clint Spiegel, for accepting an unknown and unproven student into his lab and allowing me free reign to perform the experiments as I saw fit. His knowledge in the field of ribosomes proved invaluable in helping me design and conduct experiments. I would also like to thank Dr. Gerry Prody and Dr. Sergey Smirnov for their expert analysis of this thesis, and providing me with critical feedback of my experiments and interpretations.

I also extend my gratitude towards other members of the Spiegel lab working on this project, specifically Michelle Wuerth, Justin Walter, Danny Harbeson, Catherine Shelton, and Bassam Haddad. I also thank all current and former lab members of the Spiegel lab for their insight and aid in designing experiments, as well as for providing me with a solid groundwork from which to conduct the research presented herein.

Table of Contents

List of Figures

Table of Abbreviations

Abbreviation	Name	Function
70SIC	70S initiation complex	An assembly of the 30S and 50S subunits also containing an mRNA strand and fMet-tRNA^{fMet}
aa-tRNA	Aminoacyl transfer ribonucleic acid	tRNA bound to an amino acid
AEC	Anion exchange chromatography	Technique used to purify proteins based on their isoelectric point
BCIP-NBT	5-bromo-4-chloro-3'-indolyphosphate p-toluidine-nitro-blue terazolium chloride	Reagent used to develop the color of western blots
BLI	BioLayer Interferometry	Technique used to determine binding kinetics and affinity
CD	Circular dichroism	Technique allowing for detection of secondary structure of a protein; used to determine if proteins are folded or not
CTD	C-terminal domain	The domain of a protein that contains the terminal carboxyl group
deacyl-tRNA	Deacylated transfer ribonucleic acid	tRNA not bound to an amino acid
DNA	Deoxyribonucleic acid	Storage medium for genes used by all prokaryotes and eukaryotes
EF4	Elongation Factor 4 (also known as LepA)	GTPase, function still undetermined
EF-G	Elongation Factor G	GTPase, Involved in translocation and ribosome recycling
EF-Tu	Elongation Factor Thermo-unstable	GTPase, localizes aa-tRNA to the 70S ribosome
fMet-tRNA^{fMet}	N-formylmethionine attached to transfer ribonucleic acid	The first amino acid in all prokaryotic proteins attached to tRNA
GAC	GTPase associated center	Portion of the 50S subunit where translational GTPases primarily associate
GDP	Guanosine diphosphate	Product of cleavage of GTP by GTPases

GDPNP	Guanosine 5'-[β,γ-imido]triphosphate	Non-hydrolysable analog of GTP, locks GTPases into GTP bound conformation
GTP	Guanosine triphosphate	Hydrolyzed by GTPases to provide energy for conformational change
IF1	Initiation Factor 1	Involved in translation initiation
IF2	Initiation Factor 2	GTPase, involved in translation initiation
IF3	Initiation Factor 3	Involved in translation initiation
IMAC	Immobilized metal affinity chromatography	Method of purifying proteins that contain a $(His)_6$-tag
IPTG	Isopropyl β-D-1-thiogalactopyranoside	Allolactose mimic, induces overexpression of proteins on vectors
LB	Lysogeny Broth	Liquid media used to grow bacterial cells
LepA	Leader Peptidase A	GTPase, function still undetermined
mRNA	Messenger ribonucleic acid	Intermediary step between DNA and proteins, dictates the order of amino acid addition
Ni-NTA	Nickel-nitrilotriacetic acid	Substrate used to bind molecules containing a $(His)_6$-tag
NTD	N-terminal domain	The domain of a protein that contains the terminal α-amino group
PCR	Polymerase chain reaction	DNA amplification method
PDBid	Protein data bank identification number	Code used to identify molecules that have had structures solved and that have been deposited onto www.rcsb.org
P_i	Inorganic phosphate (orthophosphate)	Product of cleavage of GTP by GTPases
PMSF	Phenylmethylsulfonyl fluoride	Serine protease inhibitor, used to prevent degradation of overexpressed proteins prior to purification
PTC	Peptidyl transferase center	Forms peptide bonds between the elongating peptide on the P-site tRNA and the amino acid on the A site tRNA

RF1	Release Factor 1	Involved in translation termination
RF2	Release Factor 2	Involved in translation termination
RF3	Release Factor 3	GTPase, Involved in translation termination
RNA	Ribonucleic acid	Many varied cellular functions
rRNA	Ribosomal ribonucleic acid	RNA present in ribosomes, catalyzes sequential amino acid addition
SDM	Site-directed mutagenesis	Method of introducing specific mutations into target genes
SDS-PAGE	Sodium dodecyl sulfate polyacrylamide gel electrophoresis	Method of separating proteins based on molecular weight
SEC	Size exclusion chromatography	Technique used to purify proteins based on their three dimensional size
SRL	Sarcin-ricin loop	Portion of the 23S rRNA essential for GTP hydrolysis catalyzed steps in translation
TBST	Tris-buffered saline with Tween 20	Reagent used to wash nitrocellulose membranes
tRNA	Transfer ribonucleic acid	Binds amino acids, and associates with the ribosome
β-ME	β-mercaptoethanol	Reagent used to reduce disulfide bonds caused by to proximal cysteine residues in a protein

Chapter 1 – Ribosomes: Form and Function

Since Watson and Crick discovered the structure of deoxyribonucleic acid (DNA) in 1953, the “central dogma” in all of molecular biology has been that DNA, the highly stable storage material nearly all life exploits for its genes, is converted into an intermediary messenger ribonucleic acid (mRNA), then expressed as a functional chain of amino acids commonly known as a protein (Watson and Crick, 1953; Crick, 1970). The reading of DNA and subsequent synthesis of mRNA is called transcription, while converting of an mRNA sequence into functional proteins is known as translation. In every known species this second step, translation, is governed by a macromolecular ribonucleoprotein called the ribosome (Figure 1-1; Palade, 1955). The ubiquitous ribosome essentially converts the genes of an organism into their interactive counterparts, proteins, allowing life as we know it to transpire. It accomplishes this through complex interactions with other proteins, transfer RNAs (tRNAs), and mRNA, as will be described in detail later. In brief, the ribosome is able to catalyze the sequential addition of specific amino acids, the building blocks of proteins, onto an elongating peptide chain as governed by the mRNA sequence and thus ultimately the DNA. The mRNA is comprised of four different nucleotides, adenine (A), uracil (U), cytosine (C), and guanine (G). The order of these nucleotides, or bases, dictates which amino acid the ribosome adds to the elongating polypeptide. Each mRNA molecule can be divided into codons, sets

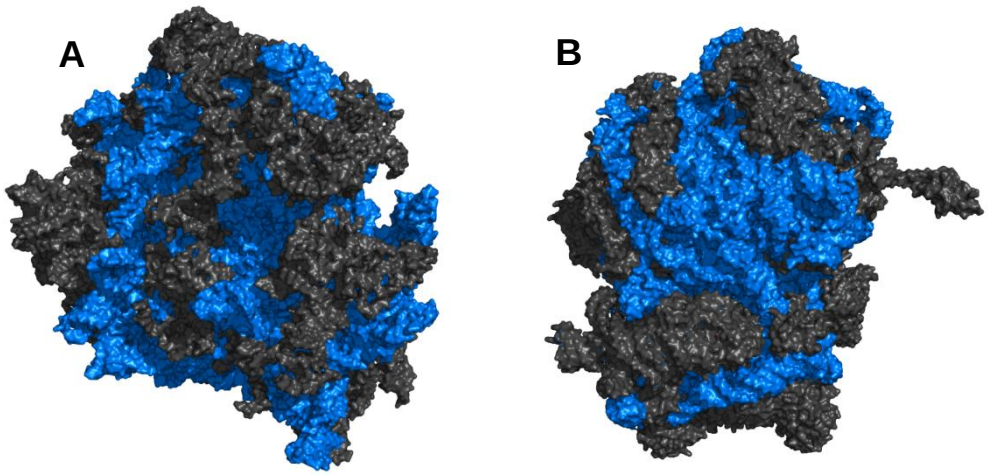

Figure 1-1. Comparison of 80S and 70S ribosomes. **(A)** Structure of the 80S eukaryotic ribosome from *Saccharomyces cerevisiae* (PDBid 4V7R). **(B)** Structure of the 70S prokaryotic ribosome from *Thermus thermophilus* (PDBid 4Z8C).

of three nucleotides that tell the ribosome which amino acid should be added to the protein next (Crick, 1968). Depending on the order of the nucleotides appearing in the codon, one of twenty different amino acids will be attached to the polypeptide.

Ribosome Structure

The ribosome is considered to be one of the most evolutionarily conserved molecules discovered to date (Gray et al., 1984; Osawa et al., 1992; Melnikov et al., 2012). Every living organism employs a ribosome to convert its mRNA into functional proteins, including plants, fungi, mammals, and invertebrates; even

viruses coopt the ribosomes present in the host cells they infect. Despite the divergence of prokaryotes and eukaryotes occurring approximately two billion years ago, the degree of homology found across domains of life makes it clear the ribosome is a product of divergent evolution (Figure 1-1; Kozak, 1999; Melnikov et al., 2012). The 70S ribosome is one of the largest macromolecules in prokaryotes, weighing an astounding 2-3 megadaltons and having a diameter of approximate 250 Å (Ramakrishnan, 2002). The eukaryotic 80S ribosome has a molecular mass of around 4 megadaltons, and can reach nearly 300 Å in diameter (Ben-Shem et al., 2010).

The prokaryotic 70S ribosome is composed of two different subunits, making it a heterodimer. The large subunit, 50S ('S' stands for Svedberg, and is a unit of sedimentation rate), is composed of two single stranded ribosomal RNA (rRNA) molecules, the 23S and 5S rRNA, which are approximately 2900 and 120 bases, respectively (Figure 1-2A). It also contains 33 ribosomal proteins (L1, L2, L3, etc.). The smaller 30S subunit contains only one 16S rRNA of 1500 nucleotides and 22 associated proteins (S1, S2, S3, etc.) (Figure 1-2B; Wilson and Nierhaus, 2003).

Ribosomes are unique in that the rRNA plays most of the enzymatic and catalytic roles as well as determines the basic internal structure, whereas the proteins are found exclusively on the exterior portions of the ribosome and are almost entirely nonenzymatic, meaning ribosomes are in fact ribozymes (Yusupov et al., 2001). From this it is inferred that ribosomal proteins evolved at a later point than the

rRNA, and as RNA likely predated both DNA and proteins, suggests a very ancient evolution (Joyce, 2002). The 23S rRNA present in the 50S subunit gives the ribosome its ability to catalyze the addition of amino acids onto a polypeptide at a location known as the 'peptidyl transferase center' (PTC) (Figure 1-3; Ammons et al., 1999; Beringer et al, 2008). While the function of the 5S rRNA present in that same subunit has not yet been discovered, it has been shown that deletion of the 5S rRNA strand is detrimental to the cell (Ammons et al., 1999). The 16S rRNA present within the 30S subunit contains the location where mRNA binds to the ribosome for translation, as well as the site the anticodon ends of tRNA molecules bind to within the 70S complex, known as the decoding site (Figure 1-3; Wilson and Nierhaus, 2003).

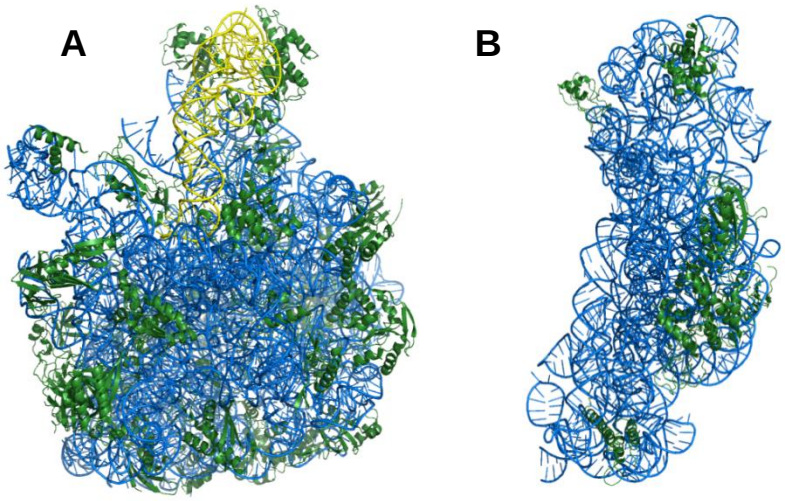

Figure 1-2. Prokaryotic ribosomal subunits. **(A)** 50S ribosomal subunit. Blue - 23S rRNA, yellow - 5S rRNA, green – proteins (PDBid 1JJ2). **(B)** 30S ribosomal subunit. Blue – 16S rRNA, green – proteins (PDBid 1FKA).

Though there are some structural differences between the prokaryotic and eukaryotic forms, the overall function of the ribosome remains unchanged, and the rRNAs and proteins present within it contain very strong sequence similarity (Verschoor et al., 1996). This parallel between the two versions means that much of the activity of the ribosome is likely to be translatable from one species to another, as well as from one domain of life to another (Ganoza et al., 2002).

tRNAs

Transfer RNA (tRNA) is a single stranded RNA molecule comprised of less than 100 nucleotides whose function is to recognize the codon dictated by the mRNA and shuttle the appropriate amino acids to the ribosome during translation (Sharp et al., 1985). tRNA molecules have a 3' end that overhangs the corresponding 5' end by approximately 5 bases, allowing the free end to recognize and bind an amino acid should it encounter the correct one (Figure 1-3A). At the opposite end of each tRNA is an anticodon region, which allows it to identify the codon on the mRNA and bind to the ribosome appropriately (Rich and Bhandary, 1976). Once an aminoacylated tRNA (aa-tRNA) enters the ribosome it is bound to one of three sites present on both the 30S and 50S subunits, the aminoacyl site (A), peptidyl site (P), or exit site (E) (Figure 1-3B). The A site binds the required aa-tRNA as specified by the mRNA and positions it within the ribosome with the help of elongation factor thermo-unstable (EF-Tu). The aa-tRNA moves from the A site to the P site when the attached amino acid becomes added to the elongating

protein. Once in the P site, the tRNA is still attached to the amino acid, which in turn, is attached to the elongating polypeptide through a spontaneous transpeptidation reaction, primarily catalyzed by the 23S rRNA. Once released from the peptide chain, the spent tRNA (deacyl-tRNA) is transferred from the P site to the E site, where it can dissociate from the ribosome complex, and bind another amino acid, allowing the cycle to continue (Rheinberger et al., 1981). All of these sites have interactions between the tRNA and the 23S rRNA found in the 50S subunit (Moazed and Noller, 1989).

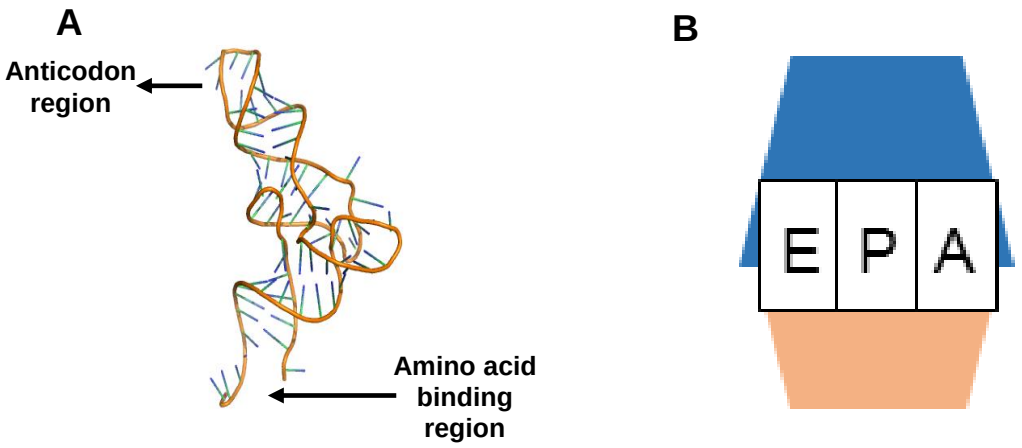

Figure 1-3. tRNA positions in the ribosome. **(A)** Initiator tRNA from *Escherichia coli*, indicating the anticodon region and the 3' aminoacyl recognition site (PDBid 3CW5). **(B)** 70S ribosome structure indicating the three tRNA binding sites.

Translation

As mentioned above, the ribosome serves to *translate* the mRNA strand into a linked chain of amino acids known as a protein. In order to fully understand how this large, complex piece of molecular machinery accomplishes translation, the process can be broken down into four distinct stages. The first stage, *initiation*, serves to bind mRNA and the first aminoacyl-tRNA to the 70S ribosome, thereby preparing the complex for the next stage, *elongation* (Ball and Kaesberg, 1973). *Elongation* is the central step in translation, as it is simply the sequential addition of amino acids onto the polypeptide chain, and it occurs repeatedly until the mRNA instructs the ribosome to stop. *Termination*, the third step, takes place after the ribosome recognizes a stop codon on the mRNA, and consists of the hydrolysis of the now full length protein from the 70S complex and its subsequent dissociation from the complex. The final step, *recycling*, dissociates the 70S ribosome into the 50S and 30S subunits and allows for the remnant mRNA and deacyl-tRNA left in the 30S subunit to dissipate. Each of these steps utilizes a host of proteins to aid the ribosome, deemed translation factors, which are associated with (and often named after) the different stages of translation.

Initiation

Initiation is the process that assembles the requisite molecules for polypeptide synthesis. The free floating 30S subunit spontaneously binds the mRNA at a purine rich segment upstream of the start codon known as the Shine-Dalgarno

sequence (Shine and Dalgarno, 1974). This region is complementary to a section of the 16S rRNA present in the 30S subunit, and Watson-Crick base pairing (A:U and C:G) allows association to be thermodynamically favorable. Upon binding of this sequence, the mRNA is positioned in such a way that the start codon, a specific arrangement of bases present in the mRNA, is positioned directly in the P site, primed for amino acid addition once the full 70S initiation complex (70SIC) is formed (Figure 1-4; Qin 2009). This start codon typically specifies an aa-tRNA bound to an N-formylmethionine (fMet) residue (fMet is often removed after translation) which is positioned in the 30S P site by translation initiation factor 2 (IF2) (Gualerzi and Pon, 1990). IF2 binds to fMet-bound tRNA (fMet-tRNA^{fMet}), and once the mRNA is positioned in the 30S subunit, correctly positions the tRNA in the P site. Initiation factor 1 (IF1) binds adjacent to the A site and is speculated to have a role in preventing premature entry of another tRNA molecule (Ramakrishnan, 2002). Initiation factor 3 (IF3), however, associates with the 30S E site and sterically prevents premature attachment of the 50S subunit (Petrelli et al., 2001). Once the mRNA is bound and IF2 positions the fMet-tRNA^{fMet}, IF3 is allowed to dissociate and IF2, a GTPase (GTPases are discussed in greater detail in chapter 2), hydrolyzes guanosine 5'-triphosphate (GTP) to guanosine 5'-diphosphate (GDP). This hydrolysis induces a conformational change in IF2, allowing it to dissociate from the 30S complex, thereby enabling the 50S subunit to bind, forming the full 70SIC, and leaving the ribosome ready to perform addition of subsequent amino acids (Luchin et al.,

1999). Many of the discrete steps involved in initiation are yet to be fully characterized, as the intricacies involved have only recently begun to be studied thoroughly and appropriately.

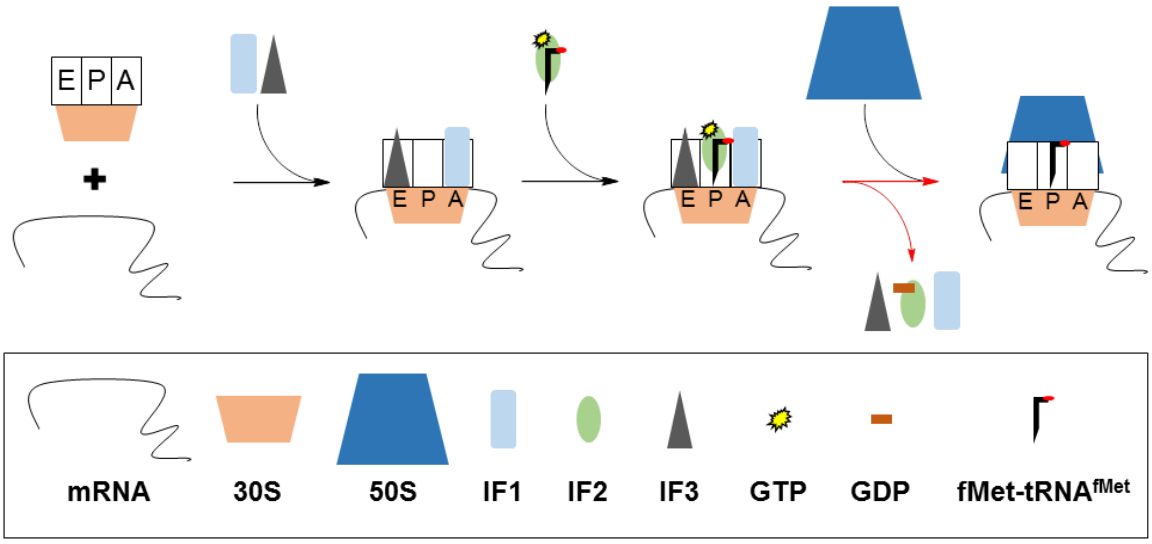

Figure 1-4. Initiation of translation. The 30S subunit spontaneously associates with mRNA, followed by the binding of IF1 and IF3. IF2 then binds with fMet-tRNA^{fMet}, and hydrolysis of GTP to GDP allows the initiation factors to dissociate and the 50S subunit to bind. Red arrows indicate steps involving the hydrolysis of GTP.

Elongation

The process of elongation can be divided into three distinct steps. First, the 70S ribosome must *accommodate* an aa-tRNA, allowing entry into the A site of the 50S subunit. Next, the amino acid bound to the tRNA undergoes *peptidyl transfer* to the elongating protein chain. Finally, *translocation* pushes the mRNA and tRNA through the 30S and 50S ribosomal subunits and readies the 70S complex for entry of another aa-tRNA.

Accommodation

As the 70S initiation complex forms, the A site of the 50S subunit opens allowing an aa-tRNA to enter the A site (Frank, et al., 2005). EF-Tu binds aa-tRNA, as well as GTP, and correctly positions it in the A site as controlled by the pairing of the codon on the mRNA strand with the anticodon region present on the tRNA (Figure 1-5; Pape et al., 2000; Schmeing et al., 2009). Correct binding leads to a series of conformational changes which cause EF-Tu to hydrolyze GTP and subsequently dissociate from the 70S complex, leaving the aa-tRNA behind (Potapov, 1982; Berchtold et al., 1993; Pape et al., 1998).

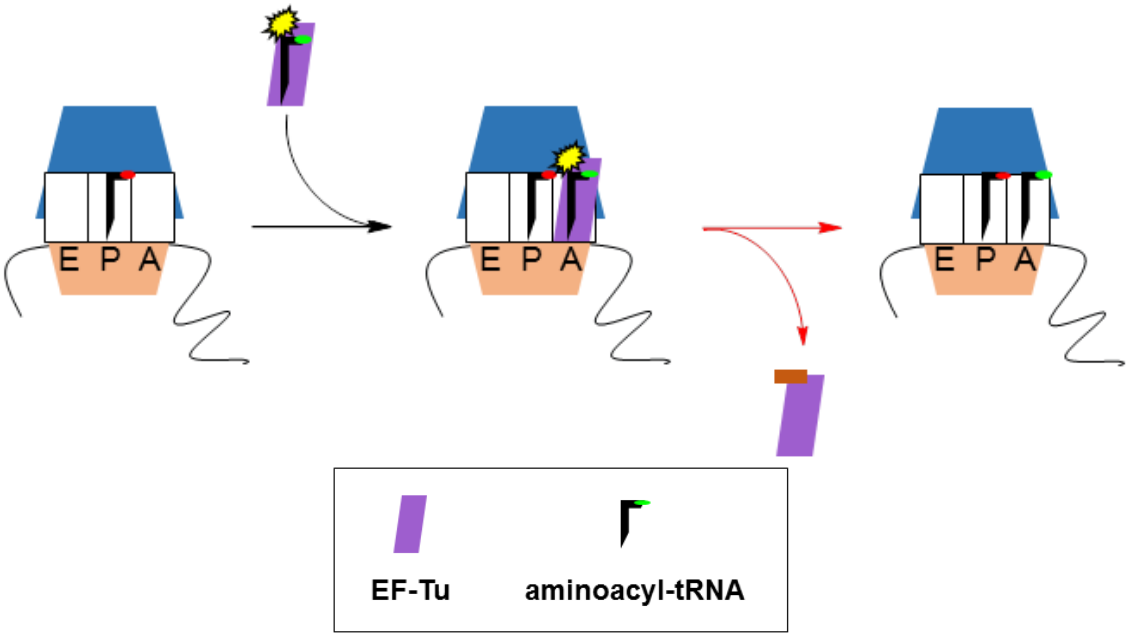

Figure 1-5. Accommodation during elongation. EF-Tu brings the correct aa-tRNA to the 70S ribosome as dictated by the mRNA. GTP hydrolysis correctly places and orients the aa-tRNA in the A site.

Peptidyl transfer

Once the aa-tRNA mentioned previously is bound to the 70S complex, the amino acid on the aa-tRNA must be attached to the elongating peptide chain. (Figure 1-6; Nissan et al., 2000; Ban et al., 2000). In order to accomplish this, the 70S complex must have the proper orientation between the A site aa-tRNA and the P site peptidyl-tRNA (Barta et al., 2001). First, the A site aa-tRNA must reorient itself to place the amino acid in a position favorable for peptide bond formation. The creation of this peptide bond is catalyzed by the 23S rRNA present in the 50S subunit through a mechanism that is not yet entirely understood (Nissen et al., 2000; Schmeing et al., 2005; Leung, et al., 2011). Briefly, nucleophilic attack by the α-amino group present on the A site aa-tRNA on the riboester bond of the peptidyl-tRNA in the P site links the A site aa-tRNA to the elongating peptide, while deacylating the tRNA in the P site, ultimately adding one amino acid to the peptide chain through the transfer of that chain to the A site. Despite over 50 years of research on ribosomes, there is still no consensus on the mechanism by which the aa-tRNA adds its amino acid to the elongating peptide, and it remains a fervently debated topic. One of the more intriguing and recent mechanisms suggests an active role for the tRNA as a catalyst, acting as a shuttle for protons between the α-amino group and the 3'-hydroxyl end of the peptidyl-tRNA (Frank et al., 2005).

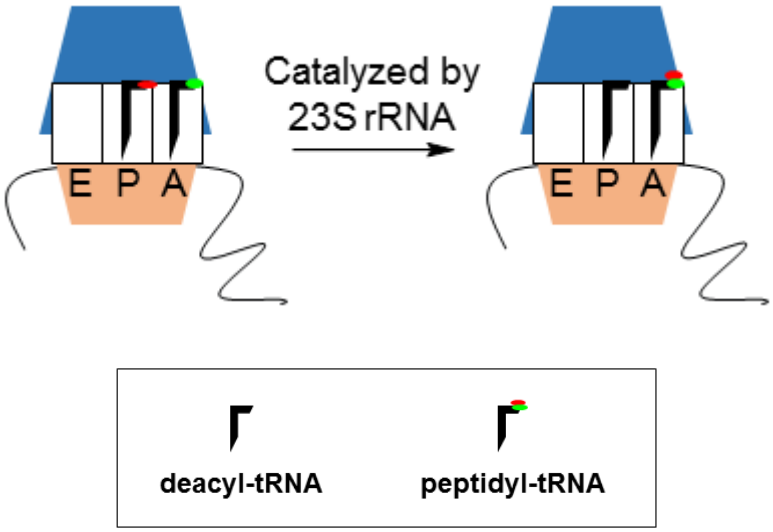

Figure 1-6. Peptidyl transfer step in elongation. First the aa-tRNA undergoes a conformational change to better position itself for peptidyl transfer. Next, transfer of elongating protein from the A site is transferred to the P site via catalysis by the 23S rRNA.

Translocation

In order to continue translation, the deacyl-tRNA in the P site must be transferred to the E site to allow exit from the ribosome, and the peptidyl-tRNA in the A site must be shifted to the P site through *translocation*. This process effectively frees the A site for the entrance of another aa-tRNA (Figure 1-7). Translocation, as it is known, is the precise and coordinated movement of mRNA and tRNA through the 70S complex so as to maintain the proper reading frame of the mRNA and place the peptidyl-tRNA in the correct orientation for another cycle of amino acid addition (Figure 1-7). Elongation factor G (EF-G), another GTPase, catalyzes the movement of both molecules through the ribosome (Zaviolov et al., 2005a; Zhou et al., 2014). EF-G binds GTP, forcing a conformational change allowing it to

associate with the 70S ribosomal complex in the pre-translocational state. Subsequent hydrolysis of the GTP to GDP provides the appropriate movement of both these molecules through the ribosome into the post-translocational state (Agrawal et al., 1999; Spiegel et al., 2007). As EF-G dissociates, another EF-Tu molecule with GTP bound inserts the next required amino acid into the A site, allowing another round of elongation to begin.

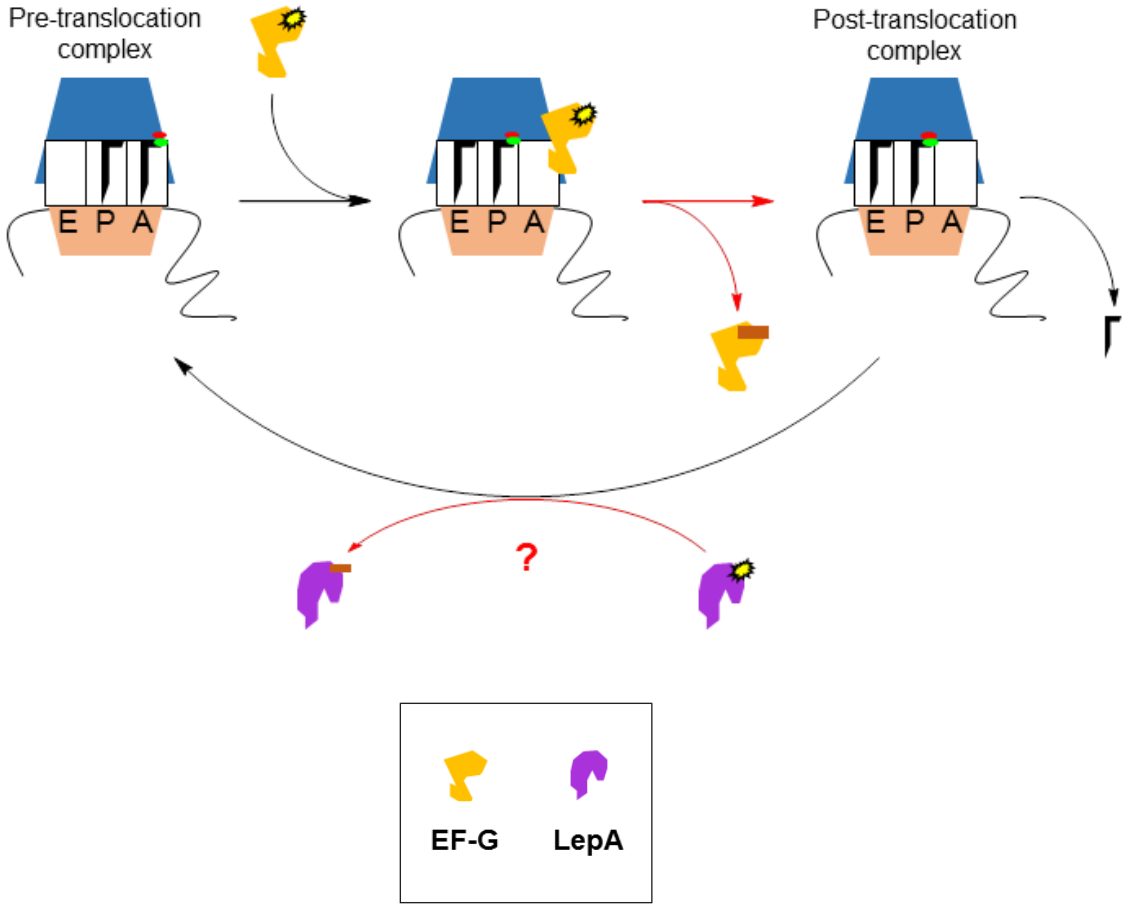

Figure 1-7. Translocation. EF-G catalyzes the transition from the pre- to the post-translocation complex, while LepA may catalyze the reverse reaction.

Leader Peptidase A

While elongation proceeds with very high fidelity, mistakes are occasionally made. Until recently, it was thought that the bacterial ribosome had no way of recovering from certain types of translation errors, but recent reports on leader peptidase A (LepA, also known as elongation factor 4, EF4) have raised questions concerning this. Several studies have suggested that LepA contains the unique ability to catalyze back-translocation, returning the ribosome to a pre-translocation state, and not allowing the mRNA or tRNA to advance, though this topic is still highly controversial (Figure 1-7; March and Inouye, 1985; Youngman and Green, 2007). This protein has been found to be highly conserved across prokaryotes, and is even present in the mitochondria found in eukaryotes (explained in further detail in Chapter 2, Figure 2-4; Evans et al., 2008). LepA has very strong structural homology with EF-G, differing only in the absence of domain IV and subdomain G', and the presence of a unique C-terminal domain (Evans et al., 2008). Despite the similarities, the overall function of LepA in vivo is still unknown. Many experts postulate that it has a role in slowing down elongation, thereby limiting the number of mistakes made. Others suggest it supports complete translocation in the presence of high cellular stress environments, such as high or low pH, high salt, or extreme temperatures (Qin et al., 2006; Pech et al., 2010). Several recent reports provided strong evidence that LepA may not catalyze back translocation at all, but rather influence translation initiation, altering the average ribosome density surrounding several

key coding regions of the prokaryotic genome to increase the translation of genes in those areas (Balakrishnan et al., 2014). The one thing that is agreed upon is that LepA unquestionably requires further investigation.

Termination

Much like the start codon signals to the ribosome that translation should commence, a stop codon communicates when to halt the addition of amino acids. To indicate termination, prokaryotes utilize three release factors (RF1, RF2, and RF3) (Figure 1-8). RF1 and RF2 are considered class I peptide release factors, and they serve to identify the three distinct versions of the prokaryotic stop codon (RF1 recognizes UAA and UAG, while RF2 recognizes UAA and UGA) (Brown and Tate, 1994; Kisselev et al., 2003; Petropoulos et al., 2014). Upon binding to the A site, RF1 or 2 (RF1/2) trigger the hydrolysis and dissociation of the newly synthesized polypeptide chain (Mora et al., 2003; Petry et al., 2005; Rawat et al., 2006). RF3, a class II peptide release factor and GTPase, associates to the 70S ribosome in the A site while bound to GDP, and as GDP is replaced with GTP, a conformational change dissociates RF1/2 from the 70S ribosome (Kong et al., 2004; Gao et al., 2007; Zaher and Green, 2011; Zhou et al., 2012b)). Hydrolysis of the GTP to GDP allows RF3 to dissociate act on another ribosome (Zavialov et al., 2002).

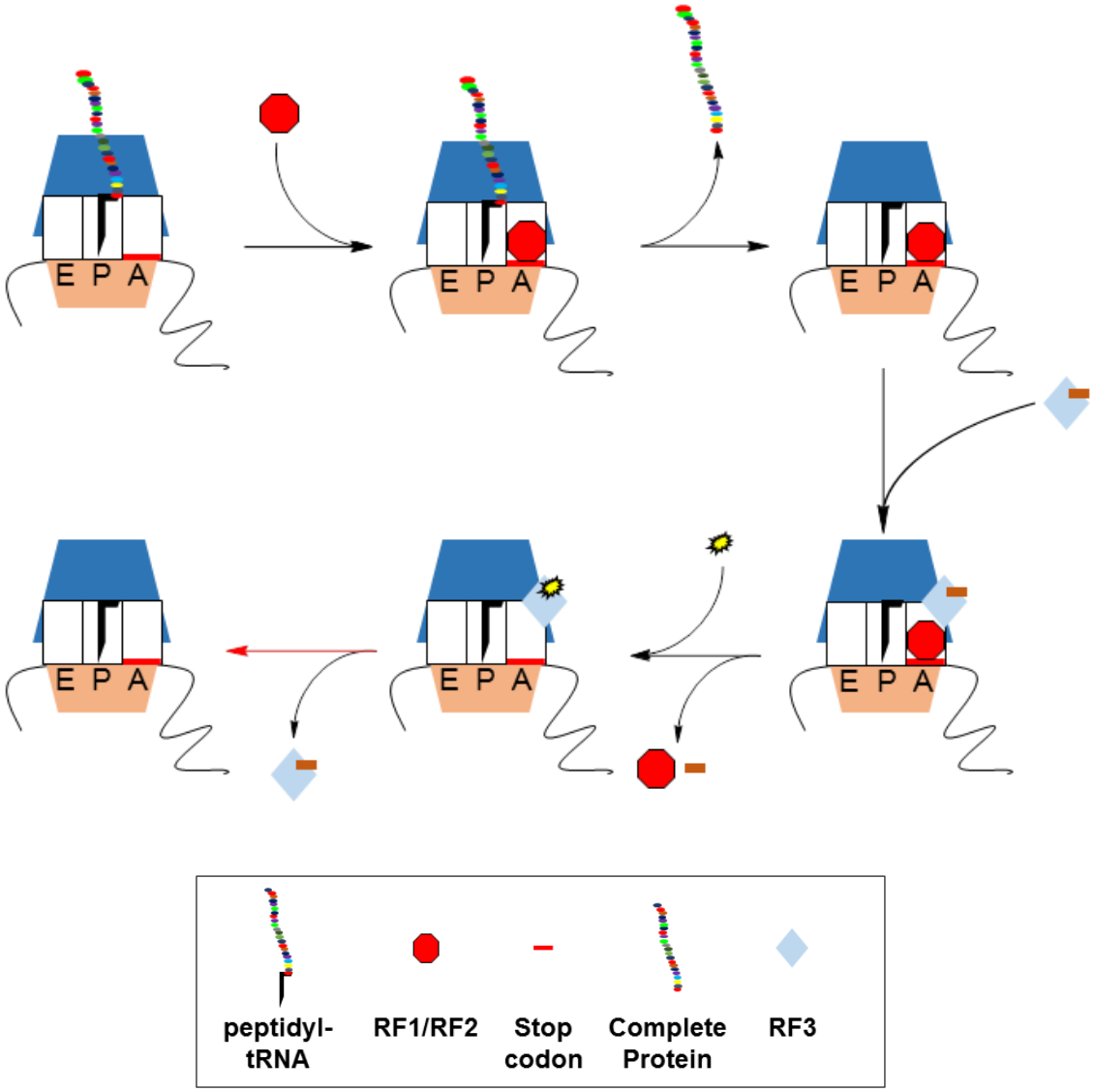

Figure 1-8. Termination of protein elongation. RF1 or RF2 recognizes and binds to the stop codon in the A site, causing hydrolysis of the elongating peptide. Binding of RF3·GDP dissociates the class 1 release factor, followed by exchange of GDP with GTP. Subsequent GTP hydrolysis causes dissociation of RF3·GDP from the ribosome.

Recycling

Following termination, the ribosome is left with deacyl-tRNA in the P site, and the mRNA stop codon in the A site (Figure 1-9). In order to dissociate this complex, a series of events occurs involving EF-G, IF3, and a protein mimic of tRNA dubbed ribosome recycling factor (RRF) (Hirashima and Kaji, 1972; Zavialov et al., 2005b). The discrete mechanism of ribosome recycling has yet to be fully described, though the most recent evidence suggests that EF-G and RRF bind first, followed by dissociation of the 50S and 30S subunits from one another (Peske et al., 2005). Crystal structures of RRF bound to the 50S subunit suggest that RRF causes considerable conformational changes, though when RRF is bound to the 70S complex these appear to be much less dramatic (Wilson et al., 2005; Weixlbaumer et al., 2007). It has been theorized that the binding of EF-G to the 70S-RRF complex causes RRF to undergo further conformational changes, similar to what is seen in the RRF-50S complex mentioned above (Wilson et al., 2005). Crystallographic data also suggests RRF, despite its structural and spatial similarities to tRNA, binds in a significantly different manner to the ribosome (Agrawal et al., 2004). After dissociation of the subunits, IF3 binds to the 30S subunit, causing another conformational change and allowing the deacyl-tRNA and the mRNA strand to dissociate. This leaves the individual subunits in the same state they were during the initiation step, ready to begin another round of translation (Figure 1-9; Hirokawa et al., 2005; Dever and Green,

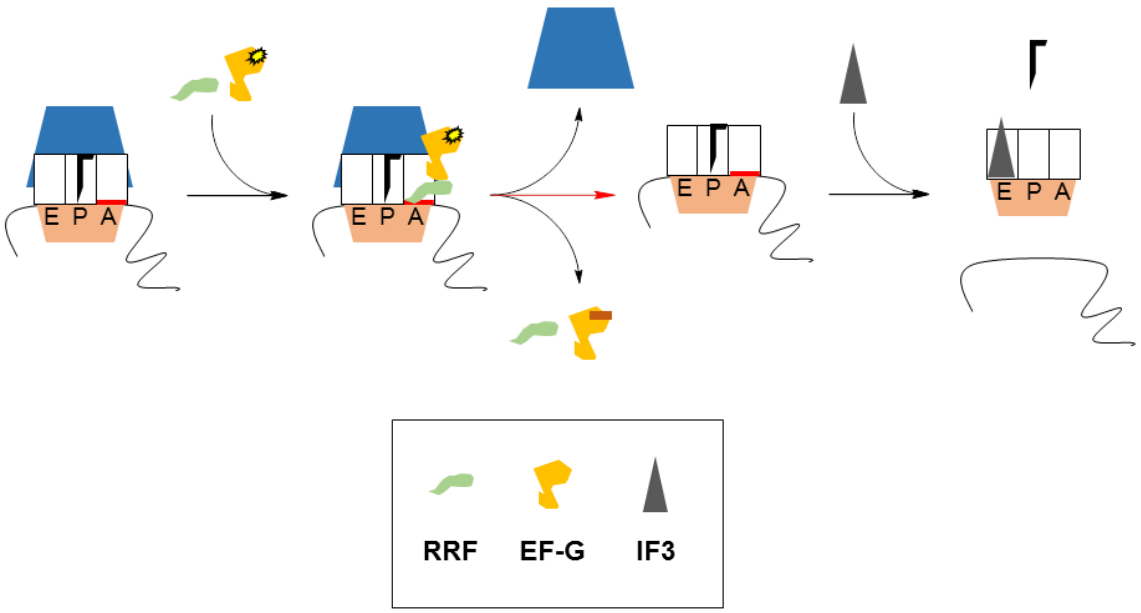

Figure 1-9. Recycling of ribosomes. After peptide dissociation, EF-G and RRF bind to the 70S complex. Upon hydrolysis of GTP, EF-G and RRF leave which enables the 50S subunit to dissociate. IF3 then associates to the 30S subunit, allowing the mRNA and deacyl-tRNA to leave, and completing a round of translation.

2012). Bound IF3 serves and an anti-association factor, preventing erroneous association of the 30S and 50S subunits prior to the next round of translation.

Ribosomal Protein L7/L12

Ribosomal protein L7/L12 is a 12 kDa protein located on the outside of the 50S ribosomal subunit (Figure 1-10). L7 and L12 are the same protein, excepting a methylated N-terminus on L7, and will therefore be collectively referred to as L12 hereafter. L12 is unique for several reasons. It is the only protein present in multiple copies in a ribosome and it is also the only protein that does not directly

interact with any rRNA, but instead binds to the protruding C-terminal domain (CTD) of L10, which in turn binds to the rRNA present in the GTPase associated center (discussed below, Figure 2-7; Diaconu et al., 2005). This binding of L12 to L10, and their interactions with L11 compose what is known as the 50S stalk region of the ribosome (Figure 1-11). Structurally, L12 contains an N-terminal domain (NTD) and a CTD that are connected via a dynamic hinge region (Figure 1-10; Liljas and Gudkov, 1987). The NTD allows for the dimerization of L12, while the role of the CTD is still not entirely clear, likely due to its highly dynamic nature (Diaconu et al., 2005). In fact, the CTD of L12 is usually poorly resolved or entirely absent in crystal structures of the 70S ribosome. The exact role of the entire L12 protein in translation has also remained elusive, despite over 15 years of study. Several recent studies have concluded that it aids the ribosome in factor binding, GTPase activity, and P_i release, though no clear consensus has been reached on the mechanisms of these roles. There is strong evidence to support the role of L12 in GTPase recognition as well as factor exchange (Uchiumi et al., 2002; Savelsbergh et al., 2005; Helgstrand et al, 2007).

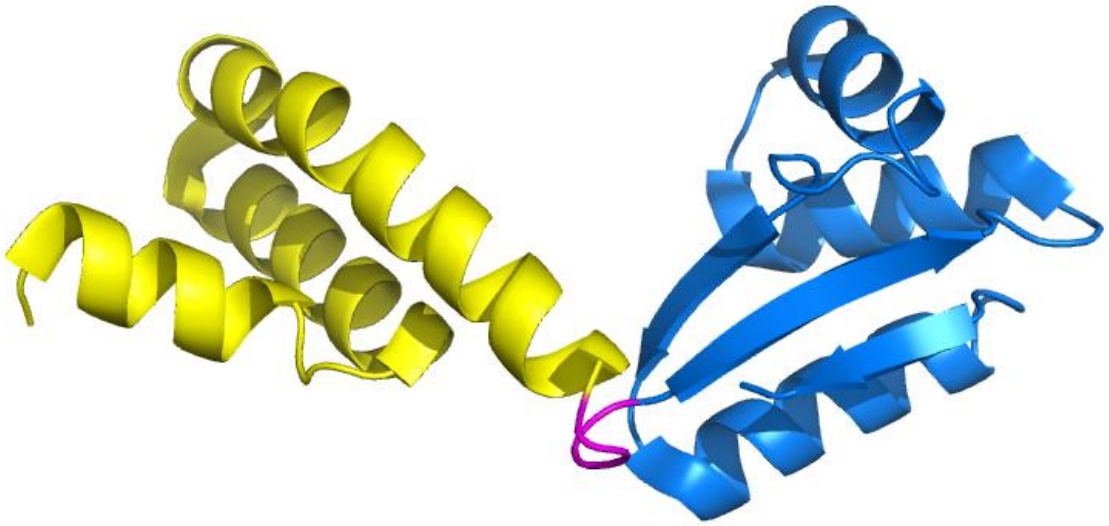

Figure 1-10. Crystal structure of L12 from *Thermotoga maritime* (PDBid 1DD4). The NTD (yellow) and the CTD (blue) are connected by a flexible hinge region (pink).

Several studies over the past decade have shown that L12 makes direct contact with a portion of the G-domain, labeled the G' domain, of EF-G. Interestingly, this G' domain present in EF-G is absent in most of the other GTPase translation factors (discussed below), suggesting this is a novel interaction that merits further study (Savelsbergh et al., 2005; Gao et al., 2009). Initial reports on the importance of L12 show conflicting results, some asserting that the removal of L12 has little to no influence on GTP hydrolysis, whereas others show a near complete abrogation of GTPase activity upon L12 removal (Diaconu et al., 2005; Nechifor et al., 2007; Mikolajka, et al., 2011). The interaction between the NTD of L11, the CTD of L12, and the G' domain form an arc-like connection (ALC), and results in a significant change in conformation (Figure 1-11; Agrawal et al., 1998).

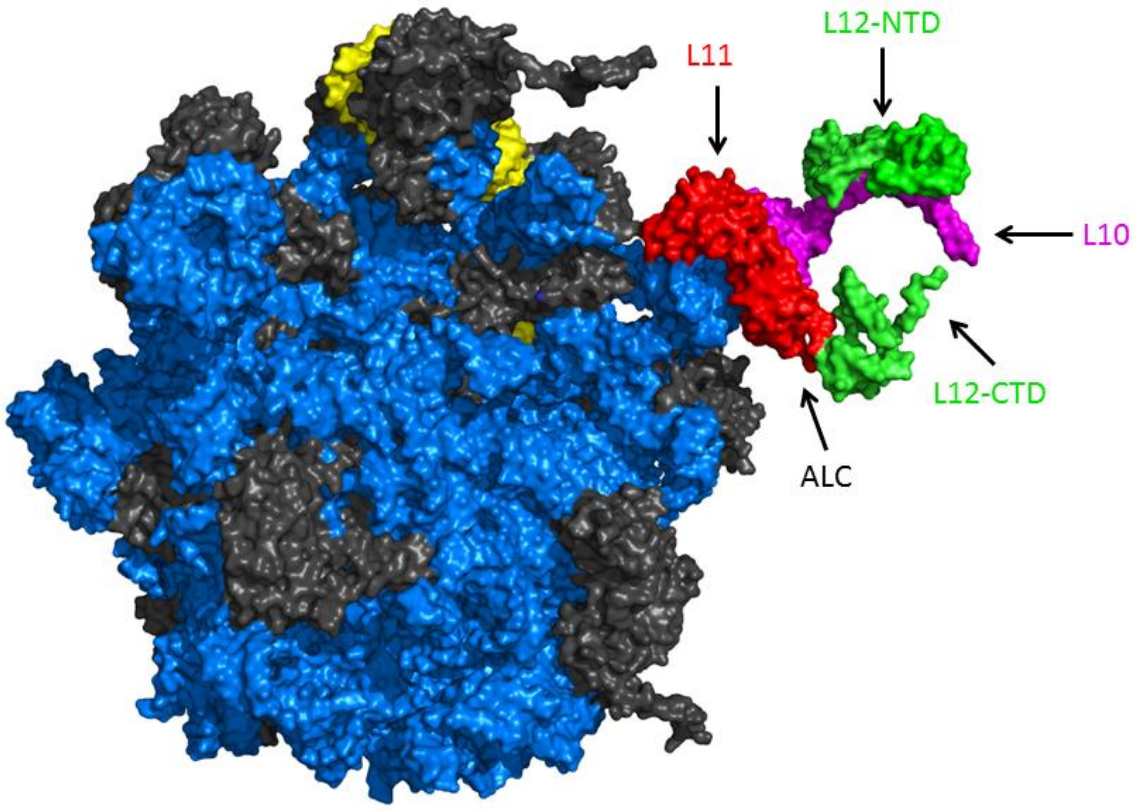

Figure 1-11. Stalk region of the 50S subunit. Visualization of L10 - magenta, L11 - red, and L12 – green ribosomal proteins attached to the 50S ribosomal subunit of *Thermus thermophilus* (PDBid 2WRJ). Arc-like connection (ALC) is the junction between the NTD of L11 and the CTD of L12 along with the G' domain of EF-G (full ALC crystal structure not available).

While much is known about the structure and function of ribosomes, still more has yet to be discovered. The role of L12 in initiation, elongation, termination, and recycling needs to be researched further, and as recent reports have shown interactions between this protein and several of the GTPase translation factors, this presents exciting possibilities. Previous reports from the Spiegel lab indicate that incomplete removal of L12 results in a substantially lower GTP hydrolysis compared to endogenous ribosomes. Recent development of a protocol to allow

for complete removal of L12 will allow for better characterization of its role in GTPase activation and binding (discussed below, Chapter 2).

Chapter 2: GTPases

Though it was necessary to mention some structural and functional information concerning translational GTPases in the previous ribosome chapter, this chapter is dedicated to comparing the similarities and differences of the G-domain containing translation factors: IF2, EF-G, RF3, and LepA. The majority of research presented herein is concerned with these translation factors and their interactions with the 70S ribosome and ribosomal protein L12.

GTPases and the GTPase superfamily

Of all the translation factors mentioned above, several belong to a class of molecules known as GTPases. As already described, these proteins have the ability to bind GTP, and hydrolyze the phosphate bond between the β and γ phosphates, forming GDP and a molecule of inorganic phosphate, PO_4^{3-} (P_i) (Figure 2-1A; Scheffzek and Ahmadian, 2005). The hydrolysis of this bond provides enough energy to the molecule to perform its intended function. In the case of translational GTPases this is often the regulation of ribosomal translation. GTP analogs, such as guanosine 5'-[β,γ-imido]triphosphate (GDPNP), have the ability to lock GTPases into their GTP bound form (Figure 2-1B). Replacement of the oxygen between the β and γ phosphates with a nitrogen atom prevents GTPases from hydrolyzing the bond, thereby forcing them into maintaining their "GTP bound states."

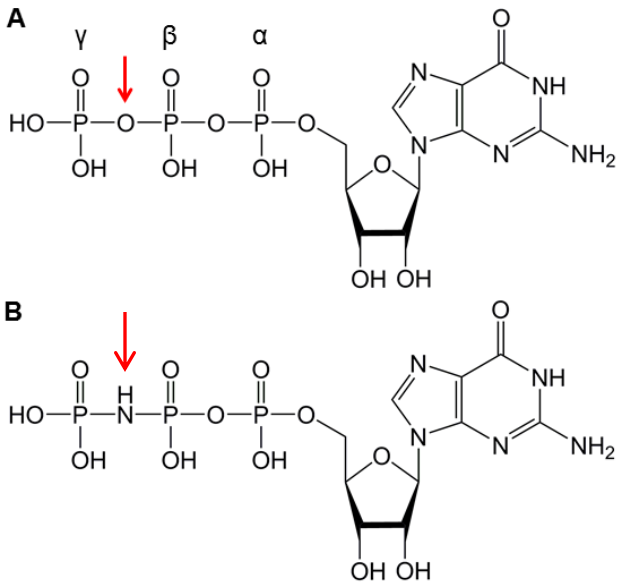

Figure 2-1. Structures of GTP and GDPNP. **(A)** Guanosine triphosphate (GTP) with the alpha, beta, and gamma phosphates labeled. Hydrolysis of the bond(↓) between the β and γ phosphates forms guanosine diphosphate (GDP). **(B)** Guanosine 5'-[β,γ-imido]triphosphate (GDPNP), a GTP analog with a nitrogen atom in place of the oxygen seen in GTP, rendering it non-hydrolysable.

The GTPase superfamily is universally conserved across all domains of life, and though there are some very similar prokaryotic and eukaryotic GTPases (e.g. elongation factor G and eukaryotic elongation factor 2, Figure 2-2), there are often significant structural differences between them (Scheffzek and Ahmadian, 2005). GTPases are also implicated in a wide variety of functions, ranging from the Ras subfamily of signal transduction molecules to the signal recognition particle (SRP) involved in transport of proteins across membranes (Wilkie, 1999). Some translational GTPases, like the aforementioned RF3, only associate with other proteins when bound to GDP, and GTP hydrolysis is the cause of

dissociation from the ribosome (Gao et al., 2007). In contrast, IF2 and EF-G are only able to bind to the ribosome in the presence of GTP, with the GDP bound state having little to no affinity for 70S ribosomes. In these cases GTP or GDP act as switches, activating or deactivating the GTPases. In this manner GTPases are able to exert their functions through conformational change caused by GTP binding and hydrolysis (Rodina et al., 1997).

All members of the GTPase family contain a highly conserved G-domain, the site where GTP or GDP bind to the molecule. In translation, IF2, EF-G, RF3, and LepA all contain this domain, and all bind to similar locations on 50S ribosomal subunit, suggesting comparable interactions with the ribosome (Moazed et al., 1988). The G-domain contains five consensus regions (G1-G5), areas that occur across a broad range of organisms and serve to properly orient the GTP or GDP into the binding pocket (Saraste et al., 1990). The G1, G2, and G3 sequences have been shown to recognize and interact with the β and γ phosphates of GTP, whereas the G4 and G5 sequences are selective for guanine based nucleosides, rather than the adenosine, uridine, and cytidine triphosphates often associated with kinases (Vetter and Wittinghofer, 2001).

Homology of translational GTPases

The translational GTPases show remarkable similarities to one another, even across species. Bacterial EF-G mentioned above is very structurally similar to eukaryotic elongation factor 2 (eEF-2) (Figure 2-2), whereas EF-Tu is

orthologous to eEF-1, providing another striking example of just how highly conserved the process of translation is. Within prokaryotes the GTPases involved in the different stages of translation also show homology among themselves (Figure 2-3). EF-G, IF2, and EF-Tu (when bound to tRNA) are all structurally similar to one another (Qin et al., 2006). RF3 and LepA also show a strong structural resemblance. This homology is unsurprising when we consider that these GTPases must all bind to similar regions of the ribosome, as they all contain a large highly conserved G domain. In fact, a comparison of domains present in three translational GTPases clearly reveals the marked homologies (Figure 2-4). EF-G, LepA, and RF3 all contain homologous I and II domains. LepA and EF-G also share III and V domains, while RF3 and EF-G both include a G' subdomain within domain I. Each of these three proteins only includes one domain not found in another translational GTPase.

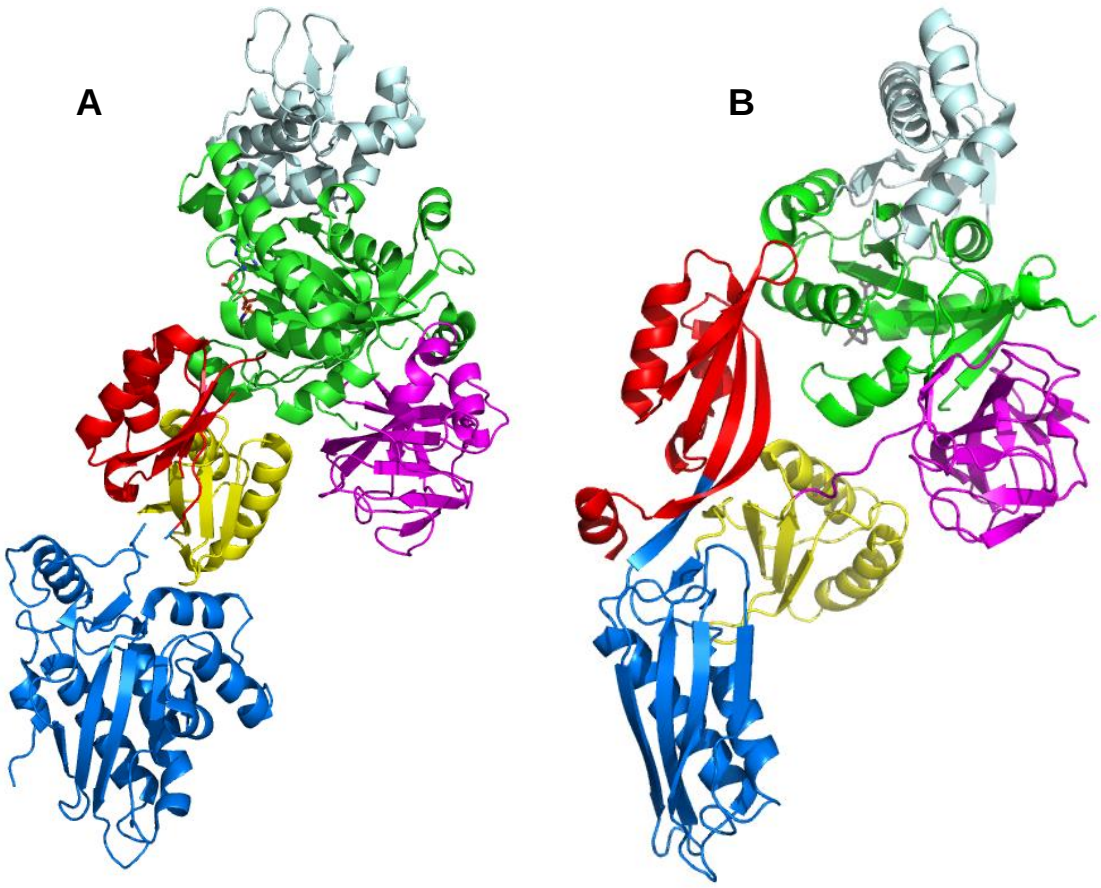

Figure 2-2. Structural comparison of eEF2 and EF-G. **(A)** eEF2 from *Saccramoneas cervesiae* (PDBid 2P8W) and **(B)** EF-G from *Thermus thermophilus* (PDBid 4M1K). Domains are color coded as follows: G – green, G' – pale blue, II – magenta, III – yellow, IV – dark blue, V – red. Both molecules are bound to GDP, appearing in grey.

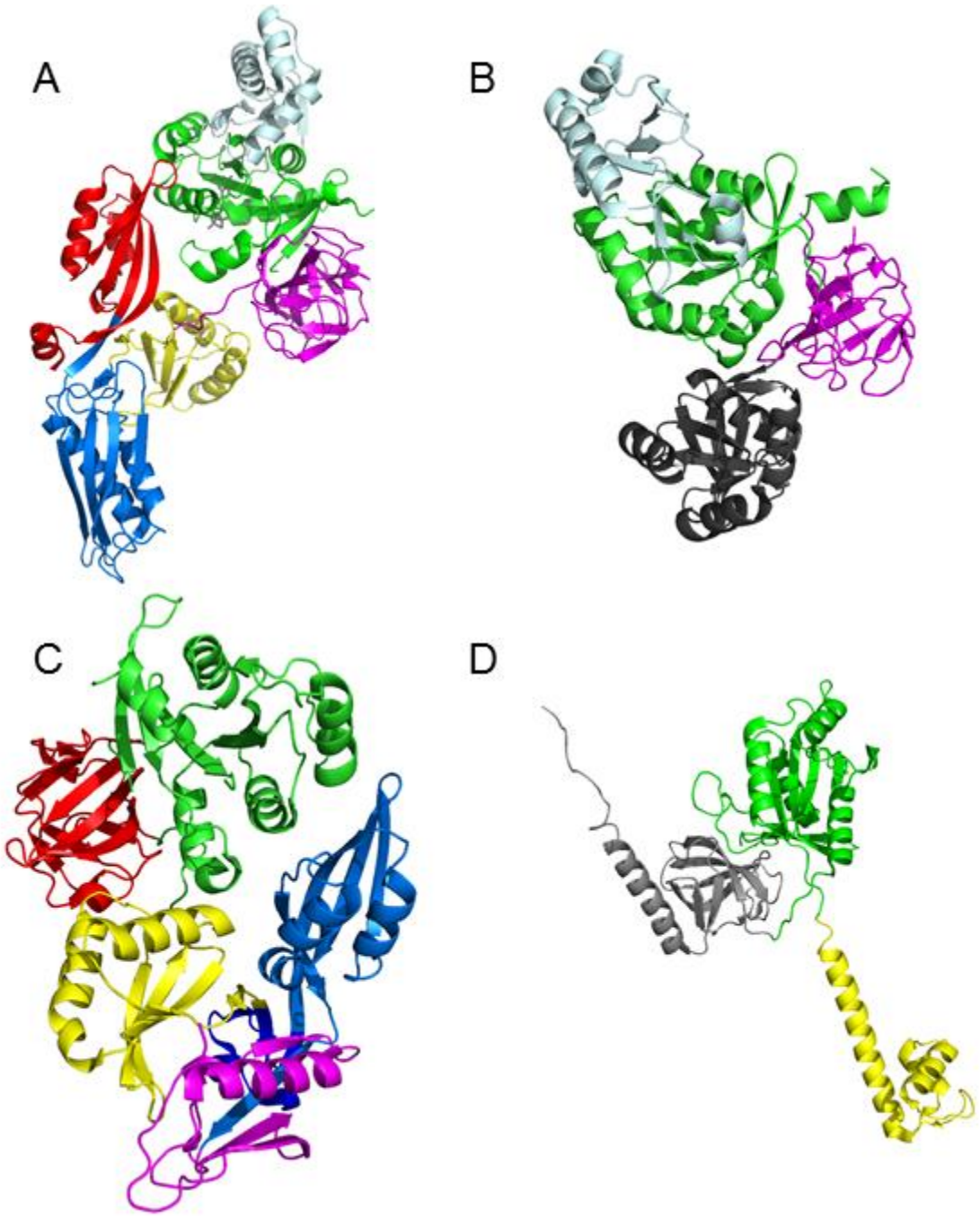

Figure 2-3. Prokaryotic translational GTPases. **(A)** EF-G bound to GDP (PDBid 4M1K), **(B)** RF3 bound to GDP (PDBid 2H5E, **(C)** LepA (PDBid 3CB4) **(D)** Initiation Factor 2 (PDBid 4B3X). Domains depicted in green indicate GTP hydrolysis activity. Domains of the same color share significant homology.

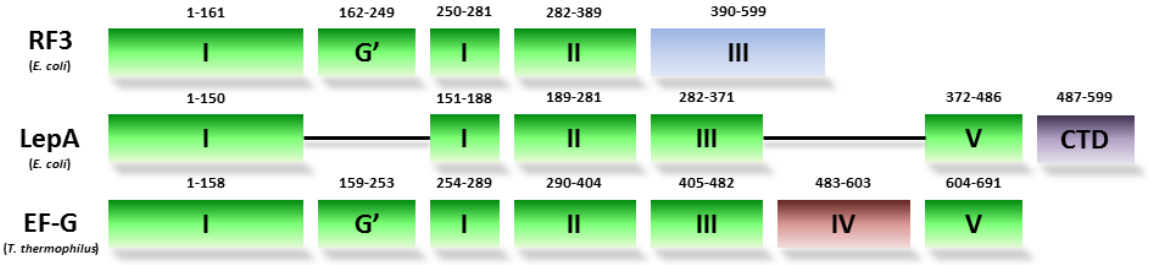

Figure 2-4. Domain alignment of RF3, LepA, and EF-G. Structurally homologous domains – green, domains unique to RF3, LepA, and EF-G – blue, purple, and red, respectively.

Translational GTPase activation

The ability of GTPases to hydrolyze GTP in solution is typically very low or nonexistent, and significant GTP hydrolysis only occurs in the presence of activators. A single activator for translational GTPases has remained elusive to this day, though not for a lack of effort to elucidate it (Rodnina et al., 1997; Mohr et al., 2002).

It has been proposed that interaction of translational GTPases with rRNA or some of the large subunit proteins causes a conformational shift in the GTPase towards a state more favorable for GTP hydrolysis (Berchtold et al., 1993). The areas of common interaction between EF-G, LepA, RF3, and IF2 are few, comprised of the L10, L11, and L12 ribosomal proteins as well as the sarcin-ricin loop (SRL) and the GTPase associated center (GAC), both part of the 23S rRNA (SRL and GAC discussed below). Since these GTPases have such strong homologies, it is likely that the mechanism surrounding their activation is similar.

Previous work in the Spiegel lab has shown that L10, L11, and L12, along with structural mimics of several portions of rRNA thought to have some interactions with translational GTPases are unable to cause a significant increase in GTP hydrolysis individually or in conjunction with one another without the presence of complete ribosomes (unpublished data in the Spiegel lab). Further investigations into the method of translational GTPase activation are necessary, and L12 is at the forefront of the target molecules, due to its direct interactions with portions of the G-domain of several translational GTPases.

Elongation Factor G

As mentioned earlier, EF-G catalyzes the translocation of the 70S ribosome from the ‘pre’ to the ‘post’ state through the hydrolysis of GTP to GDP, and has an ambiguous function in the recycling of ribosomes. Despite being, arguably, the most well characterized prokaryotic translational GTPase, the overall contribution of each domain to translocation and ribosome recycling has not been entirely determined. As shown in Figure 2-4, EF-G contains five distinct domains (I-V) and one subdomain (G’).

Domain I is the G domain where GTP binds and is hydrolyzed (Figure 2-5). Contained within domain I is a 90 residue G’ domain, not typically found in other GTPases. This small domain has direct interactions with the CTD of the L12 ribosomal protein, and these contacts are theorized to participate in the stabilization of the pre-translocation complex (Figure 2-6; Valle et al., 2003). In

fact, the only other GTPase known to stabilize this hybrid state, RF3, has a very similar G' domain (Figure 2-4; Jin et al., 2011; Zhou et al., 2012a).

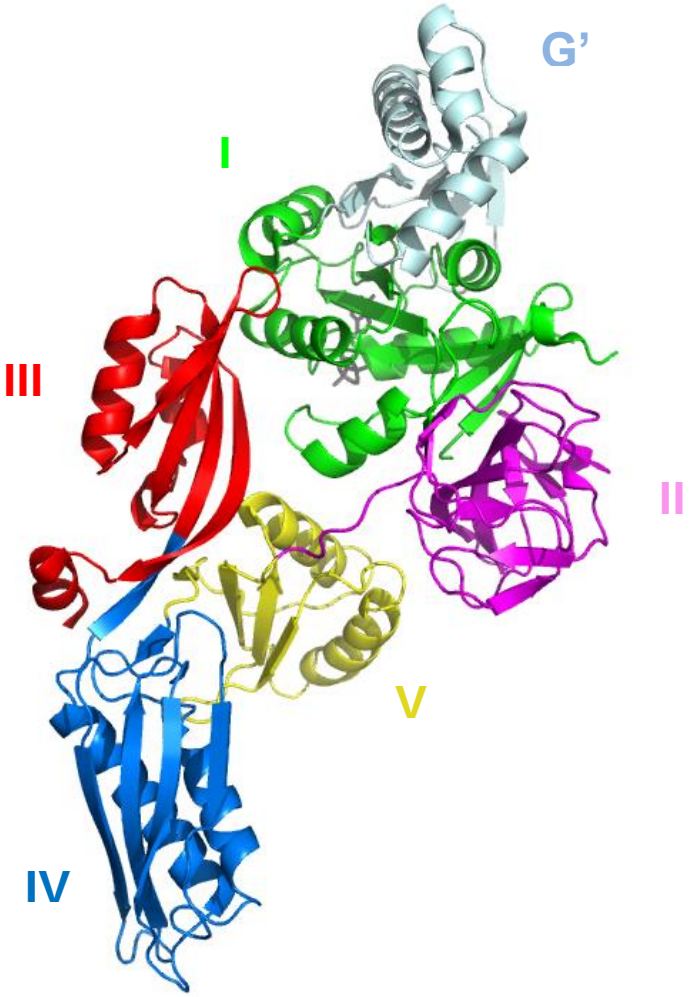

Figure 2-5. Structure of EF-G from *T. thermophilus* (PDBid 4M1K). Domains labeled and color coded for identification.

Domains II and III display a strong structural resemblance to EF-Tu (Figure 2-5). In EF-G, these domains have been shown to make key contacts with the 16S rRNA in the 30S subunit (Pulk and Cate, 2013). Interestingly, the bacteriostatic antibiotic fusidic acid binds to the interface between domains I, II, and III, preventing the release of the hydrolyzed inorganic phosphate and therefore impeding proper translocation, ultimately leading to a significant decrease in cell fitness (Laurberg et al., 2000; Gao et al., 2009; Guo et al., 2012).

Domain IV is implicated in proper tRNA translocation. Structurally, it protrudes from the body of the enzyme, connected through domains III and V (Figure 2-5). Replacement of a single residue, histidine 583, with either lysine or arginine was shown to decrease the rate of translocation by more than 100-fold, while GTP hydrolysis and EF-G binding remained uninhibited (Martemyanov and Gudkov, 1999; Savelsbergh et al., 2000a; Salsi et al., 2014).

Domain V is believed to be of high importance in communicating structural information between domains I and IV (Savelsbergh et al., 2000a). Structurally, this seems plausible (Figure 2-5). Domain V is situated directly between domains I and IV, and may be able to exert conformational changes in order to influence either of the two domains. Together, domains IV and V interact with a portion of the SRL (discussed below) and mutants with deletions of these two domains have been proven to not interact with the 23S rRNA at all, and consequently stay attached to the ribosome following GTP hydrolysis (Savelsbergh et al., 2000b).

Though the role of EF-G in translation is firmly established, the exact mechanism of its interactions with the GTPase associated center, and specifically L12, has yet to be fully characterized. As stated earlier, some reports show the loss of L12 has minimal effect on GTP hydrolysis, others show a significant decline upon removal of L12 (Savelsberg et al., 2005; Mikolajka, et al., 2011; Walter et al., 2011). Likewise, some reports even demonstrate GTPase activity in the presence of L12 alone, though the Spiegel lab has been unable to replicate this result (Savelsbergh et al., 2000b).

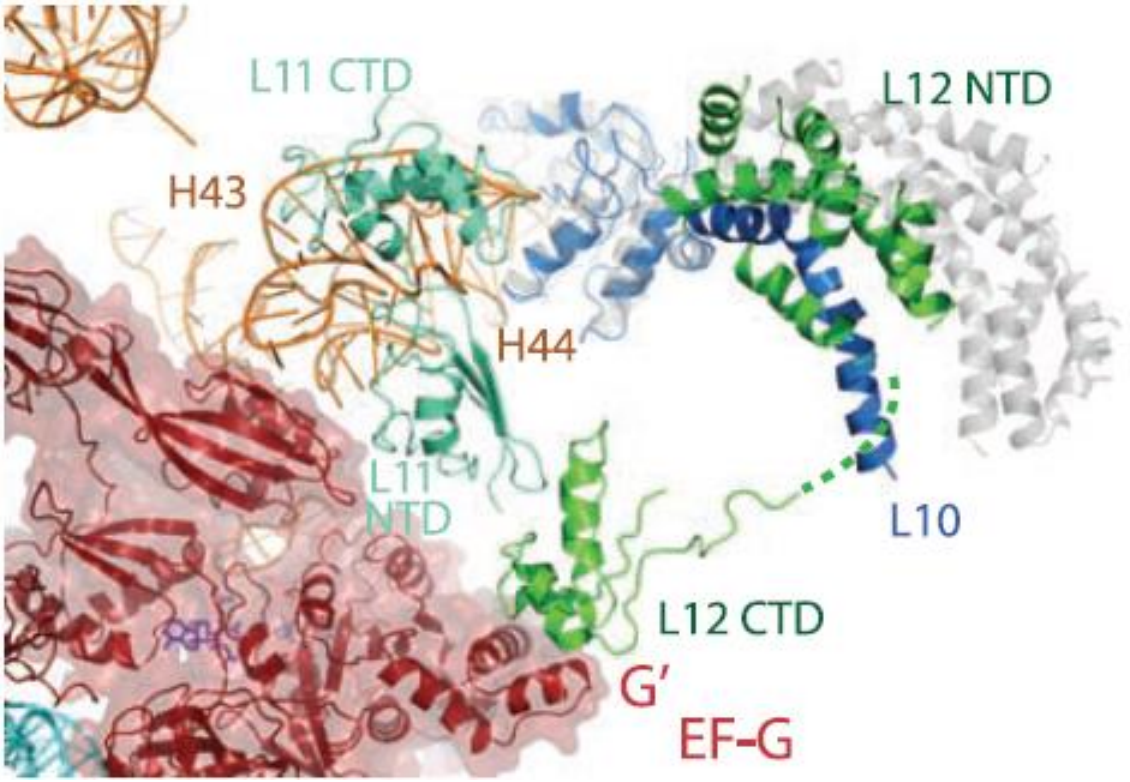

Figure 2-6. L12 interaction with the G' domain of EF-G. The L10-L12 stalk region (green and blue, top right) bends toward the L11 region (cyan) when bound to EF-G, relative to the translation factor free ribosome (gray), causing the CTD of L12 and the NTD of L11 to form interactions with the G' domain of EF-G. From Gao et al., 2009. Reprinted with permission from AAAS.

GTPase-70S binding regions

Over the course of the last 30 years the interactions between translational GTPases and the prokaryotic 70S ribosome have been intensely examined. This work has identified transient interactions between the 23S rRNA present in the 50S subunit and the G-domain of each GTPase (Moazed et al., 1988). GTPases seem to have an affinity for two portions of the rRNA: the sarcin-ricin loop (SRL),

and the GTPase-associated center (GAC), the latter of which also involves certain ribosomal proteins.

Sarcin-ricin loop

The SRL region of the 23S rRNA is where the antifungal compound sarcin and the N-glycosidase, ricin both act (Gutell et al., 1993). Though this highly conserved 12 residue region has been proven to be critical to ribosome function, its specific mechanism in translation has yet to be established. It is known, however, that the SRL makes a large number of contacts across several key areas of the 50S subunit, suggesting a possible role in factor binding through conformational change. Indeed, recent studies have shown that the SRL is not crucial for GTP hydrolysis by EF-Tu or EF-G, or for the formation of new peptide bonds to occur, but rather has a major role in maintaining EF-G within the ribosome during translocation of the mRNA and tRNA (Shi et al., 2012).

GTPase associated center

The GAC, like the SRL, is comprised of a portion of highly conserved 23S rRNA, but also involves three ribosomal proteins: L10, L11, and L12 (Figure 2-7; Diaconu et al., 2005). In most bacteria, four copies of L12 (two homodimers) attach their NTD to the C-terminal domain (CTD) of one copy of L10, forming $L10(L12)_4$ (Thermostable bacteria attach six copies of L12). This pentamer, alongside L11, binds to the 23S rRNA (Agrawal et al., 2001). The entire complex, called the ribosomal stalk, is a highly dynamic extrusion from the relatively

spherical ribosome. As the L12 protein is so prevalent and dynamic, there has been much effort recently to discover its role in translation. The interaction of translation factors with L12 has yet to be fully characterized. As mentioned above, there are known interactions between it and the G' domain of EF- G, yet little effort has been placed into determining how they influence each step of translation.

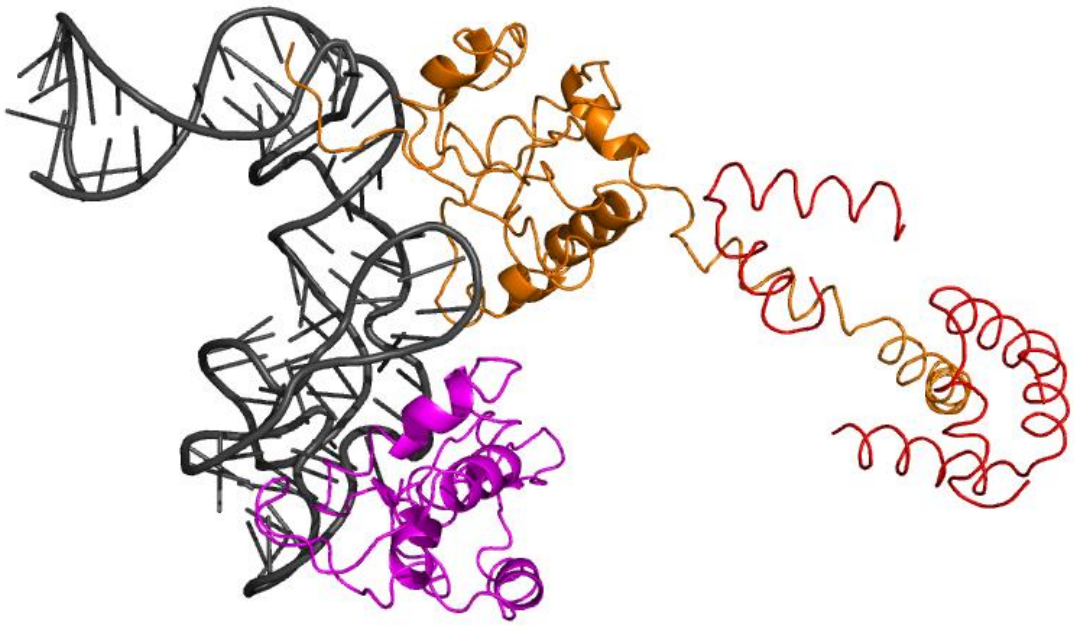

Figure 2-7. 23S rRNA interactions in the GAC. The 23S rRNA (black) has direct interactions with L10 (orange) and L11 (magenta) proteins. Only the NTD of L12 (red) was determined in this crystal structure (PDBid 2WRJ).

Project Goals

The aims of this research were threefold. First, we set out to characterize the role of L12 in ribosome-dependent GTPase activity. Through a recently developed two step L12 depletion protocol, we were able to ensure complete removal of the L12 protein from 70S ribosomes. Through a malachite green based inorganic phosphate detection assay we were able to accurately determine the GTP hydrolysis activity of translational GTPases in the presence of 70S or 70SΔL12 ribosomes. Additionally, we wanted to determine if any activity lost through the removal of L12 could be regained through the addition of independently purified L12.

Once the role of L12 in GTPase activity was established, our second aim was to determine if L12 was required for binding of translational GTPases to 70S ribosomes. A simple GTPase binding assay provided semi-quantitative determination of GTPase-70S binding with and without L12 on the ribosome. Next, BioLayer Interferometry (BLI) quantitatively assessed the binding affinity of EF-G to intact and depleted ribosomes.

The final objective of this work was to ascertain the overall role of the IV, V, and G' domains of EF-G on ribosome-dependent GTPase activity. To accomplish this, we generated and purified several domain deletion mutants of EF-G (EF-GΔG', Δ4, Δ5, and Δ4,5) and examined their GTP hydrolysis activity through the aforementioned inorganic phosphate assay.

Chapter 3 – Materials and Methods

Buffers

BLI Reaction Buffer: 20 mM Tris-HCl (pH7.5), 20mM $MgCl_2$, 30 mM NH_4Cl, 15 mM imidazole, 6 mM β-mercaptoethanol.

GTPase Lysis Buffer: 50 mM Tris-HCl (pH 7.5), 60 mM NH_4Cl, 7 mM $MgCl_2$, 15 mM imidazole, 25% (v/v) glycerol, 6 mM β-mercaptoethanol.

GTPase Wash Buffer: 50 mM Tris-HCl (pH 7.5), 50 mM KCl, 60 mM NH_4Cl, 7 mM $MgCl_2$, 15 mM imidazole, 25% glycerol (v/v), 6 mM β-mercaptoethanol.

GTPase Elution Buffer: 50 mM Tris-HCl (pH 7.5), 60 mM NH_4Cl, 7 mM $MgCl_2$, 250 mM imidazole, 25% glycerol (v/v), 6 mM β-mercaptoethanol.

GTPase Storage Buffer: 50 mM Tris-HCl (pH 7.5), 60 mM NH_4Cl, 7 mM $MgCl_2$, 25% glycerol (v/v), 1 mM dithiothreitol.

JE28 Lysis Buffer: 20 mM Tris-HCl (pH 7.5), 10 mM $MgCl_2$, 150 mM KCl, 30 mM NH_4Cl, 5 mM imidazole, 1 mM dithiothreitol.

JE28 Wash Buffer: 20 mM Tris-HCl (pH 7.5), 10 mM $MgCl_2$, 150 mM KCl, 500 mM NH_4Cl, 5 mM imidazole, 1 mM dithiothreitol.

JE28 Salt Wash Buffer: 20 mM Tris-HCl (pH 7.5), 10 mM $MgCl_2$, 150 mM KCl, 500 mM NH_4Cl, 1 mM dithiothreitol.

JE28 Elution Buffer: 20 mM Tris-HCl (pH 7.5), 10 mM $MgCl_2$, 150 mM KCl, 30 mM NH_4Cl, 150 mM imidazole, 1 mM dithiothreitol.

GTPase Reaction Buffer: 90 mM HEPES-K (pH 7.5), 100 mM NH_4Cl, 20 mM $Mg(CH_3COO)_2$.

L12 Extraction Buffer:20 mM Tris-HCl (pH 7.5), 1.0 M NH_4Cl, 20 mM $MgCl_2$, 50 % glycerol (v/v), 5 mM β-mercaptoethanol.

100/10 Buffer: 20 mM Tris-HCl (pH 7.0), 100 mM NH_4Cl, 10.5 mM $MgCl_2$, 0.5 mM ethylenediaminetetraacetic acid (EDTA, pH 8.0), 6 mM β-mercaptoethanol.

500/10 Buffer: 20 mM Tris-HCl (pH 7.0), 500 mM NH_4Cl, 10.5 mM $MgCl_2$, 0.5 mM EDTA (pH 8.0), 6 mM β-mercaptoethanol.

100/6 Buffer: 20 mM Tris-HCl (pH 7.0), 100 mM NH_4Cl, 6 mM $MgCl_2$, 0.5 mM EDTA (pH 8.0), 6 mM β-mercaptoethanol.

100/10 Buffer: 40 mM Tris-HCl (pH 7.0), 100 mM NH_4Cl, 10.5 mM $MgCl_2$, 6 mM β-mercaptoethanol.

1.1 M (37.7%) Sucrose Cushion: 37.7% (w/v) sucrose, 500 mM NH_4Cl, 10.5 mM $MgCl_2$, 0.5 mM EDTA (pH 8.0), 6 mM β-mercaptoethanol.

10% Sucrose Gradient Buffer: 20 mM Tris-HCl (pH 7.0), 100 mM NH_4Cl, 6 mM $MgCl_2$, 6 mM β-mercaptoethanol, 10% (w/v) sucrose.

35% Sucrose Gradient Buffer: 20 mM Tris-HCl (pH 7.0), 100 mM NH_4Cl, 6 mM $MgCl_2$, 6 mM β-mercaptoethanol, 35% (w/v) sucrose.

Purification Buffer: 50 mM Tris-HCl (pH7.5), 60 mM NH_4Cl, 7 mM $MgCl_2$, 0.22 µm filtered.

FPLC Buffer A: 50 mM Tris-HCl (pH7.5), 60 mM NH_4Cl, 7 mM $MgCl_2$, 15% (v/v) glycerol, 6 mM β-mercaptoethanol, 0.22 µm filtered.

FPLC Buffer B: 50 mM Tris-HCl (pH7.5), 60 mM NH_4Cl, 7 mM $MgCl_2$, 1.0 M KCl, 15% (v/v) glycerol, 6 mM β-mercaptoethanol, 0.22 µm filtered.

FPLC Storage Buffer: 50 mM Tris-HCl (pH7.5), 60 mM NH_4Cl, 7 mM $MgCl_2$, 50% (v/v) glycerol, 1 mM dithiothreitol, 0.22 µm filtered.

1X TAE Buffer: 40 mM Trisma^{TM} (pH 8.0), 1 mM EDTA, 0.1% glacial acetic acid, 0.22 µm filtered.

1X TBST: 50 mM Tris-HCl (pH 7.6), 150 mM NaCl, 0.05% Tween20.

Generation of EF-G domain mutants

The wild type *Escherichia coli FusA* gene, coding for the EF-G protein, was previously cloned into a pSV281 overexpression vector between *Xho*I and *Bam*HI cut sites (Walter et al., 2011). Both domain IV and the majority of the G' portion of the G domain were removed through site directed mutagenesis (SDM) (Agilent Technologies, QuikChange Site Directed Mutagenesis Kit). A

polymerase chain reaction (PCR) was performed to delete the desired portion of the gene utilizing primers designed via Agilent Technologies website and purchased from Integrated DNA Technologies (IDT). Reactions were performed as suggested by the SDM kit, and contained 125 ng forward primer, 125 ng reverse primer, 50 ng DNA template, 1 µL dNTP mix, 5 µL 10X QuikChange Lightning Buffer, and 1.5 µL QuikSolution reagent in a final volume of 50 µL. Primer sequences are located in Table 3-1. Reactions were incubated at an initial denaturation temperature of 95°C for 2 minutes followed by 18 cycles of 95°C denaturation (20 seconds), 60°C annealing (10 seconds), and 68°C extension (4 minutes). After a final 68°C extension for 10 minutes, plasmids were incubated with 10 units of *Dpn*I restriction endonuclease at 37°C for 5 minutes. Reactions were stored on ice until transformation. Plasmid sequences were confirmed by Nevada Genomics.

Table 3-1. DNA primer sequences for the generation of EF-GΔ4 and EF-GΔG' plasmid DNA. All primers purchased from Integrated DNA Technologies

Primer Name	Sequence
EF-GΔ4 Forward	5'-GGTTTCGCTTTCTTAAAGCCGTTCGCTTCAACGTTGAATT-3'
EF-GΔ4 Reverse	5'-AATTCAACGTTGAAGCGAACGGCTTTAAGAAAGCGAAACC-3'
EF-GΔG' Forward	5'-CGCTGCAGCTGGCGTGTGGTTCTGCGTT-3'
EF-GΔG' Reverse	5'-AACGCAGAACCACACGCCAGCTGCAGCG-3'

Transformation of expression vectors into *E. coli*

Expression vectors generated through SDM were initially transformed into an XL-10 Gold *E. coli* cell line as part of the site directed mutagenesis protocol

mentioned above. Chemically competent XL-10 Gold *E. coli* cells were thawed on ice and 45 µL was aliquoted into a prechilled 14 mL polypropylene round-bottom tube (BD Falcon). To this, 2 µL β-ME mix (Agilent) and 2 µL *Dpn*I treated PRC product were added. Mixtures were gently swirled, and allowed to incubate on ice for 30 minutes. Tubes were heat shocked at 42°C for 30 seconds, then placed immediately on ice for 2 minutes. To each reaction, 500 µL of prewarmed Lysogeny broth (LB) was added, and cells were allowed to recover at 37°C for 1 hour with gentle shanking prior to plating. Cells were evenly distributed onto LB with agar plates (LB + Agar, 1% (w/v) Bacto^{TM} Tryptone (BD Biosciences), 0.5% (w/v) yeast extract, 1% (w/v) sodium chloride, 1.5% (w/v) agar) containing 35 µg/mL kanamycin and were incubated at 37° C overnight. Plasmids from each transformation were isolated (Qiaprep Spin Miniprep Kit, Qiagen) and purified plasmids were sequenced by the Nevada Genomics Center at the University of Nevada, Reno. Once sequences were confirmed plasmids were subsequently transformed into both BL21 and NiCo21 chemically competent *E. coli* cell lines using the same heat shock protocol described above.

Restriction digestion

To accurately determine if PCR was successful, the lengths of genes of interest were examined through restriction digestion. For each reaction 10 units of *Xho*I (New England Biolabs), *Bam*HI (New England Biolabs), or *Xho*I and *BamH*I restriction endonucleases were added to every µg of DNA to be digested, and

diluted into 1X Cutsmart buffer (New England Biolabs) with a total volume of 20 µL. Reactions were allowed to proceed at 37°C for 1.5-2.5 hours, then either immediately ran on an agarose gel, or stored at -20°C.

Overexpression of $(His)_6$-tagged translation factors

To 10 mL LB, kanamycin was added to a final concentration of 35 µg/mL. A single colony was selected from the transformation described earlier and swirled in the LB. The solutions were then incubated overnight with shaking at 200 rpm, 37°C, at a 45° angle. After at least 8 hours growth the 10 mL cultures were added to 1 L portions of LB+kanamycin to inoculate them. Cells were allowed to grow at 37°C, 200 rpm until the optical density (OD) at 600 nm was approximately 0.5 AU, as monitored by spectroscopy (Hewlett-Packard 8453 spectrophotometer). The 1 L growths were then induced to overexpress the protein contained on the plasmid using isopropyl-β-D-thiogalactopyranoside (IPTG) to a final concentration of 400 µM. The incubation temperature was then lowered to 15° C, and left shaking overnight. Cells were pelleted by centrifugation (6300 X g, 15 minutes). Every 5 g of cell pellet was resuspended in ~35 mL of GTPase lysis buffer with 1 mM phenylmethylsulfonyl fluoride (PMSF) and 1 mg/mL lysozyme. Cells were agitated by gently shaking at 4° C for 45 minutes, followed by lysis through sonication (Branson Sonifier 450, 50% duty cycle, 5 output, 3 X 30 seconds). Cell debris was removed by centrifugation (36,000 X g,

45 minutes). Lysate was filtered through a 5 µm, then a 0.45 µm sterile syringe filter prior to immobilized metal affinity chromatography (IMAC).

Purification of $(His)_6$-tagged translation factors

Nickel-nitrilotriacetic acid (Ni-NTA) resin conditioned with GTPase lysis buffer was added to the clarified cell lysate, and allowed to incubate, stirring, for 2-3 hours at 4°C. Lysate/resin mixture was then added to a borosilicate gravity column, and washed with at least 5 column volumes (CV) of GTPase lysis buffer, followed by at least 5 column volumes of GTPase wash buffer, then at least 3 CV of GTPase lysis buffer. GTPases were eluted on ice using GTPase elution buffer until the flow through tested negative for protein using Bradford reagent (Coomassie Plus™ Protein Assay Reagent, Thermo Scientific). To remove imidazole, the purified protein was dialyzed overnight in 12-14 kDa molecular weight cut off (MWCO) dialysis tubing (Spectrum Laboratories, Inc.) into GTPase storage buffer. After concentration through a 30 kDa MWCO centrifugal filter (Millipore), purity was analyzed by SDS-PAGE. If GTPases appeared to be less than 95% pure, anion-exchange chromatography (AEC) and/or size exclusion chromatography were performed.

Electrophoresis

Discontinuous sodium dodecyl sulfate polyacrylamide gel electrophoresis (SDS-PAGE) was performed as previously described to determine purity and size of

isolated proteins (Cleveland et al., 1977). Samples were diluted into a loading dye containing a reducing agent (2% w/v SDS, 80 mM Tris-HCl (pH 6.8), 10% v/v glycerol, 0.002% (w/v) bromophenol blue, 5% v/v β-mercaptoethanol) and were thermally denatured at 95°C for 5 minutes prior to loading into wells. Typically between 100 and 120 volts was applied to the gel until the desired separation was seen between molecular weight markers (Fisher BioReagents). Gels were stained overnight in coomassie gel stain (0.003% w/v Coomassie Brilliant Blue G-250, 40% methanol, 10% glacial acetic acid) and unbound stain was removed through incubation with destain solution (40% methanol, 10% acetic acid) overnight. All SDS-PAGE gels contained in this document were stained with coomassie gel stain.

Agarose gel electrophoresis was performed as previously described to determine the size of genes or plasmids of interest. Agarose was dissolved in 1X TAE buffer by microwaving, followed by the addition of GelRed^{TM} 10,000X Nucleic Acid Gel Stain (Biotium) to a 1X concentration. Samples were diluted into a 6X DNA loading dye (Promega), loaded into wells, and electrophoresed at 110 volts until the desired separation was seen as visualized by ultraviolet light.

Anion Exchange Chromatography

An AKTA Prime fast protein liquid chromatography (FPLC) instrument attached to a 5 mL Q column (GE Healthcare Life Sciences) allowed for further purification of impure proteins. After the system was rinsed with FPLC buffer A, the protein

was injected onto the column. A linear gradient of 0%-50% FPLC buffer B over 75 mL eluted the translation factor. Subsequent dialysis into GTPase storage buffer removed the high salt, and proteins were concentrated with a 30 kDa MWCO centrifugal filter. Purity of the isolated protein was determined via SDS-PAGE, and GTPases were aliquoted into small volumes and stored at -80° C after freezing in liquid nitrogen.

Size Exclusion Chromatography

An AKTA Prime fast protein liquid chromatography (FPLC) instrument attached to a HiLoad 16/60 Superdex^{TM} 75 prep grade column (GE Healthcare Life Sciences) allowed for further purification of contaminated proteins. After the system was rinsed with FPLC buffer A, the protein was injected onto the column. All peaks were collected separately and analyzed via SDS-PAGE to identify the protein and assess purity. Proteins were concentrated with a centrifugal spin filter. Proteins were aliquoted and stored at -80° C after freezing in liquid nitrogen.

Purification of $(His)_6$-tagged 70S ribosomes

JE28 cells were grown as previously described (Ederth et al., 2009). Briefly, JE28 cells were grown overnight from glycerol stocks in the same manner as the above-mentioned GTPases. Upon inoculation into the 1 L LB, the OD_{600} was monitored until it reached approximately 1.0. Growth flasks were then placed in

an ice bath for 1 hour, followed by cell pelleting as mentioned above. The method of cell lysis was identical to above, excepting the substitution of JE28 lysis buffer, JE28 wash buffer, and JE28 elution buffer in place of the respective GTPase buffers, and the exchange of Ni-NTA resin for TALON^{TM} resin. After elution from the resin, ribosomes were dialyzed overnight in JE28 dialysis buffer in 12-14 kDa MWCO dialysis tubing. Ribosomes were then pelleted at 150,000 X g, resuspended with JE28 SW buffer, pelleted again, and resuspended in ribosome storage buffer. The 70S ribosomes were then quantified via UV/Vis spectroscopy, using a molar absorptivity of 39,103,438 M^{-1} cm^{-1}. Purity was assessed via SDS-PAGE, and ribosomes were subsequently aliquoted and frozen in liquid nitrogen, followed by storage at -80° C.

Purification of untagged 70S ribosomes

Endogenous ribosomes were isolated from MRE600 cells. Unlike the JE28 cells, MRE600 cells harbor no resistance to traditional antibiotics. A 5 mL overnight culture of MRE600 cells was grown at 37°C, then inoculated into 1 L of LB media, and grown at 37°C. The OD_{550} was monitored until it reached 0.4-0.5, then flasks were cooled on ice for 1 hour. Cells were pelleted at 6000 X g, 15 minutes, followed by resuspension in ~20 mL JE28 lysis buffer with 1 mM PMSF and 1 mg/mL lysozyme. After gentle shaking for 30 minutes, cells were sonicated on ice (Branson Sonifier 450, 50% duty cycle, 5 output, 3 X 30 seconds) and cell debris was pelleted by two successive rounds of centrifugation at 36,000 X g, 4°

C for 45 minutes each. The supernatant was split into two aliquots, and each was carefully layered on top of 10 mL ice cold 1.1 M sucrose cushion in Ti60 tubes (Beckman), and centrifuged in a fixed angle Type 60Ti rotor at 100,000 X g for 21 hours, 4°C. Pellets were drained, rinsed with 5 mL of 100/10 buffer, and inverted at 4°C until only a clear pellet remained at the bottom of the tube. The pellet was resuspended in 5 mL of 100/10 buffer, and then centrifuged at maximum speed in a tabletop microcentrifuge for 5 minutes to clarify the lysate. The total volume was brought up to 40 mL with ice cold 500/10 buffer, and the NH_4Cl concentration was adjusted to 500 mM through the addition of 5 M NH_4Cl. Solution was split equally between two Ti60 tubes, and centrifuged again at 100,000 X g for 5 hours at 4°C. Pellets were rinsed and resuspended as above, then pelleted again with the same conditions.

From this, each pellet was resuspended in 500 µL 100/10 buffer, and gently layered on top of two 10-35% linear sucrose gradients (prepared using built-in programs on a Gradient Station$_{ip}$, BioCorp). These gradients were centrifuged in an SW28 rotor at 55,000 X g, 13 hours, 4°C. Gradients were pumped using the GradientMaker 150, monitoring the A_{254} using an EconoUV (BioRad). The 70S fraction was conservatively collected, then diluted to 40 mL with 100/10 resuspension buffer. $MgCl_2$ concentration was brought up to 10 mM using a 2 M stock solution, and 70S ribosomes were pelleted at 100,000 X g for 17 hours at 4°C. Pellets were drained and rinsed with 5 mL 100/10 resuspension buffer, and

finally resuspended in 100 µL of 100/10 resuspension buffer. The purity of the collected 70S fraction was analyzed via SDS-PAGE, quantified as the $(His)_6$-tagged ribosomes were, then flash frozen in liquid nitrogen and stored at -80° C.

Purification of L12

Justin Water had previously cloned the L12 gene into the pSV281 vector, introducing an N-terminal $(His)_6$-tag. L12 was purified in a fully unfolded state in order to prevent co-purification of ribosomes. Lysis, wash, and elution of L12 were performed identically to that of the GTPases, excepting the introduction of 7 M urea to each buffer, to ensure unfolding. After elution, purified protein was centrifuged at 150,000 X g for 2 hours at 4°C. The supernatant was refolded through slow dialysis in two separate 1 L aliquots of GTPase storage buffer for 24 hours each. The purified protein was then concentrated using a 10 kDa MWCO spin concentrator (Millipore) and purity was assessed via SDS-PAGE. L12 was quantified using the Bradford assay, frozen in liquid nitrogen, and stored at -80°C.

Depletion and reconstitution of L12

Previous reports have provided a method to remove L12 from 70S ribosomes (Mohr et al., 2002). All solutions were stored at 4°C for 24 hours prior to depletion, and 70S ribosomes were thawed on ice immediately prior. In a microfuge tube, 450 pmol of purified $(His)_6$-tagged 70S ribosome were combined

with 450 µL of L12 extraction buffer, and allowed to incubate for 5 minutes on ice. To this, 250 µL of ice-cold 200 proof ethanol was added, and the solution was stirred at 4°C for 5 minutes, at which point another 250 µL aliquot of 200 proof ethanol was added. After an additional 5 minutes of stirring, the mixture was centrifuged at 150,000 X g for 45 minutes. The supernatant was added to a 5X excess of cold acetone, and the precipitate was saved for SDS-PAGE analysis to confirm that only L12 was removed. Pellets were resuspended in 100 µL ribosome storage buffer, and injected onto an AKTA Prime FPLC instrument attached to a 5 mL Ni-NTA column. Depleted ribosomes were collected in the initial flowthrough, while non-depleted ribosomes were eluted using JE-28 elution buffer and discarded. The reintroduction of purified L12 to depleted 70S ribosomes was accomplished through incubation of 70ΔL12 with a 5-fold excess of purified $(His)_6$-tagged L12 at 37°C for 30 minutes.

Western blots

In order to ensure the protein removed during the 70S depletions was L12, acetone precipitated proteins were separated on a 15% SDS-PAGE gel and transferred to a nitrocellulose membrane for 8 hours at 15 volts (BioRad TransBlot SD Semidry Transfer Cell). The identity of the removed protein was confirmed through a HisDetector™ Western Blot Kit (KPL). The nitrocellulose membrane was incubated in 20 mL of 1X Detector Block solution for 1 hour with gentle rocking. The HisDetector™ Nickel-AP Conjugate was then added, and

allowed to incubate for another hour. Membranes were then washed with three 10 mL aliquots of the provided Tris-buffered saline with Tween (TBST), and color was developed by placing the membrane in 10 mL of 5-bromo-4-chloro-3'-indolyphosphate p-toluidine-nitro-blue terazolium chloride (BCIP-NBT) for 15 minutes. The nitrocellulose membrane was then washed with ddH_2O and allowed to dry.

Malachite green GTPase activity assay

In order to test the activity of both purified 70S ribosomes and the GTPases, an assay to detect the presence of inorganic phosphate was adapted (Harder et al., 1994). To prepare the reaction quenching dye, Malachite Green (0.045% w/v in ddH_2O) was combined with 4.2% w/v ammonium molybdate in a 3:1 ratio, and stirred for at least 30 minutes at room temperature. For the assay, GTPase (5 μM), 70S (0.2 μM), 70SΔL12 (0.2 μM), 70SΔL12+L12 (0.2 μM), and malachite green reaction buffer (to 1X) were combined as appropriate and were incubated at room temperature for 10 minutes. Next, GTP (25 μM) was added to the applicable reactions and left to react at room temperature for 15 minutes. Reactions were quenched through the addition of malachite green reagent, and color was allowed to develop for five minutes. Reactions were analyzed in a 96 well plate at 620 nm against the appropriate controls, using a BioTek® Epoch plate reader.

Removal of $(His)_6$-tag from GTPases

Some assays required the removal of the polyhistadine tag from the GTPases. To cleave this tag from the desired proteins, previously purified Tobacco Etch Virus (TEV) protease was combined in a 1:10 w/w ratio with the translation factor. Cleavage was allowed to proceed for 4 hours at room temperature, followed by a 30 minute incubation with Ni-NTA resin. Resin flowthrough was collected and concentrated. Proteins bound to the resin were eluted with GTPase elution buffer and analyzed via SDS-PAGE to confirm successful removal of the $(His)_6$-tag through a lowering of the molecular weight, and loss of affinity for the Ni-NTA resin.

GTPase binding assay through ultracentrifugation

To determine whether ribosomes and GTPases were binding together, a ribosome binding assay previously utilized in the Spiegel lab was adapted. To S120-AT3 rotor thick-walled polycarbonate tubes, 250 µL of 10% w/v sucrose in M20 buffer was added. GTPase and 70S or 70SΔL12 were allowed to react in the presence or absence of GDPNP for 15 minutes at 37° C, and then layered on top of the sucrose solution. Reactions and the appropriate controls were centrifuged at 255,000 X g for 10 minutes at 4° C, and supernatants were discarded. Pellets were resuspended in 20 µL ddH_2O via gentle vortexing, and analyzed by SDS-PAGE.

Quantification of SDS-PAGE gels using ImageJ

ImageJ, a freeware program made available through the NIH, was utilized to quantify gel images. Images were turned into greyscale by converting them to 32 bit, and contrast and brightness were adjusted until bands were optimally visible. Lanes were selected via the rectangular selection tool, and resultant bands were plotted using the built-in tools. Integration of these bands was transferred to Excel, and normalized to a control band within each lane of the gel (typically the S6 protein present at ~35 kDa).

BioLayer Interferometry kinetics assay

GTPase, ribosome, and buffers were all prepared from the same stock buffer for BioLayer Interferometry. Prior to experiments, all GTPases, ribosomes, and nucleotide analogs were prepared in BLI reaction buffer. Ni-NTA tips (FortéBio) were hydrated in the BLI reaction buffer as well. Tips were initially blanked in buffer for 60 seconds, followed by the binding of tagged 70S ribosomes (3.5 μM) for 600 seconds. After a 60 second wash, TEV cleaved GTPase was allowed to associate to the bound 70S for 600 seconds, then dissociate for 600 seconds in the buffer. All kinetic and binding data were calculated using the built in BLItz software.

Circular dichroism

Circular dichroism (CD) spectra were collected on an Olis DSM 20 CD instrument. Prior to data collection, L12 was diluted to 0.5 mg/mL in GTPase storage buffer. Ellipticity was monitored from 200 to 270 nm in 1 nm increments at 20°C.

Chapter 4 – The role of L12 in translational GTPase activity and binding

Results

GTPase Expression and Purification

GTPases were purified through a well-established technique (see Materials and Methods). All genes were originally cloned from genomic *E. coli* DNA into a pSV expression vector (pSV281) allowing for overexpression of the desired protein driven by the lac promoter. This expression vector also contained a gene encoding kanamycin resistance, an N-terminal $(His)_6$-tag, and a TEV protease cleavage site between the $(His)_6$-tag and the protein of interest. After cell lysis, and subsequent purification steps, the resultant translation factors were analyzed by SDS-PAGE (Figure 4-1A). Concentrated translation factors were quantified through their molar extinction coefficients (calculated using ExPASy ProtParam) and the Beer-Lambert law at a wavelength of 280 nm. All GTPases were determined to have greater than 95% purity via SDS-PAGE and the correct size before being tested in any biochemical assays (Figure 4-1B).

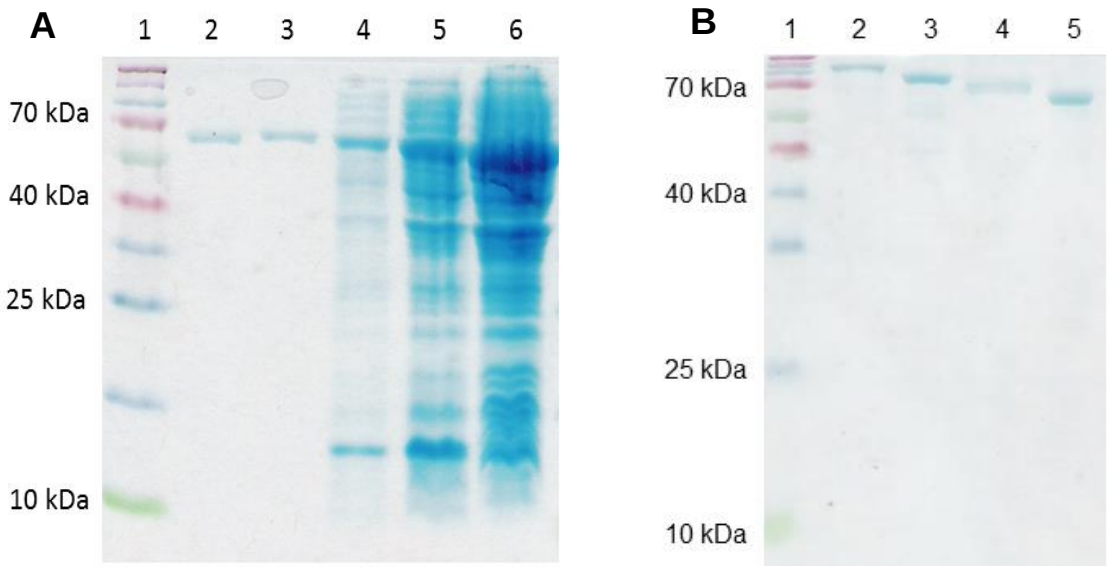

Figure 4-1. Standard purification of Translational GTPases. **(A)** Coomassie blue stained 15% SDS-PAGE gel. All proteins were overexpressed, attached to Ni-NTA, washed, then eluted and concentrated. (1) Spectra^{TM} BR Protein Ladder (Thermo Scientific), (2) RF 3 post TEV cleavage, (3) RF3 pre TEV cleavage, (4) Wash, (5) Ni-NTA flowthrough, (6) Post IPTG induction sample. **(B)** 15% SDS-PAGE gel. All GTPases purified to greater than 95% purity (1) MW ladder, (2) IF2, (3) EF-G, (4) RF3, (5) LepA.

Purification of 70S ribosomes

Two different methods were employed to purify 70S ribosomes. JE-28 cells contain an N-terminal $(His)_6$-tag on the L12 protein, present in four copies on each ribosome (Ederth et al., 2009). TALON^{TM} resin (Clontech) allowed for facile purification of 70S ribosomes from whole cell lysates, and purified ribosomes were quantified via UV/Vis spectroscopy. Purity was confirmed via SDS-PAGE (Figure 4-2A). MRE-600 cells were grown in order to purify non-tagged ribosomes through a series of ultracentrifugation steps. Comparison of JE-28 and MRE600 purified 70S ribosomes showed no discernable differences once

concentration was taken into account (Figure 4-2B). An A_{260}/A_{280} ratio of 2:1 indicated a pure 70S fraction. Yield of 70S ribosomes was much greater for MRE600 isolated ribosomes (~2000 pmol) than for affinity purified ribosomes (~500 pmol) per liter of cultured media.

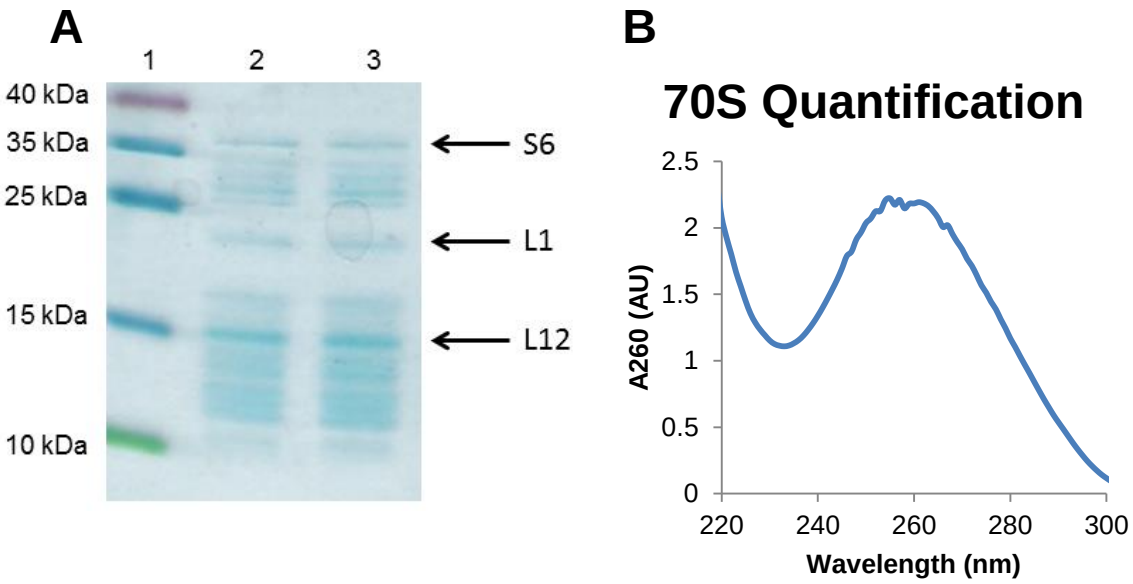

Figure 4-2. Purification of 70S ribosomes. **(A)** Coomassie stained 10% SDS-PAGE gel. (1) Spectra^{TM} BR Protein Ladder (Thermo Scientific), (2) JE-28 purified 70S vs (3) MRE600 purified 70S ribosomes. No significant difference in bands was noticed. **(B)** Typical 70S quantification curve, indicating an A260/A280 ratio of ~2.0, and showing no aberrant peaks.

Depletion of L12 from $(His)_6$-tagged ribosomes

The L12 ribosomal protein was removed from $(His)_6$-tagged 70S ribosomes through a novel two-step purification scheme (Materials and Methods). Depletion of only L12, leaving other ribosomal proteins and rRNA intact, is a time and temperature sensitive process, as previously described (Michelle Wuerth, WWU Undergraduate Honors Thesis in Biochemistry). Temperatures above 4° C, or

mixing times longer than ten minutes led to loss of other ribosomal proteins, including L10 and L11. A second step of purification, involving flowing 70S ribosomes over a Ni-NTA column after ethanol incubation ensured any ribosomes still containing L12 were removed prior to biochemical assays. Proteins removed through ethanol incubation were analyzed through SDS-PAGE to confirm that only L12 was removed (Figure 4-3A). Lane 2 shows a standard purification of L12 through non-denaturing methods (Materials and Methods). Some higher molecular weight impurities were clearly visible demonstrating L12 must be denatured to eliminate any contamination. Lane 3, purification of L12 through urea denaturation and IMAC, shows no visible impurities. Lane 4, L12 removed via ethanol precipitation with two sequential 5 minute incubation steps. The difference in molecular weight between lanes 2/3 and 4 is due to a shorter linker between the protein and the TEV cleavage site present on the ethanol precipitated proteins. After initial ethanol precipitation of L12, ribosomes were passed over a Ni-NTA column, thereby binding any with the $(His)_6$-tag still attached (Figure 4-3B). Initial flowthrough collected was assumed to be completely depleted 70S, which will be referred to as 70SΔL12 from this point forward. A western blot kit designed to detect the presence of a $(His)_6$-tag confirmed the protein depleted from the 70S ribosomes was L12 (Figure 4-4). Lane 2 displays a normal level of L12 in 70S ribosomes. Lane 3 contains a trace but detectable level of L12 after the ethanol depletion step performed by Mohr et al. (2002). This band is entirely removed after flowing the initially depleted

ribosomes over a Ni-NTA column, as seen in lane 4. Lane 5 contains the supernatant from the ethanol depletion step, confirming the protein removed contained a $(His)_6$-tag, and was the same size as L12. Urea purified L12 (lane 6) contains a $(His)_6$-tag, and appeared accordingly on the western blot, whereas lysozyme, without a tag, showed no band.

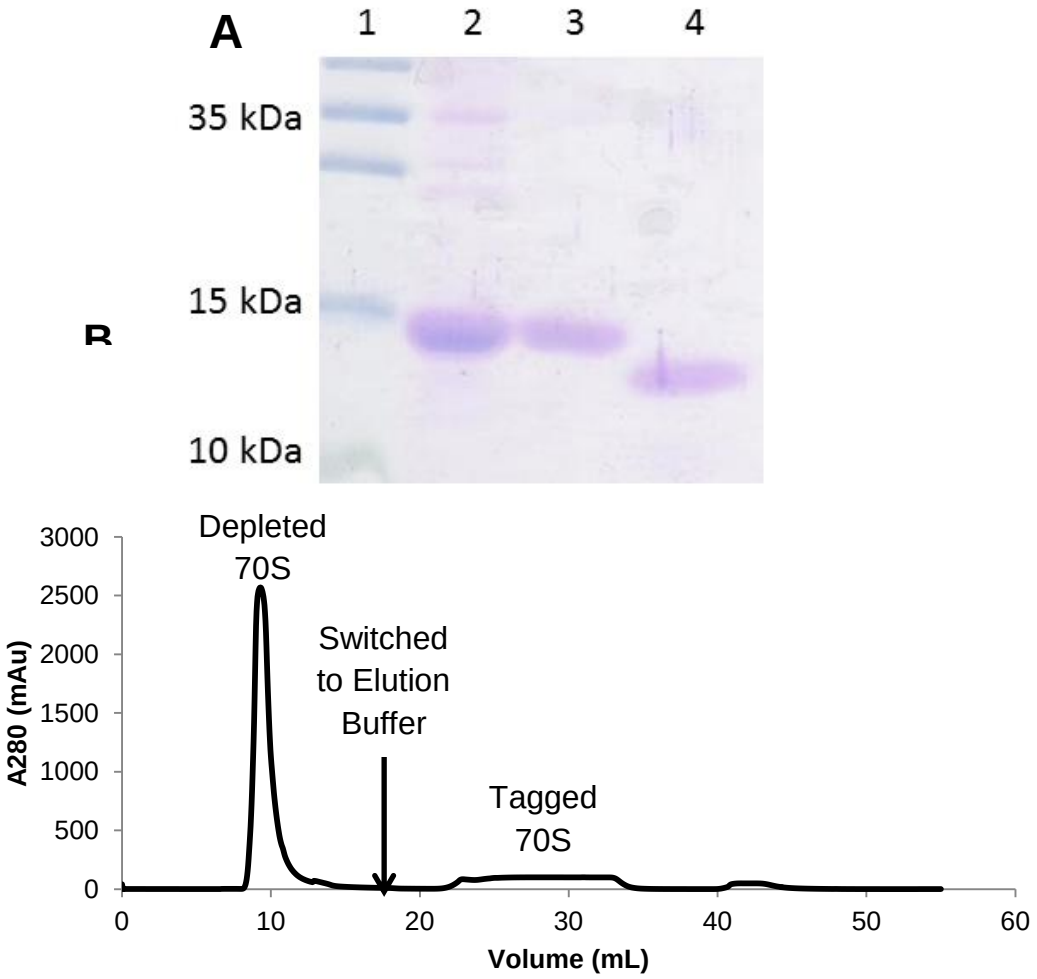

Figure 4-3. Depletion of L12 from 70S ribosomes. (**A**) Coomassie stained 17% SDS-PAGE gel indicating successful depletion of L12 from $(His)_6$-tagged 70S ribosomes. (1) MW ladder, (2) L12 purified without urea denaturation, (3) L12 purified with urea denaturation, (4) ethanol depleted L12. (**B**) Example elution profile from a Ni-NTA column of depleted ribosomes. Depleted ribosomes do not bind Ni-NTA resin (depleted 70S peak) while ribosomes still containing a $(His)_6$-tag attach to the resin, and must be eluted off with imidazole (tagged 70S peak). Experiment **A** performed by Justin Walter**.**

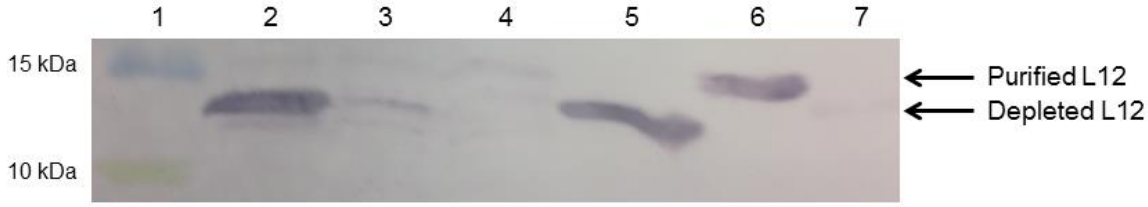

Figure 4-4. Anti-$(His)_6$-tag Western blot confirming the depleted protein was L12. A 17% SDS-PAGE gel transferred to a nitrocellulose membrane. (1) MW ladder, (2) 70S ribosomes, (3) initially depleted 70S ribosomes, (4) fully depleted 70S ribosomes, (5) supernatant from ethanol depletion, (6) purified L12, (7) lysozyme control. Experiment performed by Michelle Wuerth.

Purification of L12

The isolation of pure ribosomal proteins required complete denaturation and subsequent refolding in order to avoid ribosome contamination. Proteins were purified and eluted in 7 M urea to guarantee complete unfolding, followed by 48 hours of dialysis to refold in native buffer conditions. Successful isolation was confirmed via SDS-PAGE and Western Blot (Figure 4-3, Figure 4-4, respectively). To ensure proper folding, circular dichroism (CD) was implemented to probe the secondary structure of urea purified L12and size exclusion chromatography (SEC) ensured there were no contaminating proteins. CD spectra were indicative of strong α-helical character, showing minima around 208 nm and 220 nm (Figure 4-5). L12 contains no tryptophan residues, and therefore was quantified via a Bradford assay (Materials and Methods). Once purified,

refolded, and quantified, L12 was incubated with 70SΔL12 in order to reconstitute depleted ribosomes.

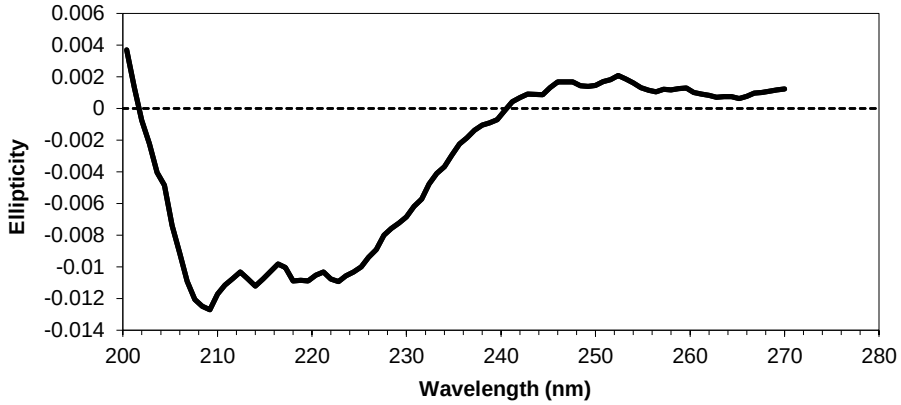

Figure 4-5. Circular dichroism spectrum of purified L12. Data collected by Justin Walter.

Effect of complete depletion of L12 on ribosome-dependent GTPase activity

After successful depletion of L12 from 70S, and purification of L12 for reconstitution studies, a simple inorganic phosphate detection assay allowed for rapid determination of the effect of L12 depletion on ribosome-dependent GTPase activities. The malachite green assay was performed as described (Materials and Methods) in the presence of 70S (intact), 70SΔL12 (depleted), and 70SΔL12+L12 (reconstituted) ribosomes. As ribosomes do not need mRNA or tRNA in order to catalyze GTP hydrolysis through GTPases, these reagents were omitted (Achila et al., 2012). In order to completely assess the activity of prokaryotic ribosomes with and without L12, an aliquot of depleted ribosomes

was incubated with purified L12, and retested for activity. Figure 4-5 shows the results for all purified GTPases using intact, depleted, and reconstituted 70S ribosomes. EF-G (Figure 4-6A), L12, and 70S alone exhibited almost no activity when incubated with GTP. Further, when EF-G was incubated with L12, no increase in activity is seen, suggesting L12 alone was not enough to stimulate GTP hydrolysis by EF-G. When 70SΔL12 was preincubated with purified L12 protein, a complete recovery of the lost activity was seen. These results held true for RF3 and IF2 as well (Figure 4-6C and D, respectively). LepA did not show a complete loss of activity with 70SΔL12, maintaining approximately 50% of the GTP hydrolysis seen in the 70S + LepA assay (Figure 4-6B). Addition of L12 to 70SΔL12 restored activity to the level seen in the 70S + LepA reaction.

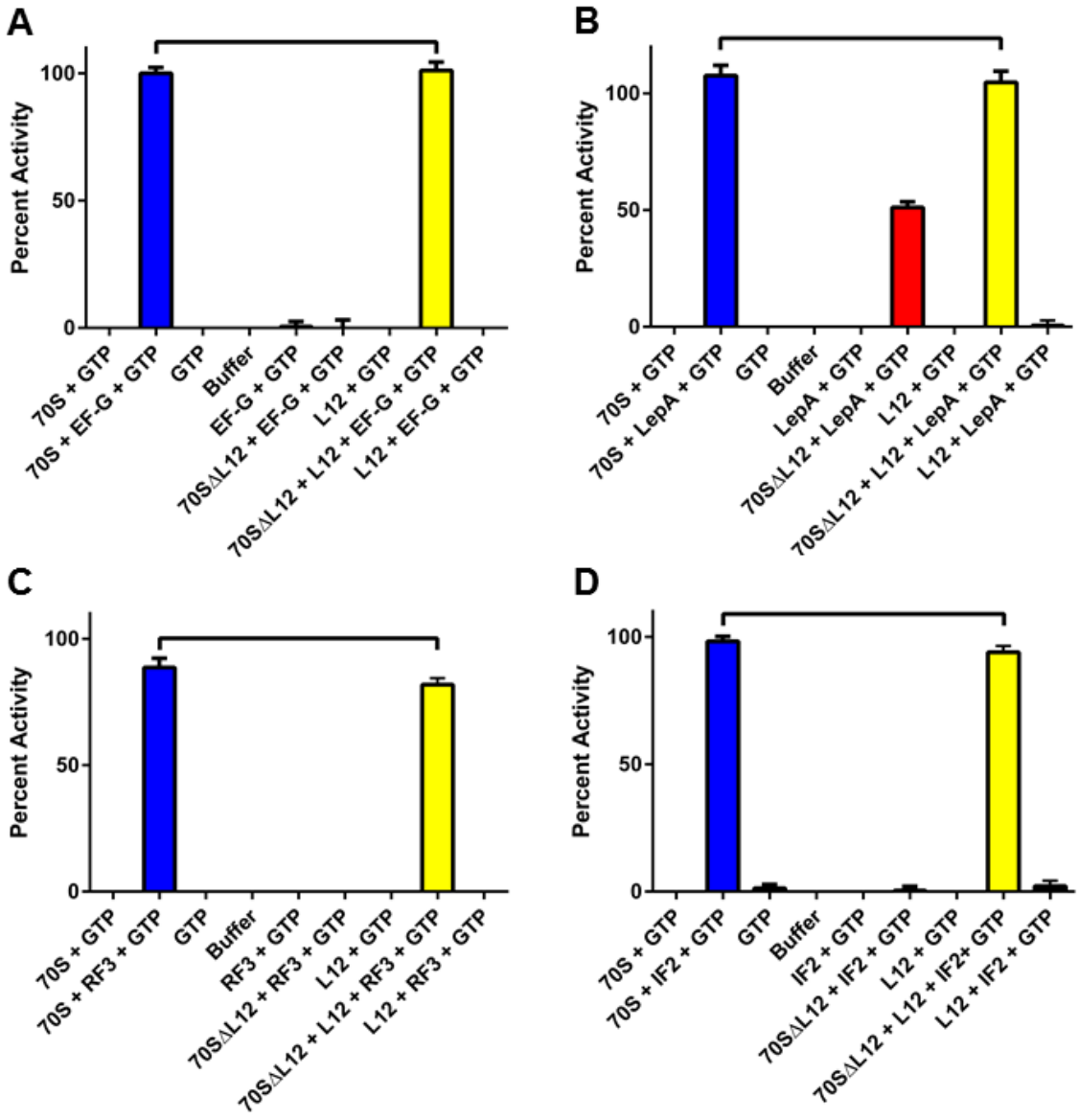

Figure 4-6. Effect of L12 depletion on ribosome dependent GTPase activity. (**A**) EF-G, (**B**) LepA, (**C**) RF3, (**D**) IF2. Brackets indicate data compared using one tailed student's t-test. No significant difference was found, using $p \leq 0.05$, $n \geq 5$ for each comparison.

It was also of interest to compare the activity of the translational GTPases with one another as a function of time. As a crude method for this comparison, a time based malachite green assay was utilized. EF-G, LepA, RF3 and IF2 were incubated in the presence of 70S, 70SΔL12, or 70SΔL12+L12, along with appropriate controls. At specific time points GTP was added. All reactions were quenched with malachite green reagent and read at the same time (Figure 4-7). Activity of each was normalized to the final 30 minute timepoint of elongation factor G, as it had the highest activity, and was assumed to be 100% given the plateau seen in GTP hydrolysis. EF-G exhibited the highest GTPase activity, reaching maximum activity around the 15 minute timepoint (Figure 4-7A). RF3 and IF2 demonstrated similar timecourses, with both not plateauing prior to the 30 minute incubation (Figure 4-7C and D, respectively). EF-G, RF3, and IF2 all show no GTP hydrolysis activity, even at a 30 minute timepoint in the presence of 70SΔL12. LepA, displaying slightly slower GTP hydrolysis than EF-G, does not lose complete activity when L12 is removed, instead showing activity similar to that shown in Figure 4-5, hovering around 50% (Figure 4-7B). The GTP hydrolysis activity was still trending upward for LepA+70SΔL12, even at the 30 minute timepoint. Reconstitution of depleted 70S ribosomes with externally purified L12 restored full activity in all cases, with no deviation from the curves obtained with intact 70S ribosomes.

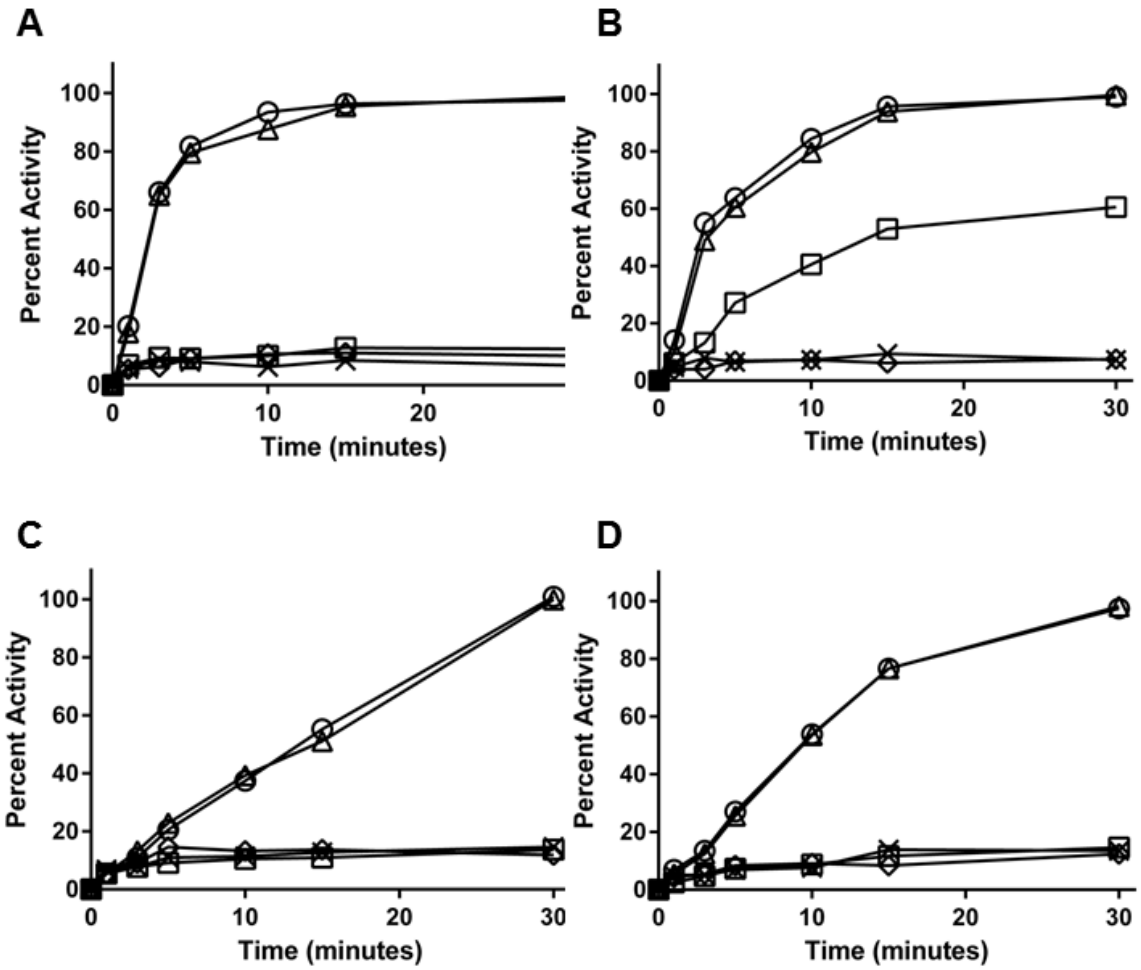

Figure 4-7. Effect of L12 depletion on time-based GTPase activity. **(A)** EF-G, **(B)** LepA, **(C)** RF3, **(D)** IF2. 70S + GTPase – open circles (O), 70SΔL12 +GTPase – open squares (□), 70SΔL12+L12 + GTPase – open triangles (Δ), 70S alone – open diamonds (◊), GTPase alone – X (X). Experiments performed in triplicate, excepting EF-G (n=5). Error bars omitted for clarity.

Effect of L12 Depletion on the binding of translational GTPases

Once GTPase activity with and without L12 was determined, it was necessary to determine whether GTPase binding was dependent upon L12 as well. In order to assess this, a GTPase binding assay via ultracentrifugation was designed. Briefly, the density of a 10% sucrose solution is such that 70S ribosomes (with or without L12) are large enough to migrate through faster than the comparatively smaller GTPases. When a GTPase binds to the 70S ribosome, however, it is able to migrate through the sucrose with the ribosomes, thereby ending up at the bottom of the sucrose, separated from any unbound GTPase (Figure 4-8). Ultracentrifugation and SDS-PAGE allowed for rapid assessment of the binding of translational GTPases to 70S and 70SΔL12 ribosomes (Figure 4-9). In the presence of endogenous 70S ribosomes and a GTP analog, EF-G tightly bound the ribosome and without this GTP analog little binding occurred (Figure 4-9A, lanes 5 and 4, respectively). In the control lanes, EF-G did not appear at all (lane 2), while 70S ribosomes pelleted readily (lane 3). In comparison, 70SΔL12 stimulated almost no binding of EF-G (Lanes 9-10), regardless of the presence of GDPNP. IF2 and RF3 exhibited similar results as EF-G (Figure 4-9C, Table 4-1). LepA exhibited different results than the other three GTPases. Like IF2, RF3, and EF-G, low level of binding was seen in the 70S + LepA lane, and addition of GDPNP caused a significant increase in this binding (Figure 4-9C, Table 4-1). However, removal of L12 did not inhibit binding as strongly as was seen with the

other translational GTPases. The removal of L12 prevented even a baseline amount of GTPase to bind to the ribosome for EF-G, IF2, and RF3 (Table 4-1). EF-G binding to 70SΔL12 with GDPNP was roughly half that of intact 70S ribosomes without a GTP analog, indicating a very low affinity. IF2 showed an even lower affinity for 70SΔL12, at approximately one third the binding found as compared to no nucleotide. RF3 showed around one sixth the binding under the same conditions. LepA in the absence of L12 showed approximately one and a half times the binding seen without GDPNP, a markedly higher result compared to the other GTPases.

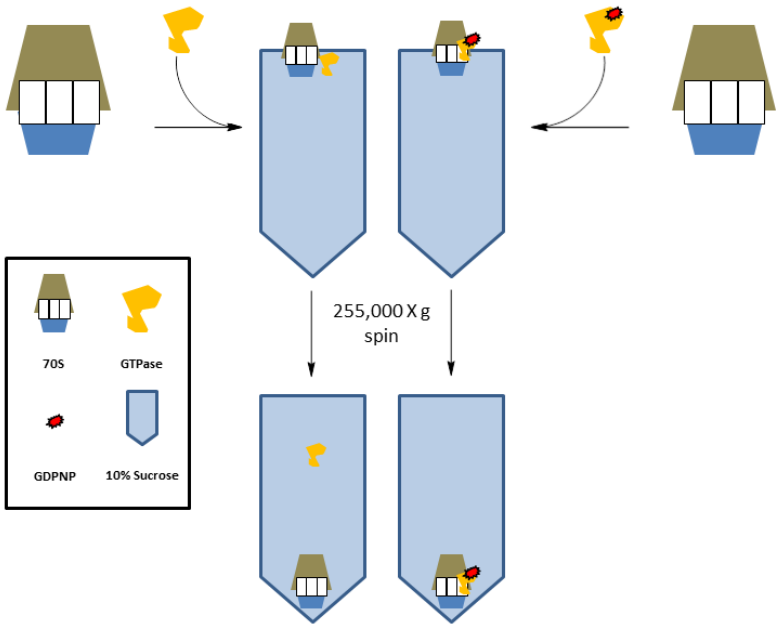

Figure 4-8. Schematic representation of the GTPase binding assay. GTPase was incubated with 70S ribosomes in the presence or absence of GDPNP. After layering on top of a sucrose cushion, reactions were centrifuged at 250,000 X g for 10 minutes. Resulting pellets were analyzed via SDS-PAGE.

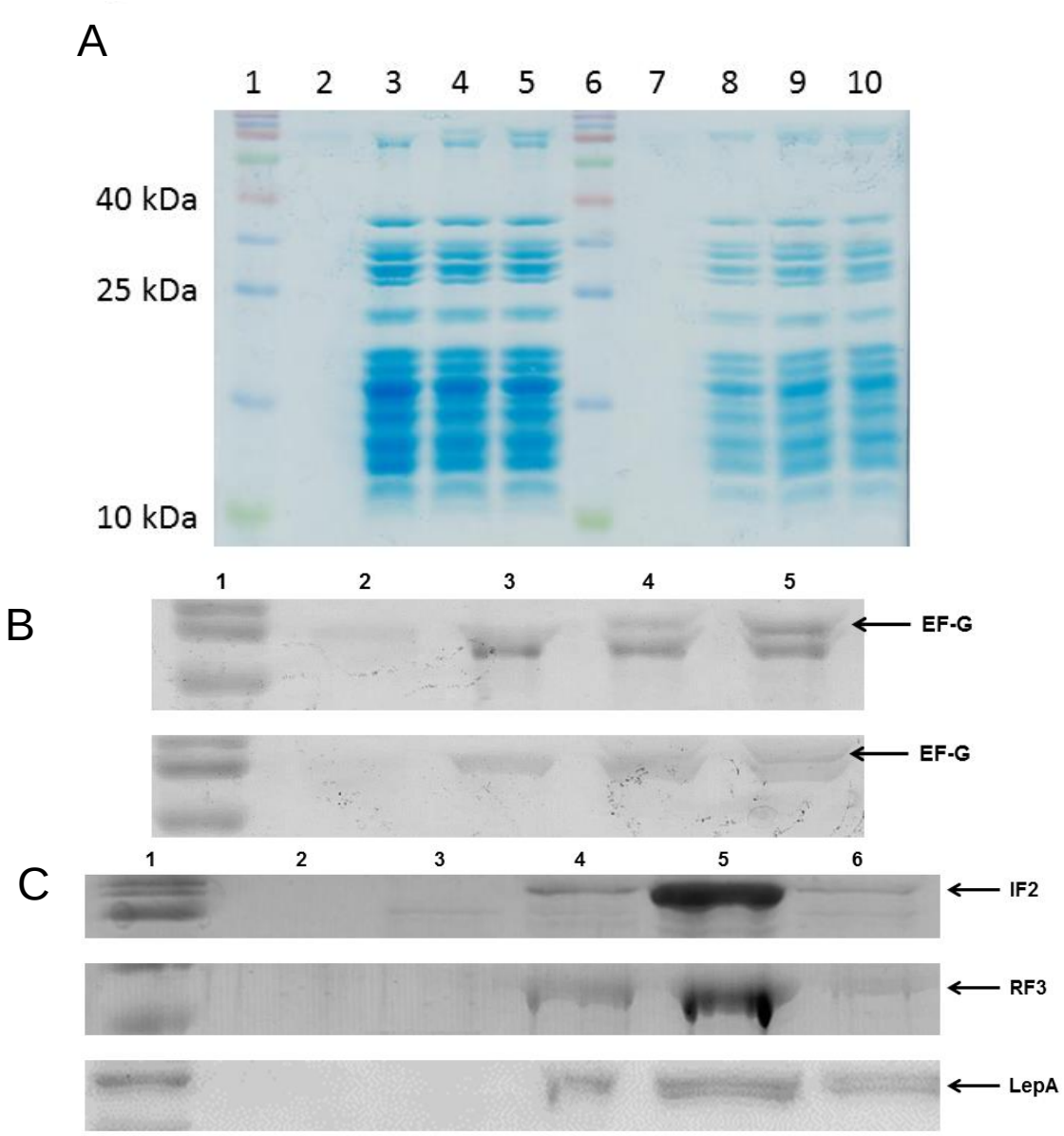

Figure 4-9. Results of GTPase binding assays. **(A)** Coomassie stained 15% SDS-PAGE gel indicating the effects of L12 depletion on translational GTPase binding. (1) MW ladder, (2) EF-G alone, (3) 70S alone, (4) EF-G+70S, (5) EF-G+70S+GDPNP, (6) Spectra^{TM} BR Protein Ladder (Thermo Scientific), (7) EF-G alone, (8) 70SΔL12 alone, (9) EF-G+70SΔL12, (10) EF-G+70SΔL12+GDPNP. **(B)** Coomassie stained 15% SDS-PAGE gel. Enhancement of lanes 1-5 (top) or 6-10 (bottom) from A. **(C)** Coomassie stained 15% SDS-PAGE gel. (1) MW ladder, (2)RF3/IF2, (3) 70S, (4) RF3/IF2 + 70S, (5) RF3/IF2 + 70S + GDPNP, (6) RF3/IF2 + 70SΔL12 + GDPNP.

Table 4-1. Quantification of select lanes from GTPase binding assays. Normalized to 70S + GTPase for each translation factor. Data are the average of at least two experiments. Band intensities normalized to the S6 protein present in each lane.

		GTPase			
		EF-G	RF3	IF2	LepA
Complex	70S + GTPase	1.0	1.0	1.0	1.0
	70S + GTPase + GDPNP	3.8	4.6	3.5	4.1
	70SΔL12 + GTPase + GDPNP	0.4	0.2	0.2	1.5

Binding Kinetics of Depleted 70S ribosomes

Once initial studies concerning GTP hydrolysis and binding of translation factors to 70S ribosomes with and without L12 were completed, we sought a method of quantitatively determining the binding affinity of translational GTPases to intact or depleted ribosomes. To this end, BioLayer Interferometry (BLI), a technique akin to surface plasmon resonance, allowed for rapid determination of overall 70S-GTPaes affinity. Purified 70S ribosomes were bound to Ni-NTA BLI tips via the L12 $(His)_6$-tag, followed by a brief rinse with BLI reaction buffer to remove any unbound ribosomes. Subsequently, TEV cleaved GTPases (thereby containing no $(His)_6$-tag) were incubated with the 70S-bound tips to determine association, and then rinsed in BLI reaction buffer again to determine dissociation. Initial tests were performed with only tagged 70S ribosomes and TEV cleaved EF-G (Figure 4-10, Table 4-2). The association constant, k_a, is similar for all three concentrations of EF-G tested, averaging at 1.47E+3 $M^{-1}s^{-1}$, while the k_d

averages 1.88E-4 s^{-1}. Combined, these give a K_D of 1.58E-7 M, or approximately 100 nM, similar to previously reported values (Lancaster et al., 2008).

Once protocols had been established and proper times and concentrations decided upon, the effect of L12 was determined. In order to conclude if EF-G bound to 70SΔL12, EF-G was preincubated with either 70S or 70SΔL12 ribosomes. Following initial binding and washing of tagged 70S ribosomes to the Ni-NTA tip, EF-G (TEV cleaved) + 70S (wild type, containing no $(His)_6$-tag), or GTPase (TEV cleaved) + 70SΔL12, were allowed to associate, followed by dissociation. Binding curves and kinetic data were generated via the BLItz software (Figure 4-11, Table 4-3). Trials 1, 2, and 3 all demonstrate similar k_a, k_d, and K_D values to those found in Figure 4-10 and Table 4-2, as expected. Upon the introduction of 70SΔL12, we saw no significant difference in the association of EF-G to the ribosomes bound on the Ni-NTA tip, and only slight decrease in dissociation was noted, leading to an increased binding affinity (Trial 4). When this same protocol was repeated, but with non-$(His)_6$-tagged 70S ribosomes rather than 70SΔL12, the k_a sharply decreased, indicating little to no association of EF-G to the 70S on the Ni-NTA tip. Additionally, the k_d remained similar to the other five trials, indicating similar rates of dissociation across the board.

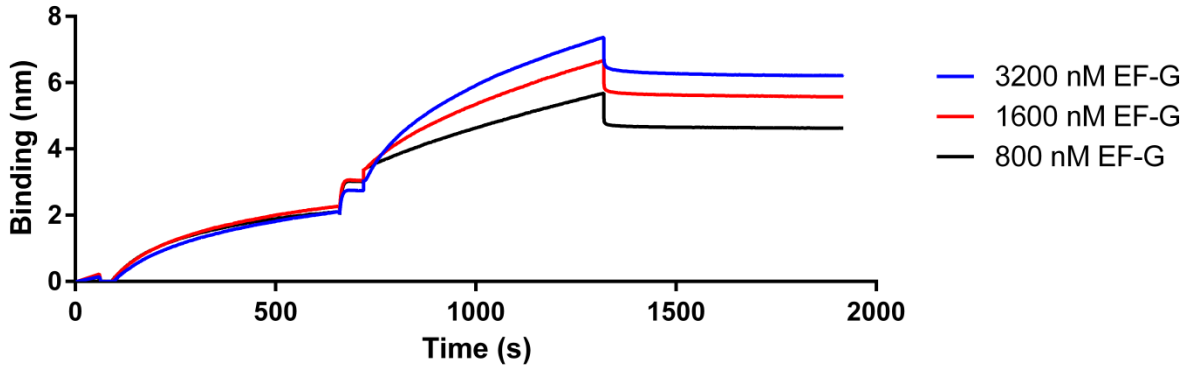

Figure 4-10. BLI analysis of 70S and EF-G binding, with Table 4-2. 0-60s: buffer blank, 60-660s: binding of 70S ribosomes to the Ni-NTA tip, 660-720s: buffer wash, 720-1320s: association of EF-G, 1320-1920s: dissociation of EF-G.

Table 4-2. Kinetic data for 70S ribosomes binding EF-G, with Figure 4-10. All calculations were performed via built in BLItz software.

Trial	Bound Protein	Associated Protein	Concentration (nm)	k_a (1/Ms)	k_a Error	k_d (1/s)	k_d Error	K_D (nM)
1	70S	EF-G (TEV Cleaved)	3200	8.30 E+02	4.14 E+01	2.38 E-04	6.93 E-06	290
2	70S	EF-G (TEV Cleaved)	1600	1.48 E+03	1.32 E+01	1.60 E-04	2.66 E-06	110
3	70S	EF-G (TEV Cleaved)	800	2.11 E+03	6.09 E+01	1.68 E-04	4.03 E-06	80

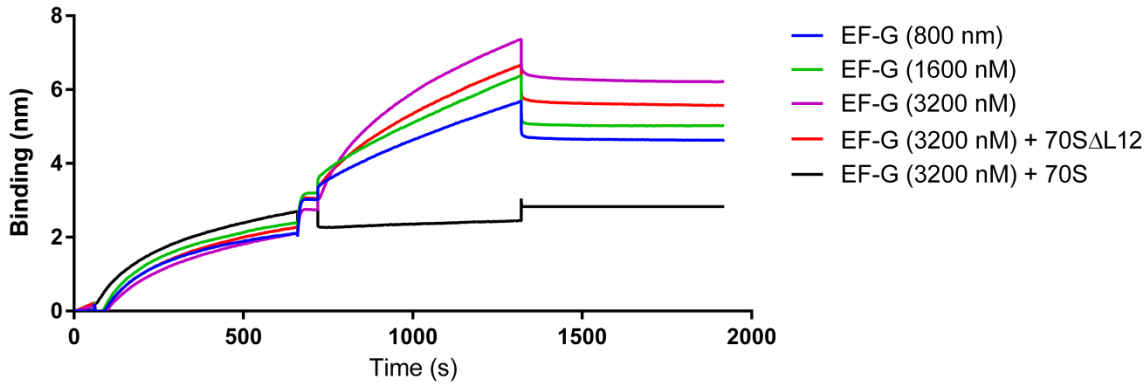

Figure 4-11. BLI analysis of EF-G binding with and without L12 on the 70S ribosome. 100-660s: binding of 70S to the Ni-NTA tip, 660-720s: buffer wash, 720-1320s: association of EF-G of EF-G + 70S/70SΔL12, 1320-1920s: dissociation of EF-G. With Table 4-3.

Table 4-3. Kinetic data for 70S ribosomes binding EF-G in the presence of 70S or 70SΔL12. With Figure 4-11. All calculations were performed via the built in BLItz software

Trial	Bound Protein	Associated Protein	Concentration (nm)	k_a ($M^{-1}s^{-1}$)	k_a Error	k_d (s^{-1})	k_d Error	K_D (nM)
1	70S	EF-G (TEV cleaved)	800	1.06 E+03	2.42 E+01	6.10 E-05	4.12 E-06	58
2	70S	EF-G (TEV cleaved)	1600	1.65 E+02	3.44 E+01	1.05 E-05	7.86 E-06	64
3	70S	EF-G (TEV cleaved)	3200	3.65 E+02	1.35 E+01	3.21 E-05	2.04 E-06	88
4	70S	EF-G (TEV cleaved) + 70SΔL12	3200	1.96 E+02	1.04 E+01	1.48 E-06	3.71 E-06	10
5	70S	EF-G (TEV cleaved) + 70S (untagged)	3200	1.12 E-02	2.08 E-02	6.12 E-05	5.17 E-06	5.5 E+6

Discussion

GTPase activation requires more than individual large ribosomal subunit proteins in solution

Despite translation being one of the most fundamentally conserved processes discovered to date, and one of the most investigated areas across scientific fields, there still exists a staggering number of uncertainties in our current understanding of protein biosynthesis. Over the past fifteen years, researchers have made immense strides in the understanding of the structure and function of both the prokaryotic and eukaryotic ribosomes, yet many of the nuances of translation remain a mystery.

One of the most crucial holes in the study of translational GTPases is the lack of knowledge surrounding their method(s) of activation. As mentioned earlier, for close to twenty years the mechanism behind the activation of translational GTPases has been sought, and not until recently has any progress occurred. In 2000, a study was published on the role of L12 in the activation of EF-G and EF-Tu, showing ribosomal protein L12 alone is enough to stimulate GTP hydrolysis in the presence of these GTPases, albeit at a extremely high 40 μM concentration (Savelsbergh et al., 2000b). The authors noted that the rate of GTPase activity was significantly lower in the presence of L12 as compared to intact ribosomes. Since this study, there has been a constant trickle of information surrounding the activation of translational GTPases, but little

consensus among the top researchers in the field. To date, there is very little evidence surrounding the role of L12 in activating EF-G, LepA, RF3, and IF2.

Previous work performed by Michelle Wuerth and Justin Walter in the Spiegel lab indicated that ribosomal proteins L10, L11, and L12 purified through chemical denaturation followed by dialysis to refold do not stimulate GTPase activity on their own, even at concentrations exceeding 50 μM. The data presented here both confirm these results, as well as advance the understanding of the role L12 plays in GTPase activation and binding.

L12 alone is unable to activate GTPase activity

Thus far, the Spiegel lab has been unable to recapitulate the GTPase activity induced by L12 alone noted by Savelsbergh et al. (2000a, b). There are several possibilities for this.

First, the L12 purified by Walter and Wuerth was impure, unfolded, or improperly folded. To address this concern, we analyzed the purified protein via SDS-PAGE (Figure 4-3), and found no visible contamination. Western blot analysis proved the purified protein was the recombinant version of L12 that was overexpressed and purified via IMAC (Figure 4-4, Figure 4-3A respectively). Next, we performed circular dichroism on the purified L12, and found distinct peaks present that are associated with alpha helical structure (Figure 4-5). As this protein is nearly entirely alpha helical, excepting the flexible hinge region connecting the NTD and

CTD (Figure 1-10), we can conclude with reasonable certainty that it is not unfolded. Additionally, when purified L12 is added to an aliquot of fully depleted ribosomes, the lost activity is regained, with no significant deviation from that of intact 70S ribosomes (Figures 4-6 and 4-7).

Second, the result obtained by Savelsbergh et al. (2000a, b) may be due to contamination of their samples by trace amounts of 70S ribosomes, GTPases, or another 50S stalk protein, such as L10. It seems logical that L12 would harbor some natural affinity for L10, as they bind together *in vivo*. It is also possible that the L12 was contaminated with trace amounts of ribosomes. As no denaturation method was implemented by Savelsbergh et al. (2000a,b) to purify L12, it cannot be asserted that no active 70S was present. Previously, the Spiegel lab showed that without unfolding of the protein, purification was incomplete (Walter et al., 2011). Additionally, even in the presence of very high concentrations of L12 (~ 50 μM, data not shown), EF-G is unable to hydrolyze GTP without 70S ribosomes. While this has not yet been tested with the other translational GTPases (IF2, RF3, and LepA, it follows that the L12 protein itself is not sufficient to activate the GTPases, and requires some other activating agent.

Complete depletion of L12 from 70S ribosomes leads to total abrogation of GTP hydrolysis

Previous studies in the Spiegel lab have shown that incomplete removal of the L12 protein from $(His)_6$-tagged ribosomes leads to a significant decrease in GTP hydrolysis by translational GTPases (Walter, Master's Thesis). Recently, a method to completely remove all L12 from tagged 70S was developed (Wuerth, WWU Honors Thesis in Biochemistry). While preliminary evidence suggested that the removal of all L12 from ribosomes confers absolute loss of catalytic GTP hydrolysis, this had only been tested on EF-G one time, and still remained to be further investigated with all the translational GTPases.

Here we demonstrate that, following the two-step depletion of L12 from 70S ribosomes, EF-G is unable to catalyze the hydrolysis of GTP, as initially shown by Michelle Wuerth. Additionally, incubating the 70SΔL12 ribosomes with purified L12 led to a full return of the lost activity, with no significant difference in enzymatic rate or overall activity (p-value = 0.7396, n=5) (Figure 4-6). As a control to this experiment, L12 was added in conjunction with GTPases and GTP in order to ascertain the extent to which L12 catalyzes GTP hydrolysis. Using L12 purified through urea denaturation and subsequently refolded, the activity was identical to that of EF-G + GTP alone. These results indicated that for EF-G at least, the presence of L12 is not enough to activate the GTPase function.

This same methodology was exercised to test the effect of L12 depletion on other translational GTPases with strong homology to EF-G. RF3 and IF2 performed in a similar manner to EF-G in these assays. Both of these GTPases showed lower activity in 70SΔL12+L12 tests than with intact 70S ribosomes , though not to a statistically significant degree (RF3 p-value = 0.1673, IF2 p-value = 0.2026) (Figure 4-6). A one-tailed student's t-test was applied to determine statistical significance, comparing the complete 70S reaction with that of the 70ΔL12+L12. The differences seen in the IF2 and RF3 assays can be attributed to the experiments being performed with a separate aliquot of 70SΔL12+L12, which was improperly quantified after L12 addition, leading to a lower than expected concentrations. When the lower concentration of 70SΔL12+L12 is taken into account, the discrepancy seen between the 70S and 70SΔL12+L12 vanishes.

LepA displayed a unique result in this experiment. Though the structural homology between LepA and EF-G is striking (for domain comparison see Figure 2-4), when incubated with 70SΔL12, LepA maintained an activity level roughly half that of the activity seen with wild type 70S ribosomes. Additionally, L12 in in the presence of LepA and GTP revealed the same lack of activity found with either L12 + GTP, or LepA + GTP (Figure 4-6). Previous results in the Spiegel lab have shown that LepA maintains some activity above baseline in the presence of depleted 70S ribosomes, though these results were obtained with only the initial step of ethanol incubation for depletion, not the secondary step

which removes all $(His)_6$-tag containing proteins. This new result indicates LepA has some baseline level of GTP hydrolysis independent of the L12 protein, whereas IF2, RF3, and EF-G do not. This result was not unexpected, as Justin Walter made note of it in his Master's Thesis, but does confirm that the activity noted by him was not due to incomplete removal of L12 from the 70S. The strong homology between EF-G and LepA suggests similar mechanisms of activation, so any deviations between the two translation factors warrants further investigation.

Over the course of these experiments, it was also noted that IF2 and RF3 had significantly lower rates of GTP hydrolysis compared to EF-G and LepA (Figure 4-7). Others have noted that both of these translation factors require the presence of mRNA and/or tRNA to achieve maximal rates of catalysis, and that lower activity through interactions with vacant ribosomes is expected (Roll-Mecak et al., 2000; Zavialov et al., 2001; Roll-Mecak et al., 2004).

This result confirms the notion that L12 alone in solution is unable to activate translational GTPases, contrary to the results reported by Savelbergh et al., (2000a,b). Additionally, it validates the theory that upon complete removal of L12, all GTPase activity is lost from EF-G, IF2, and RF3, and LepA activity is significantly impaired. Hydrolysis of GTP is returned to normal levels through the reintroduction of L12 to depleted 70S ribosomes with no significant variation between wild type ribosomes and the reconstituted 70S ribosomes.

Loss of L12 from the ribosomal stock leads to a decreased binding affinity for translational GTPases

After it had been established that the removal of all L12 from 70S ribosomes led to a substantial decrease (LepA) or complete loss of activity (EF-G, RF3, and IF2), it was crucial to determine whether the translational GTPases were still able to bind to 70SΔL12.

GTPase binding assays through ultracentrifugation were designed to test basic association of GTPases to 70S ribosomes in both wild type and 70SΔL12 states (Figure 4-8). Previous reports have employed similar assays to show binding of the GTPases to 70S ribosomes in the presence of antibiotics, or with translation factor mutants (e.g. Kolupeva et al., 2005; De Laurentiis and Wieden, 2015). Disappointingly, these reports failed to show experiments such as SDS-PAGE or western blots, leading us to believe there must have been some amount of GTPase binding even in the absence of nucleotide analogs. Indeed, we see that a small, but significant, amount of GTPase associates with the 70S ribosomes in the absence of GDPNP, though it is a trace amount in comparison to the nucleotide analog-containing lane (Figure 4-9A and B lanes 4-5). As this is not seen in the EF-G only lane (Figure 4-9, lane 2), it suggests the result is not due to contamination or excessive centrifugation but rather a natural affinity of the GTPases to bind to the 70S ribosomes, even in the absence of GTP or GDPNP. This binding does not indicate GTP hydrolysis is occurring (controls shown in

Figures 4-6 and 4-7). When this was repeated using 70SΔL12, nearly all the association between EF-G and the 70S ribosomes vanished, indicating that the lack of GTPase activity seen in the malachite green inorganic phosphate assays (Figures 4-6 and 4-7) is likely due to a lack of binding, not explicitly due to a decrease in the ability to hydrolyze GTP without the L12 protein. Specifically, we see that IF2 and RF3 have the same binding profile as that of EF-G, while LepA is able to bind to 70SΔL12 to a much higher degree. While the LepA+70S and LepA+GDPNP+70S lanes are very similar to those seen with the other translational GTPases, the removal of L12 still permits LepA to bind at nearly 1.5 times the level seen in the no nucleotide control, a result not seen with IF2, RF3, or EF-G (Table 4-1).

BioLayer Interferometry

In order to more precisely quantitate the binding affinity of GTPases to 70S or 70SΔL12 ribosomes, BioLayer Interferometry experiments were conducted. The BLI data shown earlier (Figures 4-10 and 4-11) indicate that the removal of L12 causes a complete abrogation in GTPase binding to 70S ribosomes. Initial experiments performed tested the binding affinity of EF-G to complete 70S ribosomes (Figure 4-10, Table 4-2). K_D values in the range of 5-100 nM were generated, which correlate well with previously published values. Lancaster et al. (2008) published a K_D of ~26 nM for the binding of EF-G to the 50S subunit, while Munishkin and Wool (1997) reported a K_D of 700 nM for binding to intact

70S ribosomes, albeit with a different, less precise method of quantitation. Our data, averaging ~160 nM (n=2 at each concentration) for the initial studies, falls directly between these two oft-cited values (Munishkin and Wool, 1997; Lancaster et al., 2008).

In order to ascertain the effect of L12 depletion on binding, 70S ribosomes with or without L12 were incubated with EF-G prior to the association of EF-G to the ribosomes bound on the BLI tip. When incubated with 70SΔL12, EF-G showed no significant change in affinity towards binding to intact 70S ribosomes (Figure 4-11, red), as was be expected. If significant association occurred between 70SΔL12 and EF-G, we would see either no increase in binding, or a more gradual increase. Instead, the slope of this line is approximately equivalent to that of the positive control reactions (Figure 4-11, blue, green, and magenta). The slight increase in k_a seen for this trial is likely do to an altered concentration of EF-G, compared to that stated. The 3200 nM EF-G solution was made prior to the addition of saturating concentration of 70S or 70SΔL12, thereby lowering the concentration to 2600 nM. In contrast to this, a distinct lack of binding is seen intact 70S ribosomes are incubated with EF-G prior to association with 70S ribosomes bound to the Ni-NTA tip (Figure 4-11, black). The lack of an increase in binding here demonstrates that the majority of the EF-G was bound to 70S ribosomes in solution rather than those immobilized on the Ni-NTA tip. Together, these results indicate that 70S ribosomes have little to no affinity for EF-G when

the L12 protein is not present. Quantitatively, we see similar K_D values for the trials containing only EF-G, or EF-G with 70SΔL12. The decrease in K_D seen in the EF-G + 70SΔL12 trial is due to the increase in K_a noted above. The K_D for EF-G + 70S however was >10,000 fold higher, indicating that little to no EF-G in solution was able to bind to the immobilized 70S ribosomes.

Conclusions

The work presented here confirms much of what has been suspected by the Spiegel lab concerning the role of the L12 ribosomal protein in the activation of translational GTPases. We established that L12 is necessary for complete activation of translational GTPases EF-G, RF3, IF2, and LepA. Removal of this protein either completely abolishes (EF-G, RF3, and IF2) or significantly diminishes (LepA) the ribosome dependent GTPase activity, and reintroduction of this protein restores this activity with no significant differences noticed between pre- and post-depletion 70S ribosomes.

GTPase association to the 70S ribosome is also significantly inhibited upon removal of the L12 protein. The GTPase binding assays by ultracentrifugation demonstrate that GDPNP bound EF-G, IF2, RF3, and LepA exhibit a much stronger binding to 70S over 70SΔL12 ribosomes. LepA did show a significantly higher binding to 70SΔL12 than the other translational GTPases however, this result that warrants further investigation.

Thus far, we have been unable to test the binding of any translational GTPase using BioLayer Interferometry save EF-G, but experiments are currently being undertaken to determine if the same conditions yield similar results for LepA, IF2, and RF3. Further investigation of all translational GTPases will be necessary to determine the mechanism behind the ability of LepA to function without L12.

Future Work

We have shown that the L12 protein is essential for the activity and binding of EF-G, RF3, and IF2. However, the interesting results obtained with LepA need to be investigated further. Specifically, we will probe the interactions of LepA domain mutants with 70SΔL12 ribosomes to determine which domain allows for 50% activity to be maintained in the absence of L12. SDM can be used to generate these mutants, and the same assays employed above will allow for rapid characterization of the mutants with intact and depleted ribosomes.

Chapter 5 – Effect of EF-G domain deletion on GTP Hydrolysis Activity

Results

The IV and G' coding regions of the FusA gene can be successfully deleted from the wild-type EF-G gene

The Spiegel lab had previously created mutants of EF-G that deleted either the 5, or the 4 and 5 domains. These two mutants have been well characterized (Savelsbergh et al., 2000a; Walter et al., 2011; unpublished work in the Spiegel lab). In order to further investigate the role of the G' and 4 domains on GTPase activity, these two domains were targeted for individual deletion (Figure 5-1). Primers to remove the 4 domain of EF-G were designed based on the domain structure of EF-G, and residues 483-603 were marked for deletion. SDM was performed through PCR as described (Materials and Methods) and the resultant plasmid was transformed into XL-10 Gold chemically competent *E. coli* cells. Restriction digestion of this plasmid determined if the generated mutant genes were the correct size (Figure 5-2). We can see from lane 4 where the appropriate bands for full length EF-G and the pSV281 vector should appear. The *FusA* gene, coding for EF-G is ~2200 base pairs (bp) (lane 4, bottom band), while the pSV is ~5600 bp (lane 4, top band). After SDM to delete domain 4, we expect to see a loss of ~360 bp from the full length EF-G gene. Lanes 7 through 10 clearly

indicate a band midway between the 1500 and 2000 bp markers, approximately the correct size for EF-GΔ4. To confirm that the desired sequence was generated, plasmids were sequenced at the Nevada Genomics Center (University of Nevada, Reno; Figure 5-3). Due to the method of SDM employed to generate this mutant, half of each primer should bind to either side of the region to be deleted. Assuming successful deletion of the 4 domain, we should see the full primer sequence (Table 3-1), with no interrupting bases present in the sequencing results. Figure 5-3A contains the full sequence of the EF-G DNA, with the first half of the forward primer highlighted in yellow, and the second half in blue. Figure 5-3B and C show successful removal of the 4 domain from the EF-G gene, whereas Figure 5-3D demonstrates unsuccessful deletion (non-adjacent primer sequences).

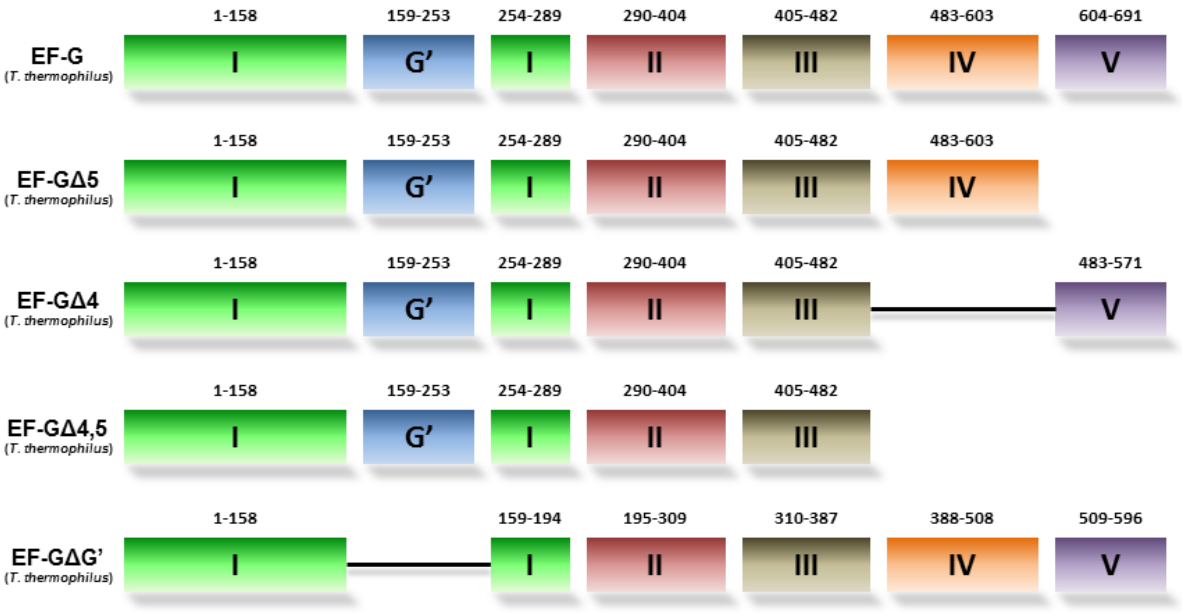

Figure 5-1. Domain comparison of EF-G and associated mutants, showing the amino acid residues after deletion of the indicated domain. Domains are color coded for easy visualization of retained domains.

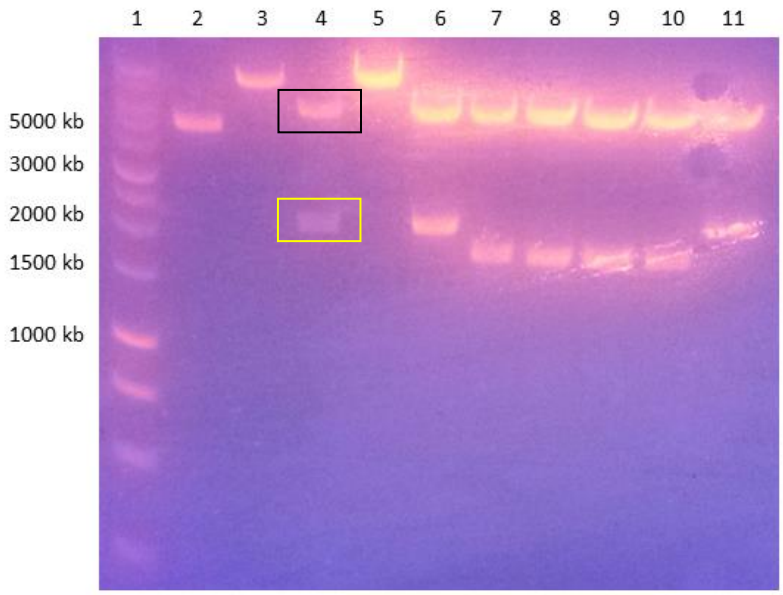

Figure 5-2. Restriction digestion of EF-GΔ4 plasmid. GelRed (Biotium) stained 1% agarose gel. (1) 1 kb DNA ladder, (2) pEF-G uncut, (3) pEF-G cut with *Xho*I, (4) pEF-G cut with *Xho*I and *Bam*HI, (5) pEF-GΔ4 cut with *Xho*I, (6-11) pEF-GΔ4 cut with *Xho*I and *Bam*HI. Black box: empty pSV vector. Yellow box: Full length EF-G gene.

Figure 5-3. Confirmation of the deletion of the 4 domain from EF-G. **(A)** The full reverse complement sequence of EF-G DNA. Blue: binding site for the first half of the forward primer, yellow: binding site for the second half of the primer. **(B and C)** Sequences showing successful deletion of the domain 4 DNA, demonstrating the complete removal of all bases between the two primer binding sites. **(D)** Unsuccessful deletion of the domain 4 of EF-G.

The G' domain of EF-G had been successfully removed via site directed mutagenesis by other groups (Nechifor et al., 2007; Mikolajka et al., 2011). In an attempt to further investigate the function the G' domain plays in GTP hydrolysis activity and 70S ribosome-GTPase binding, primers were designed to mirror the more successful G' deletion mutant found by Mikolajka et al. (2011). SDM was performed as it was for EF-GΔ4, and residues 167-260 of *E. coli* EF-G were targeted for deletion. Subsequent restriction digestion of the PCR product was analyzed to determine if the correct size gene was produced. Digestion of the full EF-G gene in the pSV showed identical results to Figure 5-2 (Figure 5-4, lanes 2 through 4). Digestion of the mutant plasmid with *Xho*I and *Bam*HI showed a band present just below the 2000 bp markers, corresponding to an approximately 280 bp loss, as expected (Figure 5-4, lanes 5-9). Sequencing results confirmed successful generation of EF-GΔG' through the appearance of the full forward primer sequence in the mutant plasmid (Figure 5-5).

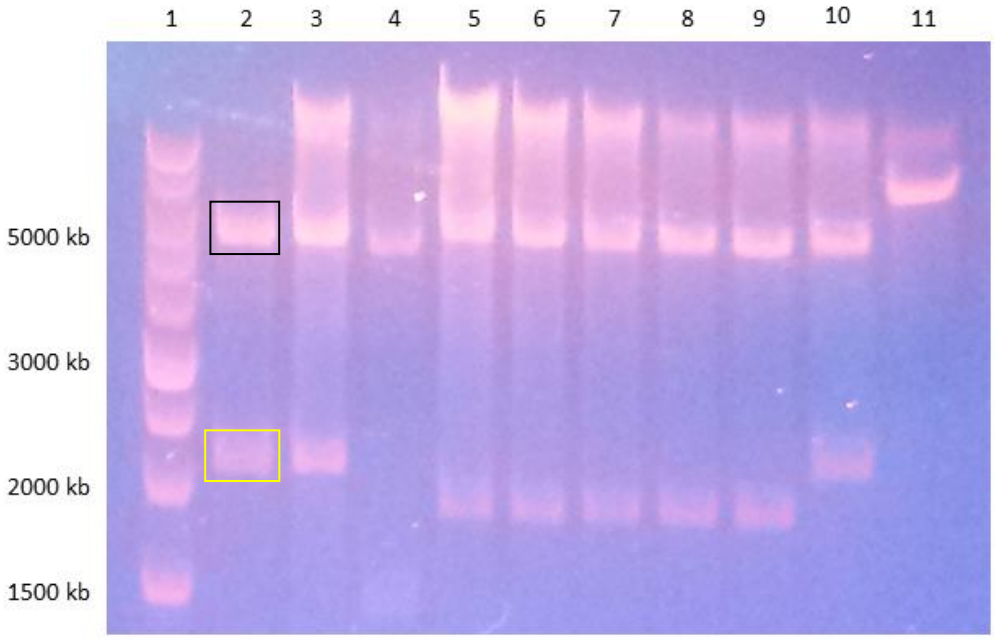

Figure 5-4. Restriction digestion of EF-GΔG' DNA. GelRed (Biotium) stained 1% agarose gel. (1) 1 kb DNA ladder, (2) pEF-G cut with *Bam*HI and *Xho*I, (3) pEF-G cut with *Bam*HI and *Xho*I, (4)p EF-G cut with *Bam*HI, (5-10) pEF-GΔG' cut with *Bam*HI and *Xho*I, (11) pEF-GΔG' *Bam*HI. Black box – empty pSV vector. Yellow box – full length EF-G gene.

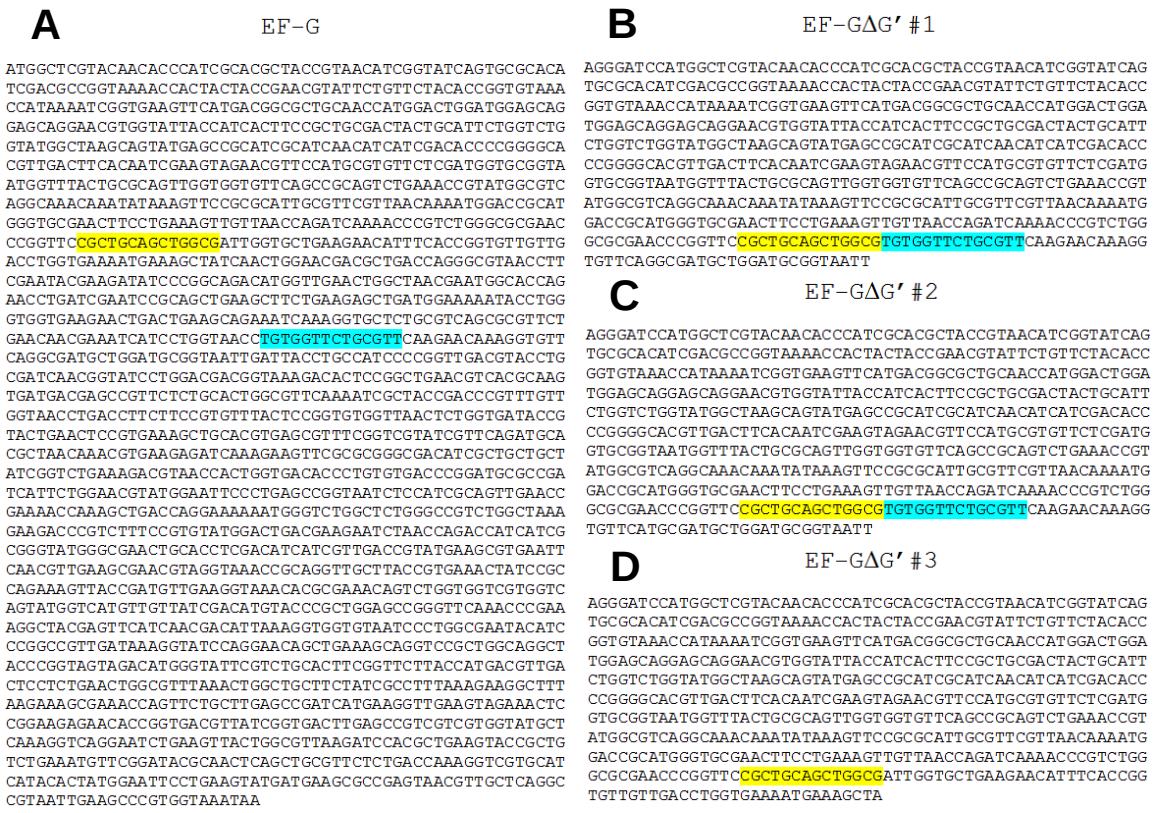

Figure 5-5. Confirmation of the deletion of the G' subdomain from EF-G. **(A)** The full sequence of EF-G DNA. Yellow: sequence of the first half of the forward primer, blue: sequence of the second half of the forward primer. **(B and C)** Sequences showing successful deletion of the G' domain DNA, demonstrating the complete removal of all bases between the two primer binding sites. **(D)** Unsuccessful deletion of the G' subdomain DNA.

EF-GΔ4 and EF-GΔG' do not express and purify cleanly

Once sequences had been confirmed for both EF-GΔG' and EF-GΔ4, the proteins were expressed as described above (Materials and Methods) and purified. Initial efforts proved futile, as SDS-PAGE results showed extremely impure protein in both cases (Figure 5-6).

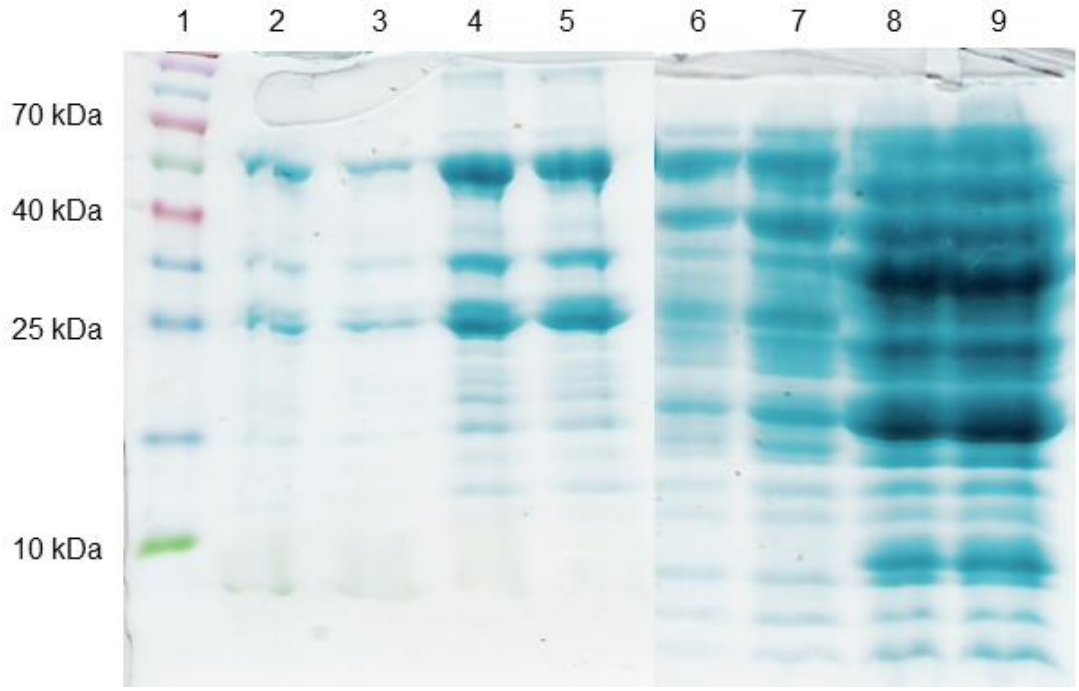

Figure 5-6. Initial purification efforts of EF-GΔ4 and EF-GΔG'. Coomassie stained 15% SDS-PAGE gel. (1) MW ladder, (2) EF-GΔ4 #1 from NiCo21 cells, (3)EF-GΔ4 #1 from BL-21 cells, (4) EF-GΔ4#2 from NiCo21 cells, (5) EF-GΔ4#2 from BL-21 cells, (6) EF-GΔG'#1 from BL-21 cells, (7) EF-GΔG'#2 from BL-21 cells, (8) EF-GΔG'#1 from NiCo21 cells, (9) EF-GΔG'#2 from NiCo21 cells.

After experimentation with several different growth temperatures, induction temperatures, purification buffers, and additional purification steps, EF-GΔ4 was eventually purified cleanly, using an overexpression temperature of 20°C rather than the typical 15°C for traditional translational GTPases. Additionally, EF-GΔ4 purified with fewer contaminating bands if the concentration of IPTG was kept below 400 μM and the post induction incubation time was kept below 8 hours as demonstrated by the prevalent low molecular weight contamination bands seen

in lanes 4 and 5, as opposed to lane 3 (Figure 5-7). Anion exchange chromatography was utilized to further purify this mutant protein.

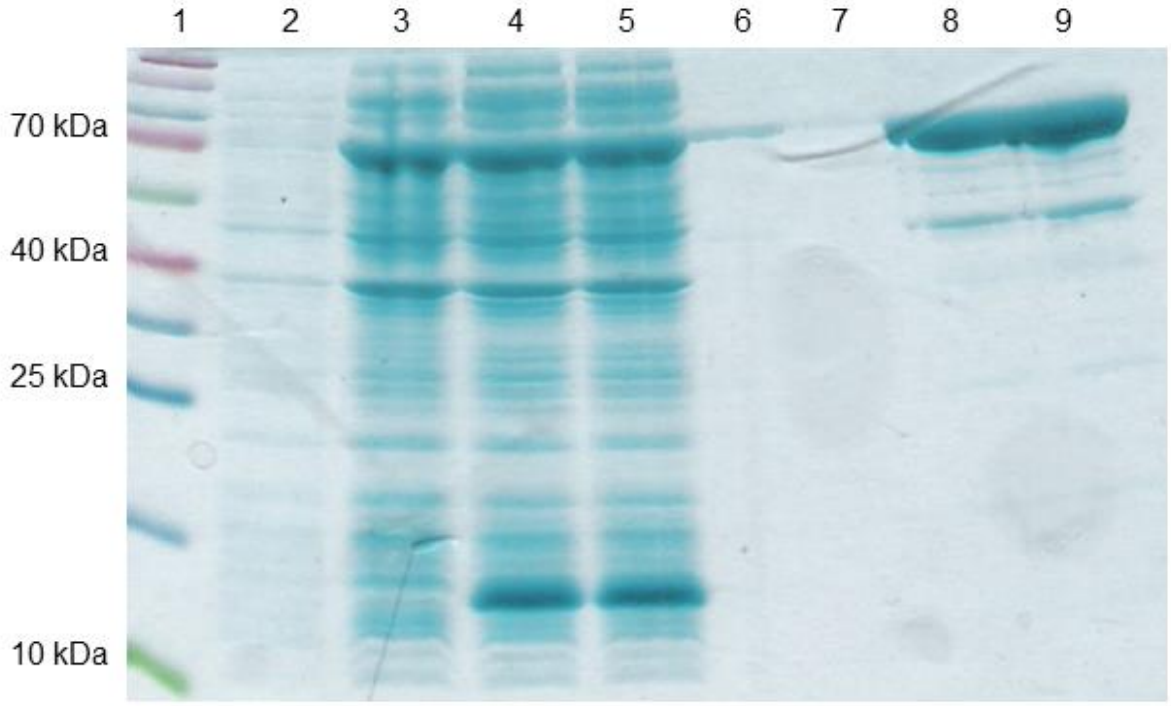

Figure 5-7. Purification of EF-GΔ4. Coomassie stained 15% SDS-PAGE gel. (1) MW Ladder, (2) 0 µM IPTG, 12 hour induction, (3) 400 µM IPTG, 8 hour induction, (4) 400 µM IPTG, 12 hour induction, (5) 400 µM IPTG, 16 hour induction, (6-7) Post AEC fractions, (8-9) Concentrated post IMAC fractions.

EF-GΔG' proved to be more recalcitrant. A brief email exchange with Mikolajka et al. (2011) indicated that they had the same troubles in isolating and purifying this mutant. As with EF-GΔ4, many different growth and induction temperatures were attempted, along with different concentrations of IPTG. Ultimately, the same conditions that proved effective for EF-GΔ4 were attempted for EF-GΔG', with

moderate success (Figure 5-8). Substituting TALON^{TM} resin yielded a much larger quantity of protein than the Ni-NTA resin (Figure 4-8). AEC increased purity significantly (Figure 5-9).

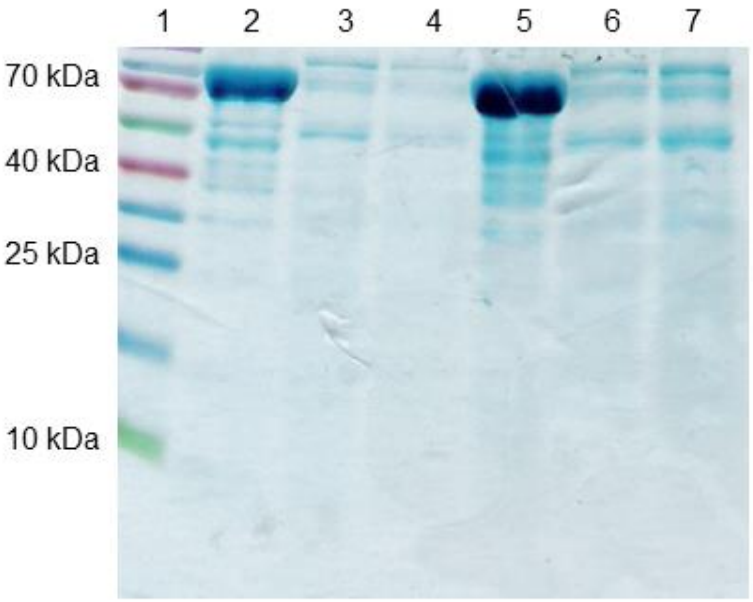

Figure 5-8. EF-GΔG' purification with Ni-NTA and TALON^{TM} resins. Coomassie stained 15% SDS-PAGE gel. (1) MW Ladder, (2) Ni-NTA elution, (3-4) Ni-NTA washes, (5) TALON elution, (6-7) TALON washes.

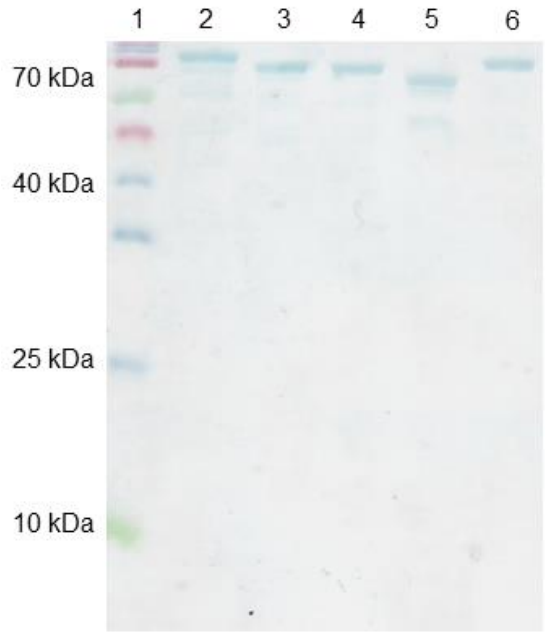

Figure 5-9. EF-G and all associated domain mutants. Coomassie stained 15% SDS-PAGE gel. (1) MW ladder, (2) EF-G, (3) EF-GΔ4, (4) EF-GΔ5, (5) EF-GΔ4,5, (6) EF-GΔG'. Impurities seen in EF-GΔ4,5 are due to insufficient washing and were removed via AEC.

GTP hydrolysis by EF-G domain mutants

Once all domain mutants were sufficiently pure, the GTP hydrolysis activity of each was evaluated using the malachite green inorganic phosphate assay described earlier. The level of each domain mutant was compared to that of the wild type EF-G protein in the presence or absence of 70S ribosomes (Figure 5-10). There was no significant change in activity upon the removal of the $(His)_6$-tag from EF-G, indicating the presence or removal of this tag does not alter the GTP hydrolysis activity of EF-G in a significant way (Figure 5-10, blue and red). EF-GΔ4 and EF-GΔ4,5 exhibit very similar activities, both maintaining around 65% of

the maximum activity (Figure 5-10, yellow and magenta). EF-GΔ5 has a higher activity than that seen in EF-GΔ4 or EF-GΔ4,5, at around 85%. The G' deletion mutant has the lowest activity, at approximately 15% that of full length EF-G.

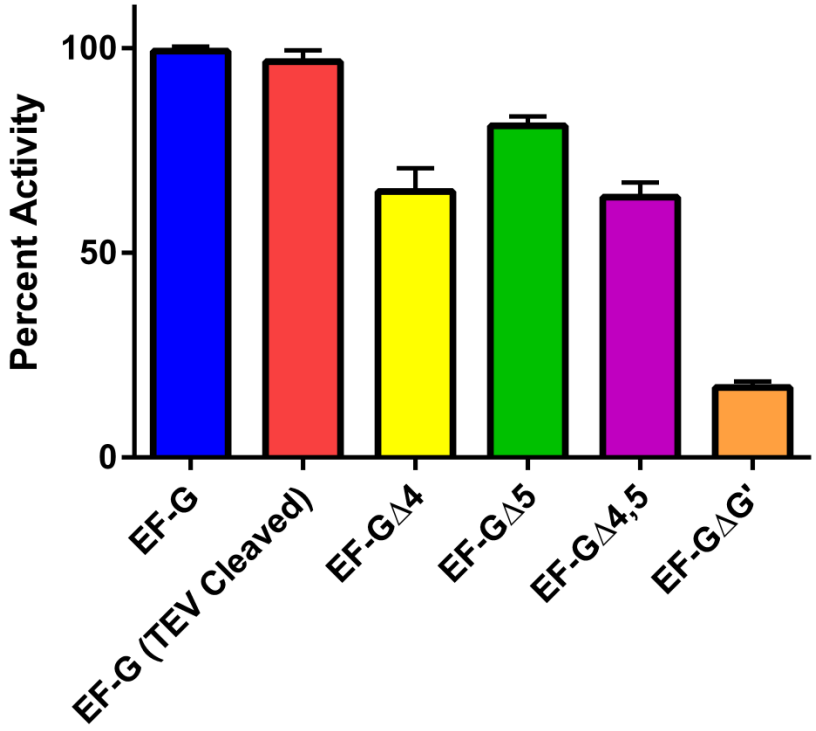

Figure 5-10. GTP hydrolysis by EF-G domain mutants. All data were normalized to full length $(His)_6$-tagged EF-G. All experiments were performed in triplicate.

Discussion

The removal of an entire domain from a protein is often a risky experiment. The excision of an internal domain, such as the G' or the IV domain of EF-G has the possibility of interrupting significant secondary and tertiary structural elements within the protein, causing it to become unstable, misfolded, or expressed within inclusion bodies, and therefore extremely difficult to purify. However, both EF-GΔ4 and EF-GΔG' were expressed and purified successfully in the past, though both remain understudied (Rodnina et al., 1997; Mikolajka et al., 2011). Generation of these domain mutants allowed the Spiegel lab to investigate the function of each domain in relation to the full length EF-G.

EF-GΔ4 and EF-GΔG' are both expressed in the soluble fraction, and require no denaturation steps for purification

When Rodnina et al. (1997) first designed the EF-GΔ4 mutant they noted that it was expressed in inclusion bodies, and required denaturation and subsequent dialysis to obtain pure, functional protein. Fortunately, the EF-GΔ4 we purified is both soluble and readily purified through IMAC and AEC (Figure 5-6, Figure 5-7).

The EF-GΔG' mutant was designed based on previous work from the lab of Dr. Cooperman at the University of Pennsylvania (Mikolajka et al., 2011). While the protein we isolated was soluble and could be sufficiently purified through IMAC and AEC, (Figure 5-6 and Figure 5-8) it precipitated out of solution at concentrations greater than ~1 mg/mL, making any in vitro assay difficult to

perform. In conferring with the Cooperman lab it was disclosed that the EF-GΔG' protein they reported was also exceedingly difficult to work with, and had solubility issues causing them to cease working with it immediately after the publication in which it was reported. In an effort to reduce the amount of EF-GΔG' precipitating, it was stored at a low concentration, and concentrated immediately prior to experimentation. This allowed us to work with EF-GΔG' concentrations up to 4 mg/mL in GTP hydrolysis assays while not having precipitation occur immediately upon thawing the protein on ice.

All EF-G domain mutants tested maintain some GTPase activity

In order to investigate if the domain mutants retained their ability to hydrolyze GTP, the malachite green assay described earlier (Chapter 4) was applied again (Figure 5-10). Compared to full length EF-G, none of the domain deletions retained complete GTPase activity. The Spiegel lab has shown previously that EF-GΔ5 demonstrated an average of ~80% of the activity of full length EF-G, while EF-GΔ4,5 maintained approximately 65% activity, and those results are replicated here (Walter et al., 2011; unpublished work). EF-GΔ4 surprisingly showed the same relative activity as EF-GΔ4,5, retaining 65% GTP hydrolysis activity compared to full length EF-G. This suggests that the deletion of the 4 domain from EF-GΔ4,5 may be a strong determinant in GTP hydrolysis activity, an idea supported by work from Savelsbergh et al. (2000b). The EF-GΔG' mutant had an activity almost 10 fold lower than that of full length EF-G. This is in

agreement with the data provided by Mikolajka et al. (2011) in which they reported a greater than 10 fold reduction in GTPase activity upon the deletion of the G' subdomain. This result is not altogether surprising given that the G' subdomain has been shown to make direct interactions with the L12 protein (Datta et al., 2005; Connell et al., 2007; Gao et al., 2009). As demonstrated in chapter 4, the loss of the ability of L12 to bind EF-G led to an immediate abolition of GTP hydrolysis. Given that some activity is maintained by EF-GΔG', it follows that the L12 protein likely has some interactions with EF-G that are not located on the G' domain. Moreover, as LepA is devoid of a G' domain yet has reduced activity in the absence of L12, an as-of-yet undescribed interaction between L12 and EF-G must exist.

The role of EF-G domains in translocation and recycling

While the role of EF-G in translocation is firmly established, the overall function of each domain remains controversial. Much of this chapter was dedicated to discussing the isolation and purification of EF-G and the associated domain mutants (EF-GΔ4, EF-GΔ4,5, EF-GΔ5, and EF-GΔG'). It seems likely that EF-GΔ4 and EF-GΔ4,5, having similar GTPase activity, will influence translocation similarly. While domain 4 is known to play a role in proper tRNA translocation, as shown by Savelsbergh et al. (2000a), the role of domain 5 is still theoretical. It is thought to serve to communicate between domains 1 and 4, suggesting that EF-GΔ4 and EF-GΔ4,5 may have the same effect, as they both lack the 4 domain,

and would therefore not allow proper communication between the domains. As so much is still an unknown concerning the role of EF-G in ribosome recycling, it is difficult to speculate on how these domain mutants might influence this complex process.

EF-GΔG', in contrast to EF-GΔ4, had very low GTP hydrolysis activity, which may be due to slower dissociation of the translation factor from the ribosome than with full length EF-G (Gao et al., 2009). Gao et al. showed that, when incubated with 70S ribosomes and GTP for a prolonged period of time (upwards of 18 hours, versus 1 hour for full length EF-G), the eventual GTP hydrolysis activity reached levels equivalent to full length EF-G. If the role of the L12 protein is to facilitate binding and dissociation of translational GTPases, then it follows that the removal of the G' domain interaction with L12 would lead to a substantially decreased activity. The G domain likely plays an important role in ribosome recycling, as it is a GTP depended process, however the G' domain may not be necessary here. Further study is needed to better understand the role of each domain in translocation and ribosome recycling.

Conclusions

Several domain deletion constructs of EF-G have been successfully generated, purified, and evaluated for ribosome-dependent GTPase activity. The EF-GΔ4 and Δ4,5 mutants maintain about 65% GTP hydrolysis activity, whereas EF-GΔ5 exhibits 80-85% of the activity seen in full length EF-G. EF-GΔG' retains a low level of GTPase activity in comparison to wild type EF-G, but still maintains ribosome-dependent GTP hydrolysis. While the precise role of the G' domain remains elusive, the notion that GTPase activity is significantly lower, though still present, points toward a more intricate role for the L12 ribosomal protein than previously theorized (Savelsbergh et al., 2000b; Gao et al., 2009).

Future Work

Each EF-G domain mutant needs to be evaluated for the GTP hydrolysis activity in the presence of 70SΔL12 ribosomes. Of particular interest is the EF-GΔG' mutant, as the L12-EF-G interaction is well established (Gao et al., 2009). The ability of each mutant to bind 70S and 70SΔL12 ribosomes through the GTPase binding assays described for IF2, RF3, and LepA is also of interest. Additionally, the role of each domain in ribosome recycling can easily be assessed through a ribosome recycling assay in the presence of RRF (Luchin et al., 1999; Kiel et al., 2006). The methods for each of these experiments are already well established (Materials and Methods). Additionally, the role of the each domain in the stabilization of ribosomal translocation can be easily assessed through single

molecule fluorescence resonance energy transfer technique. Completion of these studies will allow us to determine the overall role of each domain in EF-G activity, binding, translocation, and recycling of ribosomes.

References

Achila, D., Gulati, M., Jain, N. and Britton, R.A. (2012). Biochemical characterization of ribosome assembly GTPase rbgA in *Bacillus subtilis*. Journal of Biological Chemistry *287*, 8417–8423.

Agrawal, R.K., Penczek, P., Grassucci, R.A. and Frank, J. (1998). Visualization of elongation factor G on the *Escherichia coli* 70S ribosome: The mechanism of translocation. Proceedings of the National Academy of Sciences *95*, 6134–6138.

Agrawal, R.K., Heagle, A.B., Penczek, P., Grassucci, R.A. and Frank, J. (1999). EF-G-dependent GTP hydrolysis induces translocation accompanied by large conformational changes in the 70S ribosome. Nature Structural & Molecular Biology *6*, 643–647.

Agrawal, R.K., Linde, J., Sengupta, J., Nierhaus, K.H. and Frank, J. (2001). Localization of L11 protein on the ribosome and elucidation of its involvement in EF-G-dependent translocation1. Journal of Molecular Biology *311*, 777–787.

Agrawal, R.K., Sharma, M.R., Kiel, M.C., Hirokawa, G., Booth, T.M., Spahn, C.M.T., Grassucci, R.A., Kaji, A. and Frank, J. (2004). Visualization of ribosome-recycling factor on the *Escherichia coli* 70S ribosome: Functional implications. Proceedings of the National Academy of Sciences *101*, 8900–8905.

Ammons, D., Rampersad, J. and Fox, G.E. (1999). 5S rRNA gene deletions cause an unexpectedly high fitness loss in *Escherichia coli*. Nucleic Acids Research *27*, 637–642.

Balakrishnan, R., Oman, K., Shoji, S., Bundschuh, R. and Fredrick, K. (2014). The conserved GTPase LepA contributes mainly to translation initiation in *Escherichia coli*. Nucleic Acids Research gku1098.

Ball, L.A. and Kaesberg, P. (1973). Cleavage of the N-terminal formymlethionine residue from a bacteriophage coat protein in vitro. Journal of Molecular Biology *79*, 531–537.

Ban, N., Nissen, P., Hansen, J., Moore, P.B. and Steitz, T.A. (2000). The complete atomic structure of the large ribosomal subunit at 2.4 Å resolution. Science *289*, 905–920.

Barta, A., Dorner, S. and Polacek, N. (2001). Mechanism of ribosomal peptide bond formation. Science *291*, 203–203.

Ben-Shem, A., Jenner, L., Yusupova, G. and Yusupov, M. (2010). Crystal structure of the eukaryotic ribosome. Science *330*, 1203–1209.

Berchtold, H., Reshetnikova, L., Reiser, C.O.A., Schirmer, N.K., Sprinzl, M. and Hilgenfeld, R. (1993). Crystal structure of active elongation factor Tu reveals major domain rearrangements. Nature *365*, 126–132.

Beringer, M. (2008). Modulating the activity of the peptidyl transferase center of the ribosome. RNA *14*, 795–801.

Blanchard, S.C., Kim, H.D., Gonzalez, R.L., Puglisi, J.D. and Chu, S. (2004a). tRNA dynamics on the ribosome during translation. Proceedings of the National Academy of Sciences *101*, 12893–12898.

Blanchard, S.C., Gonzalez, R.L., Kim, H.D., Chu, S. and Puglisi, J.D. (2004b). tRNA selection and kinetic proofreading in translation. Nature Structural & Molecular Biology *11*, 1008–1014.

Brown, C.M. and Tate, W.P. (1994). Direct recognition of mRNA stop signals by *Escherichia coli* polypeptide chain release factor two. Journal of Biological Chemistry *269*, 33164–33170.

Cleveland, D.W., Fischer, S.G., Kirschner, M.W. and Laemmli, U.K. (1977). Peptide mapping by limited proteolysis in sodium dodecyl sulfate and analysis by gel electrophoresis. Journal of Biological Chemistry *252*, 1102–1106.

Connell, S.R., Takemoto, C., Wilson, D.N., Wang, H., Murayama, K., Terada, T., Shirouzu, M., Rost, M., Schüler, M., Giesebrecht, J., et al. (2007). Structural basis for interaction of the ribosome with the switch regions of GTP-bound elongation factors. Molecular Cell *25*, 751–764.

Crick, F.H. (1968). The origin of the genetic code. Journal of Molecular Biology *38*, 367–379.

Crick, F.H. (1970). Central dogma of molecular biology. Nature *227*, 561–563.

Czworkowski, J., Wang, J., Steitz, T.A. and Moore, P.B. (1994). The crystal structure of elongation factor G complexed with GDP, at 2.7 A resolution. EMBO Journal *13*, 3661–3668.

DeLaurentiis, E.I. and Wieden, H.J. (2015). Identification of two structural elements important for ribosome-dependent GTPase activity of elongation factor 4 (EF4/LepA). Scientific Reports *5*.

Dever, T.E. and Green, R. (2012). The elongation, termination, and recycling phases of translation in eukaryotes. Cold Spring Harbor Perspectives in Biology *4*, a013706.

Diaconu, M., Kothe, U., Schlünzen, F., Fischer, N., Harms, J.M., Tonevitsky, A.G., Stark, H., Rodnina, M.V. and Wahl, M.C. (2005). Structural basis for the function of the ribosomal L7/12 stalk in factor binding and GTPase activation. Cell *121*, 991–1004.

Ederth, J., Mandava, C.S., Dasgupta, S. and Sanyal, S. (2009). A single-step method for purification of active His-tagged ribosomes from a genetically engineered *Escherichia coli*. Nucleic Acids Research *37*, e15–e15.

Evans, R.N., Blaha, G., Bailey, S. and Steitz, T.A. (2008). The structure of LepA, the ribosomal back translocase. Proceedings of the National Academy of Sciences *105*, 4673–4678.

Frank, J., Sengupta, J., Gao, H., Li, W., Valle, M., Zavialov, A. and Ehrenberg, M. (2005). The role of tRNA as a molecular spring in decoding, accommodation, and peptidyl transfer. FEBS Letters *579*, 959–962.

Ganoza, M.C., Kiel, M.C. and Aoki, H. (2002). Evolutionary Conservation of Reactions in Translation. Microbiology and Molecular Biology Reviews *66*, 460–485.

Gao, H., Zhou, Z., Rawat, U., Huang, C., Bouakaz, L., Wang, C., Cheng, Z., Liu, Y., Zavialov, A., Gursky, R., et al. (2007). RF3 induces ribosomal Conformational changes responsible for dissociation of class I release factors. Cell *129*, 929–941.

Gao, Y.-G., Selmer, M., Dunham, C.M., Weixlbaumer, A., Kelley, A.C. and Ramakrishnan, V. (2009). The structure of the ribosome with elongation factor G trapped in the posttranslocational state. Science *326*, 694–699.

Gray, M.W., Sankoff, D. and Cedergren, R.J. (1984). On the evolutionary descent of organisms and organelles: a global phylogeny based on a highly

conserved structural core in small subunit ribosomal RNA. Nucleic Acids Research *12*, 5837–5852.

Gualerzi, C.O. and Pon, C.L. (1990). Initiation of mRNA translation in prokaryotes. Biochemistry *29*, 5881–5889.

Guo, X., Peisker, K., Bäckbro, K., Chen, Y., Koripella, R.K., Mandava, C.S., Sanyal, S. and Selmer, M. (2012). Structure and function of FusB: an elongation factor G-binding fusidic acid resistance protein active in ribosomal translocation and recycling. Open Biology *2*, 120016.

Gutell, R.R., Gray, M.W. and Schnare, M.N. (1993). A compilation of large subunit (23S and 23S-like) ribosomal RNA structures: 1993. Nucleic Acids Research *21*, 3055–3074.

Harder, K.W., Owen, P., Wong, L.K., Aebersold, R., Clark-Lewis, I., and Jirik, F.R. (1994). Characterization and kinetic analysis of the intracellular domain of human protein tyrosine phosphatase beta (HPTP beta) using synthetic phosphopeptides. Biochemical Journal *298*, 395–401.

Helgstrand, M., Mandava, C.S., Mulder, F.A.A., Liljas, A., Sanyal, S. and Akke, M. (2007). The ribosomal stalk binds to translation factors IF2, EF-Tu, EF-G and RF3 via a conserved region of the L12 C-terminal Domain. Journal of Molecular Biology *365*, 468–479.

Hirashima, A. and Kaji, A. (1972). Purification and properties of ribosome-releasing factor. Biochemistry *11*, 4037–4044.

Hirokawa, G., Nijman, R.M., Raj, V.S., Kaji, H., Igarashi, K. and Kaji, A. (2005). The role of ribosome recycling factor in dissociation of 70S ribosomes into subunits. RNA *11*, 1317–1328.

Jin, H., Kelley, A.C. and Ramakrishnan, V. (2011). Crystal structure of the hybrid state of ribosome in complex with the guanosine triphosphatase release factor 3. Proceedings of the National Academy of Sciences *108*, 15798–15803.

Joyce, G.F. (2002). The antiquity of RNA-based evolution. Nature. *418*, 214–221.

Kisselev, L., Ehrenberg, M. and Frolova, L. (2003). Termination of translation: interplay of mRNA, rRNAs and release factors? The EMBO Journal *22*, 175–182.

Kolupaeva, V.G., Unbehaun, A., Lomakin, I.B., Hellen, C.U.T. and Pestova, T.V. (2005). Binding of eukaryotic initiation factor 3 to ribosomal 40S subunits and its role in ribosomal dissociation and anti-association. RNA *11*, 470–486.

Kong, C., Ito, K., Walsh, M.A., Wada, M., Liu, Y., Kumar, S., Barford, D., Nakamura, Y. and Song, H. (2004). Crystal structure and functional analysis of the eukaryotic class II release factor eRF3 from *S. pombe.* Molecular Cell *14*, 233–245.

Kozak, M. (1999). Initiation of translation in prokaryotes and eukaryotes. Gene *234*, 187–208.

Lambert, T. (2012). Antibiotics that affect the ribosome. Revue Scientifique et Technique *31*, 57–64.

Walter, J.D., Hunter, M., Cobb, M., Traeger, G., and Spiegel, P.C. (2011). Thiostrepton inhibits stable 70S ribosome binding and ribosome-dependent GTPase activation of elongation factor G and elongation factor 4. Nucl. Acids Res. *40*, 360–370.

Laurberg, M., Kristensen, O., Martemyanov, K., Gudkov, A.T., Nagaev, I., Hughes, D. and Liljas, A. (2000). Structure of a mutant EF-G reveals domain III and possibly the fusidic acid binding site1. Journal of Molecular Biology *303*, 593–603.

Leung, E.K.Y., Suslov, N., Tuttle, N., Sengupta, R. and Piccirilli, J.A. (2011). The Mechanism of peptidyl transfer catalysis by the ribosome. Annual Review of Biochemistry *80*, 527–555.

Liljas, A. and Gudkov, A.T. (1987). The structure and dynamics of ribosomal protein L12. Biochimie *69*, 1043–1047.

Luchin, S., Putzer, H., Hershey, J.W.B., Cenatiempo, Y., Grunberg-Manago, M. and Laalami, S. (1999). In vitro study of two dominant inhibitory GTPase mutants of *Escherichia coli* translation initiation factor IF2 direct evidence that GTP hydrolysis is necessary for factor recycling. Journal of Biological Chemistry *274*, 6074–6079.

March, P.E. and Inouye, M. (1985). GTP-binding membrane protein of *Escherichia coli* with sequence homology to initiation factor 2 and elongation

factors Tu and G. Proceedings of the National Academy of Sciences *82*, 7500–7504.

Martemyanov, K.A. and Gudkov, A.T. (1999). Domain IV of elongation factor G from *Thermus thermophilus* is strictly required for translocation. FEBS Letters *452*, 155–159.

Schmeing, M.T., Huang, K.S., Strobel, S.A. and Steitz, T.A. (2005). An induced-fit mechanism to promote peptide bond formation and exclude hydrolysis of peptidyl-tRNA. Nature *438*, 520–524.

Melnikov, S., Ben-Shem, A., Garreau de Loubresse, N., Jenner, L., Yusupova, G. and Yusupov, M. (2012). One core, two shells: bacterial and eukaryotic ribosomes. Nature Structural & Molecular Biology*19*, 560–567.

Mikolajka, A., Liu, H., Chen, Y., Starosta, A.L., Márquez, V., Ivanova, M., Cooperman, B.S. and Wilson, D.N. (2011). Differential effects of thiopeptide and orthosomycin antibiotics on translational GTPases. Chemistry & Biology *18*, 589–600.

Moazed, D. and Noller, H.F. (1989). Interaction of tRNA with 23S rRNA in the ribosomal A, P, and E sites. Cell *57*, 585–597.

Moazed, D., Robertson, J.M. and Noller, H.F. (1988). Interaction of elongation factors EF-G and EF-Tu with a conserved loop in 23S RNA. Nature *334*, 362–364.

Mohr, D., Wintermeyer, W. and Rodnina, M.V. (2002). GTPase activation of elongation factors Tu and G on the ribosome. Biochemistry *41*, 12520–12528.

Moore, P.B. (2009). The ribosome returned. Journal of Biology *8*, 8.

Mora, L., Zavialov, A., Ehrenberg, M. and Buckingham, R.H. (2003). Stop codon recognition and interactions with peptide release factor RF3 of truncated and chimeric RF1 and RF2 from *Escherichia coli*. Molecular Microbiology *50*, 1467–1476.

Munishkin, A. and Wool, I.G. (1997). The ribosome-in-pieces: binding of elongation factor EF-G to oligoribonucleotides that mimic the sarcin/ricin and thiostrepton domains of 23S ribosomal RNA. Proceedings of the National Academy of Sciences *94*, 12280–12284.

Nechifor, R., Murataliev, M. and Wilson, K.S. (2007). Functional interactions between the G′ subdomain of bacterial translation factor EF-G and ribosomal protein L7/L12. Journal of Biological Chemistry *282*, 36998–37005.

Nissen, P., Hansen, J., Ban, N., Moore, P.B. and Steitz, T.A. (2000). The structural basis of ribosome activity in peptide bond synthesis. Science *289*, 920–930.

Osawa, S., Jukes, T.H., Watanabe, K. and Muto, A. (1992). Recent evidence for evolution of the genetic code. Microbiolgical Reviews *56*, 229–264.

Palade, G.E. (1955). A small particulate component of the cytoplasm. Journal of Biophysical and Biochemical Cytology *1*, 59–68.

Pape, T., Wintermeyer, W. and Rodnina, M.V. (1998). Complete kinetic mechanism of elongation factor Tu-dependent binding of aminoacyl-tRNA to the A site of the E.coli ribosome. The EMBO Journal *17*, 7490–7497.

Pape, T., Wintermeyer, W. and Rodnina, M.V. (2000). Conformational switch in the decoding region of 16S rRNA during aminoacyl-tRNA selection on the ribosome. Nature Structural & Molecular Biology *7*, 104–107.

Pech, M., Yamamoto, H., Karim, Z. and Nierhaus, K.H. (2010). Unusual features of the unusual ribosomal elongation factor EF4 (LepA). Israel Journal of Chemistry *50*, 117–125.

Peske, F., Rodnina, M.V. and Wintermeyer, W. (2005). Sequence of steps in ribosome recycling as defined by kinetic analysis. Molecular Cell *18*, 403–412.

Petrelli, D., La Teana, A., Garofalo, C., Spurio, R., Pon, C.L. and Gualerzi, C.O. (2001). Translation initiation factor IF3: two domains, five functions, one mechanism? The EMBO Journal *20*, 4560–4569.

Petropoulos, A.D., McDonald, M.E., Green, R. and Zaher, H.S. (2014). Distinct roles for release factor 1 and release factor 2 in translational quality control. Journal of Biological Chemistry *289*, 17589–17596.

Petry, S., Brodersen, D.E., Murphy IV, F.V., Dunham, C.M., Selmer, M., Tarry, M.J., Kelley, A.C. and Ramakrishnan, V. (2005). Crystal structures of the ribosome in complex with release factors RF1 and RF2 bound to a cognate stop codon. Cell *123*, 1255–1266.

Potapov, A.P. (1982). A stereospecific mechanism for the aminoacyl-tRNA selection at the ribosome. FEBS Letters *146*, 5–8.

Pulk, A. and Cate, J.H.D. (2013). Control of ribosomal subunit rotation by elongation factor G. Science *340*, 1235970.

Qin, H., Grigoriadou, C. and Cooperman, B.S. (2009). Interaction of IF2 with the ribosomal GTPase-associated center during 70S initiation complex formation. Biochemistry *48*, 4699–4706.

Qin, Y., Polacek, N., Vesper, O., Staub, E., Einfeldt, E., Wilson, D.N. and Nierhaus, K.H. (2006). The highly conserved LepA is a ribosomal elongation factor that back-translocates the ribosome. Cell *127*, 721–733.

Ramakrishnan, V. (2002). Ribosome structure and the mechanism of translation. Cell *108*, 557–572.

Rawat, U., Gao, H., Zavialov, A., Gursky, R., Ehrenberg, M. and Frank, J. (2006). Interactions of the release factor RF1 with the ribosome as revealed by cryo-EM. Journal of Molecular Biology *357*, 1144–1153.

Rheinberger, H.J., Sternbach, H. and Nierhaus, K.H. (1981). Three tRNA binding sites on *Escherichia coli* ribosomes. Proceedings of the National Academy of Sciences *78*, 5310–5314.

Rich, A. and Bhandary, U.L. (1976). Transfer RNA: molecular structure, sequence, and properties. Annual Review of Biochemistry *45*, 805–860.

Rodnina, M.V., Savelsbergh, A., Katunin, V.I. and Wintermeyer, W. (1997). Hydrolysis of GTP by elongation factor G drives tRNA movement on the ribosome. Nature *385*, 37–41.

Roll-Mecak, A., Cao, C., Dever, T.E. and Burley, S.K. (2000). X-ray structures of the universal translation initiation factor IF2/eIF5B: conformational changes on GDP and GTP binding. Cell *103*, 781–792.

Roll-Mecak, A., Alone, P., Cao, C., Dever, T.E. and Burley, S.K. (2004). X-ray structure of translation initiation factor eIF2γ implications for tNA and eIF2α binding. Journal of Biological Chemistry *279*, 10634–10642.

Salsi, E., Farah, E., Dann, J. and Ermolenko, D.N. (2014). Following movement of domain IV of elongation factor G during ribosomal translocation. Proceedings of the National Academy of Sciences *111*, 15060–15065.

Saraste, M., Sibbald, P.R. and Wittinghofer, A. (1990). The P-loop — a common motif in ATP- and GTP-binding proteins. Trends in Biochemical Sciences *15*, 430–434.

Savelsbergh, A., Matassova, N.B., Rodnina, M.V. and Wintermeyer, W. (2000a). Role of domains 4 and 5 in elongation factor G functions on the ribosome. Journal of Molecular Biology *300*, 951–961.

Savelsbergh, A., Mohr, D., Wilden, B., Wintermeyer, W. and Rodnina, M.V. (2000b). Stimulation of the GTPase activity of translation elongation factor G by ribosomal protein L7/12. Journal of Biological Chemistry *275*, 890–894.

Savelsbergh, A., Mohr, D., Kothe, U., Wintermeyer, W. and Rodnina, M.V. (2005). Control of phosphate release from elongation factor G by ribosomal protein L7/12. The EMBO Journal *24*, 4316–4323.

Scheffzek, K. and Ahmadian, M.R. (2005). GTPase activating proteins: structural and functional insights 18 years after discovery. Cellular and Molecular Life Sciences *62*, 3014–3038.

Schmeing, T.M., Huang, K.S., Kitchen, D.E., Strobel, S.A. and Steitz, T.A. (2005). Structural insights into the roles of water and the 2′ hydroxyl of the P site tRNA in the peptidyl transferase reaction. Molecular Cell *20*, 437–448.

Schmeing, T.M., Voorhees, R.M., Kelley, A.C., Gao, Y.-G., Murphy, F.V., Weir, J.R. and Ramakrishnan, V. (2009). The crystal structure of the ribosome bound to EF-Tu and aminoacyl-tRNA. Science *326*, 688–694.

Sharp, S.J., Schaack, J., Cooley, L., Burke, D.J. and Söll, D. (1985). Structure and transcription of eukaryotic tRNA genes. Biochemistry *19*, 107–144.

Shi, X., Khade, P.K., Sanbonmatsu, K.Y. and Joseph, S. (2012). Functional role of the sarcin-ricin loop of the 23S rRNA in the elongation cycle of protein synthesis. Journal of Molecular Biology *419*, 125–138.

Shine, J. and Dalgarno, L. (1974). The 3′-rerminal sequence of *Escherichia coli* 16S ribosomal RNA: complementarity to nonsense rriplets and ribosome binding sites. Proceedings of the National Academy of Sciences *71*, 1342–1346.

Spiegel, P.C., Ermolenko, D.N. and Noller, H.F. (2007). Elongation factor G stabilizes the hybrid-state conformation of the 70S ribosome. RNA *13*, 1473–1482.

Uchiumi, T., Honma, S., Nomura, T., Dabbs, E.R. and Hachimori, A. (2002). Translation elongation by a hybrid ribosome in which proteins at the GTPase center of the *Escherichia coli* ribosome are replaced with rat counterparts. Journal of Biological Chemistry *277*, 3857–3862.

Valle, M., Zavialov, A., Sengupta, J., Rawat, U., Ehrenberg, M. and Frank, J. (2003). Locking and unlocking of ribosomal motions. Cell *114*, 123–134.

Verschoor, A., Srivastava, S., Grassucci, R. and Frank, J. (1996). Native 3D structure of eukaryotic 80s ribosome: morphological homology with E. coli 70S ribosome. Journal of Cell Biology *133*, 495–505.

Vetter, I.R. and Wittinghofer, A. (2001). The guanine nucleotide-binding switch in three dimensions. Science *294*, 1299–1304.

Walter, J.D. Activation and inhibition of GTPase translation factors in the prokaryotic ribosome. (2010). WWU master's thesis.

Walter, J.D., Hunter, M., Cobb, M., Traeger, G. and Spiegel, P.C. (2011). Thiostrepton inhibits stable 70S ribosome binding and ribosome-dependent GTPase activation of elongation factor G and elongation factor 4. Nucleic Acids Research *40*, 360–370.

Watson, J.D. and Crick, F.H.C. (1953). The structure of DNA. Cold Spring Harbor Symposia on Quantitative Biology *18*, 123–131.

Weixlbaumer, A., Petry, S., Dunham, C.M., Selmer, M., Kelley, A.C. and Ramakrishnan, V. (2007). Crystal structure of the ribosome recycling factor bound to the ribosome. Nature Structural & Molecular Biology*14*, 733–737.

Wilkie, T.M. (1999). G proteins, chemosensory perception, and the C. elegans genome project: An attractive story. Bioessays *21*, 713–717.

Wilson, D.N. and Nierhaus, K.H. (2003). The ribosome through the looking glass. Angewandte Chemie International Edition *42*, 3464–3486.

Wilson, D.N., Schluenzen, F., Harms, J.M., Yoshida, T., Ohkubo, T., Albrecht, R., Buerger, J., Kobayashi, Y. and Fucini, P. (2005). X-ray crystallography study on ribosome recycling: the mechanism of binding and action of RRF on the 50S ribosomal subunit. The EMBO Journal *24*, 251–260.

Wuerth, M.E. A novel depletion technique for studying the role of protein L12 in activation of ribosome dependent GTPases. (2011). WWU undergraduate honors thesis.

Youngman, E.M. and Green, R. (2007). Ribosomal translocation: LepA does it backwards. Current Biology *17*, R136–R139.

Yusupov, M.M., Yusupova, G.Z., Baucom, A., Lieberman, K., Earnest, T.N., Cate, J.H.D. and Noller, H.F. (2001). Crystal structure of the ribosome at 5.5 Å resolution. Science *292*, 883–896.

Zaher, H.S. and Green, R. (2011). A primary role for release factor 3 in quality control during rranslation elongation in *Escherichia coli*. Cell *147*, 396–408.

Zavialov, A.V., Buckingham, R.H. and Ehrenberg, M. (2001). A Posttermination Ribosomal complex is the guanine nucleotide exchange factor for peptide release factor RF3. Cell *107*, 115–124.

Zavialov, A.V., Mora, L., Buckingham, R.H. and Ehrenberg, M. (2002). Release of peptide promoted by the GGQ motif of class 1 release factors regulates the GTPase activity of RF3. Molecular Cell *10*, 789–798.

Zavialov, A.V., Hauryliuk, V.V. and Ehrenberg, M. (2005a). Guanine-nucleotide exchange on ribosome-bound elongation factor G initiates the translocation of tRNAs. Journal of Biology *4*, 9.

Zavialov, A.V., Hauryliuk, V.V. and Ehrenberg, M. (2005b). Splitting of the posttermination ribosome into subunits by the concerted action of RRF and EF-G. Molecular Cell *18*, 675–686.

Zhou, J., Lancaster, L., Trakhanov, S. and Noller, H.F. (2011). Crystal structure of release factor RF3 trapped in the GTP state on a rotated conformation of the ribosome. RNA *18*, 230–240.

Zhou, J., Korostelev, A., Lancaster, L. and Noller, H.F. (2012). Crystal structures of 70S ribosomes bound to release factors RF1, RF2 and RF3. Current Opinion in Structural Biology *22*, 733–742.

Zhou, J., Lancaster, L., Donohue, J.P. and Noller, H.F. (2014). How the ribosome hands the A-site tRNA to the P site during EF-G-catalyzed translocation. Science *345*, 1188–1191.